Mineral Resources Estimation with Data and Parameter Uncertainty

by

Tolonbek Karpekov

A thesis submitted in partial fulfillment of the requirements for the degree of

Master of Science

in

Mining Engineering

Department of Civil and Environmental Engineering

University of Alberta

Abstract

Uncertainty in resource estimation affects long-term development, planning, and investment decisions. Therefore, there is a need to make the best decisions considering all available data and different modeling approaches. This thesis develops a conceptual framework for resource modeling with uncertainty. A conceptual framework is presented for establishing resource uncertainty with numerical models. The framework is based on carefully assembled modeling practices to capture and represent uncertainty. An overview, concepts, and implementation aspects are presented in order to understand the nature of modeling with uncertainty, as well as provide justification for the developed modeling approaches. The integration of concepts into a modeling workflow improves the quantification of uncertainty in different input parameters and transfers the results to final resource uncertainty and sensitivity analysis. In order to demonstrate the developed concepts and workflow, two case studies are performed. The results show that workflow is effective, practical, and robust for resource modeling with uncertainty.

To my father **Boris** and to my mother **Toktobyby**.

Much Love!

Acknowledgements

I would like to express my deep appreciation and gratitude to my supervisor, Dr. Clayton V. Deutsch for his endless support, patience, and without whom this thesis would not have been possible. I want to thank him for his continuous inspiration, motivation, and guidance throughout my journey. You are great research idea generator and facilitator.

I would also thank all members of the Centre for **Compuatational Geostatistiscs (CCG)**, particularly Ryan Martin, Tyler Acorn, Felipe A. C. Pinto, Mostafa Hadavand, and Mehdi Rezvandehny for their thoughts and comments regarding my research work, as well as Dr. Johnathan Manchuk for his professional comments and feedback.

Special thanks to my good friends Karen, Brett, Jazgul, and Seyil for your friendship and support.

Last, but not the least, I want to thank my father Boris, and my mother Toktobyby, and siblings who have always encouraged me to work hard and follow my own path. Thank you so much for all your endless love, support, and encouragement.

Contents

List of Tables

List of Figures

List of Symbols

$\mathbf{A}$	a square matrix
$\mathbf{h}$	the lag vector
C	an additive factor
$\mathbf{R}$	correlation matrix
P_i	the eigenvector projection matrix
X	the relative error
$\mathbf{z}$	the true value, vector
$\mathbf{u}_\alpha$	the sample location
$\mathbf{V}_i$	left eigenvector
α	probability type error I
β	probability type error II
$\mathbf{U}_i$	right eigenvector
r	the random number
i	the number of variables
f	the facies
p	probability
N	the number of realizations
$a_{i,min}$	the minimum base case variogram range distribution
$a_{i,max}$	the maximum base case variogram range distribution

List of Abbreviations

AER	Alberta Energy Regulatory
ACE	Alternating Conditional Expectation
AuEq	Gold Equivalent
EDA	Exploratory Data Analysis
CB	Conventional Bootstrap
CDF	Conditional Distribution Function
CDF	Conditional Finite Domain
CPU	Central Processing Unit
DF	Distance Function
GSLIB	Geostatistical Software Library and User's Guide
LMC	Linear Model of Corregionalization
MAF	Minimum/Maximum Autocorrelation Factors
MASL	Metres Above Sea Level
MCS	Monte Carlo Simulation
MRB	Mass Recoverable Bitumen
MVSB	Multivariate Spatial Bootstrap
PCA	Principal Component Analysis
PCA-R	Principal Component Analysis-Sphere
QM	Quantity of Metal
RF	Random Function
RN	Random Number
SBS	Spatial Bootstrap
SDF	Signed Distance Function
SIS	Sequential Indicator Simulation
SGS	Sequential Gaussian Simulation

Chapter 1

Introduction

1.1 Background

Geostatistics was developed in many fields including mining and petroleum. Pioneering researchers include Youden (1951) and Matheron (1962). As a scientific field, Geostatisitics was developed and established by Journel (1978, 1986), Isaaks (1989), and Cressie (1993). Modern geostatistics largely overlaps with spatio-temporal statistics and can be defined as a branch of statistics that specializes in the analysis and interpretation of spatially and temporally referenced data (Journel 1986). Understanding uncertainty is a great challenge. Numerical geological models are constructed at different scales for different purposes. Uncertainty is inevitable due to our lack of understanding in the geologic processes and incomplete data. Geological spatial distributions are complex due to inherent uncertainty caused by natural variability and sparse sampling. This uncertainty may have an impact on the mining project. A large number of uncertainty models have been proposed for different purposes with the goal of identifying sources of uncertainties. It is important to have a resource model with a reasonable understanding of uncertainty. Determining which method/model is appropriate can be based on prior experience, preference, and company policy. Alternative options available for resource modeling with uncertainty must be analyzed and evaluated in terms of ease of use, computational cost, and the reliability of the resulting model.

1.2 The Problem

There is uncertainty at every stage of a mining operation. In particular, the resource model is an important component of the mining system. It forms the basis of mine planning activities and helps in decision making. Modeling uncertainty is application tailored (Caers 2011). If the application changes then the modeling workflow to model the uncertainty will be different, hence the final model of uncertainty will be different. It is difficult and challenging to construct a resource model that includes all aspects of uncertainty. Although not the focus of this thesis, managing a model of uncertainty remains an issue. This problem includes transferring the uncertainty through mine planning and decision making. The uncertainty must be built in from the beginning of the modeling process; it cannot be added on once the model is constructed. It is important to understand the uncertainty, and if required, select suitable data acquisition that can reduce the uncertainty to an acceptable level. Therefore, there is a need for a theoretical and practical framework for the systematic treatment of uncertainty in resource modeling. This thesis aims to address this problem.

1.3 Significance of the Research

A resource model is an important component of a mining project. A carefully constructed model provides valuable decision support information, giving a practitioner a range of possibilities to evaluate different decisions and actions. Uncertainty issues are incompletely addressed in modern software and work practices despite the importance of the uncertainty in resource modeling. Producing an accurate and unbiased resource model of uncertainty that is properly conditioned to the input parameters with different complex geological settings is not an easy task. For this reason, a theoretical framework that is robust and practical with respect to uncertainty in each input parameter is important. This thesis addresses uncertainties in the data, boundaries, and input modeling parameters, and realizations of important variables including grades. The thesis study assembles, captures, and transfers the

uncertainty in input parameters in different geological settings. A theoretical and practical workflow is developed by analyzing the existing modeling approaches and selecting best practices for a treatment of the uncertainty.

1.4 Literature Review

1.4.1 Review of Resource and Geological Modeling on Reserves

Computerized resource models were introduced in the late 1970s. Numerous approaches have been applied and used to measure uncertainty in resource models over the years. Reeve & Glacken (1998) describes the history of resource estimation for large mineral deposits. Arvidson (1998) put together data over 100 years to generate a resource estimation study on a gold deposit. Another research (Murphy et al., 1998) provides an overview of the resource estimation process in gold deposits. Lutherborrow (1999) describes the history of resource estimation and recent developments. There is another overview of various methodologies and techniques for resource estimation by Carras (1998). The importance of the geology in ore reserve estimation has been studied and summarized by King et al., (1982) and Grace (1986). Geostatistics provides tools for spatial modeling of geology (Journel & Huijbregts 1978). Philip & Watson (1986) discuss components of geostatistical estimation.

Surprisingly little has been published on resource modeling with uncertainty; mainly some questions of detail have been discussed. On the other hand, much has been done and published in health, medicine, biology, and ecology (Bárdossy & Fodor 2001). Some authors address geological uncertainty primarily in coal resource estimation including Li et al., (2008) and Knights et al., (2008).

For many decades the mining industry regarded resources/reserves estimation and classifications as straightforward requiring basic mathematical and geological knowledge (De Souza Eduardo et al., 2005). According to these authors, many of the methods were based on geometrical procedures and spatial data distribution. As a result, uncertainty was ignored. Bárdossy & Fodor (2001) present an overview of the main types of uncertainties in geology. They outlined the best uncertainty oriented

approaches along with traditional methods of uncertainty. Mann (1993) presented a short review of the uncertainty problem in geology. The author suggests that all scientists are aware of uncertainty and specify the uncertainty in each measured or derived values; however, this is not a case in geology. Therefore, there is a need to identify and characterize the uncertainty in each input parameter used in resource estimation.

1.4.2 Review of Resource Modeling with Uncertainty

Geostatistics was developed and established as a scientific field by Journel (1978, 1986), Isaaks (1989), and Cressie (1993) after its first introduction by Youden (1951) and Matheron (1962). Hengl et al., (2009) analyzed bibliometric indices of the scientific field of geostatistics using statistical and spatial data analysis. They also gave an introduction to the history of the geostatistics. Uncertainty can be defined and characterized in many different ways. Mann (1993) describes uncertainty as a simple concept ostensibly understood to mean that which is indeterminate, not certain, containing doubt, indefinite, problematical, not reliable or dubious. Other research describes uncertainty as the term associated with a limitation of our knowledge, or some kind of error, or inexactness (Funtowicz & Ravetz 1990). Some uncertainty cannot be avoided because of inherent uncertainty related to natural processes or complexities caused by nonlinear relationships (Katz 2002).

Refsgaard et al., (2006) studied the role of uncertainty at different stages in the modeling process. They briefly review fourteen different (partly complementary) methods commonly used in uncertainty assessment and characterization. They demonstrated the applicability of the methods by mapping according to purpose of application, stages of modeling processes and types of uncertainties addressed. Their conclusion was that uncertainty assessment is not something that can be added and it needs to be taken into account at the early stages and considered throughout the modeling process. In addition, they discuss other aspects of uncertainty, particularly in policy and public participation processes that may be helpful in managing uncertainty and decision-making.

An overview of the methods to evaluate uncertainty of deterministic models in decision support was conducted by Uusitalo et al., (2015). They review various methods that have been or could be applied to evaluate the uncertainty related to deterministic models outputs. They also indicate that the best way of evaluating the uncertainty depends on the definitions of source models and the amount of quality information available to the modeller. They conclude that decision support models can be very valuable when it comes to managing complex problems and efficiently summarize various and distinct consequences related to alternative management measures.

Uncertainty arises due to our limited sampling of the true distribution. Geostatistics uses all available site specific and analogue knowledge to construct models of uncertainty, taking care to ensure that these models reasonably represent our state of incomplete knowledge (Wilde & Deutsch 2010). The authors defined a number of formats to express acceptable uncertainty in data by categorizing them as relative, absolute, and misclassification. According to the authors, expressing the uncertainty usually requires a specification of a volume, a $\pm$ measure of uncertainty, and the probability to be within the $\pm$ measure. They recommend using relative format for expressing the uncertainty in most cases, unless there is a significant threshold where misclassification is important.

Bear et al., (2010) did research on modeling under uncertainty. They say that deterministic approaches are good assuming that a full knowledge and understanding of all the processes and models are understood. These processes and models are used to predict future responses to measure availability of information on all parameters in the model. However, this situation is not common in practice because there is significant uncertainty in the input parameters.

One of the important contributions of spatial statistics or geostatistics is that it provides a measure of uncertainty in the regionalized variable (Isaaks & Srivastava 1989). Uncertainty in modeling comes from different sources, which may be classified into different categories (Wu & Li 2006 and Funtowicz & Ravetz 1990). These sources of uncertainty may come from the boundaries, data, and input parameters, and so

on. Some types of uncertainties are difficult to handle due to inherent uncertainty as a result of natural processes. At some point, treatment of these uncertainties may be impossible. However, the main goal of dealing with uncertainties in different input parameters is to quantify and select the best approaches to treat the uncertainty.

In addition to the geostatistical methods that have been successfully applied to assess and measure resource uncertainty, Kogan (1989) studied the accuracy of estimates and its prospects and properties by assigning confidence intervals. Bailey et al., (2012) present an overview of approaches to the analysis and modeling of multivariate geostatistical modeling. They gave an overview of existing approaches for the multivariate geostatistical data analysis, where multivariate data was indexed spatially and was continuous across space. Their approach was divided into classes such as factor models and spatial random field models.

Many areas of application involve testing physical parameters in a laboratory. They have the advantage of repeated testing and can reduce uncertainty by increasing the number of test subjects. This is not the case with geostatistical models that are derived numerically where data collection is expensive. Some thoughts on uncertainty quantification is collected by Deutsch et al., (2002). Their preliminary research report formed a conceptual basis for different research/application studies. According to the authors, geostatistics is used for heterogeneity characterization; however, assessment of the uncertainty requires more implementation details and assumptions.

Another research conducted by Babak et al.,(2006) discusses a new method for assessing uncertainty in input parameters that accounts for the histogram and variogram. Their stochastic method was based on multivariate Gaussian distribution. They compared the spatial bootstrap method with a new proposed CFD approach. The authors proposed a practical technique for uncertainty quantification in the histogram. Their approach allowed to assess the uncertainty by sampling original data that accounts for spatial correlation. They also define a number of limitations of using the spatial bootstrap where it does not account for the area of interest and only considers the histogram. They also studied the variogram uncertainty using real

data. They conclude that the proposed method is convergent, design independent, and invariant under parameterization.

Many methodologies are available to practitioners for quantifying mean uncertainty, which may cause confusion in selecting an appropriate technique. Although there is an abundance of literature for these methods, comparatively few resources are dedicated to the use of mean uncertainty within a geostatistical modeling workflow (Barnett et al., 2014). The authors present a practical guide to use of uncertainty in mean in geostatistical modeling. They provide two workflow steps to estimate the uncertainty. According to the authors, many parameters are important within geostatistical modeling, however, uncertainty of the global mean is one of the most critical. They claim that over the last decade numerous methods for quantifying mean uncertainty have been proposed; however, their practical implementation within geostatistical modeling is not usually specified.

A realistic evaluation of uncertainty is important during the planning of mining operations. A better evaluation of uncertainty could avoid problems during the production and help in mine planning (Villalba & Deutsch 2009). They reviewed the current techniques to evaluate uncertainty. This included the conventional bootstrap (CB), spatial bootstrap (SB), and conditional finite domain (CFD). The bootstrap is a popular application of Monte Carlo simulation technique that was developed by Efron (1983). The bootstrap is useful for complex statistics. This include proportions, average above cutoff, and the correlation between variables. The spatial bootstrap (Journel & Bitanov 2004 and Feyen & Caers 2006) for a single variable is an extension of the bootstrap (Efron & Tibshinari 1986) resampling technique that accounts for spatial correlation. According to the authors, all of them are based on an assumption that the distribution of the data is representative for entire domain. The samples are drawn randomly from the cumulative distribution function (CDF) of original data, taking into account the spatial correlation, conditioning to data, and the domain.

There is uncertainty in the boundaries between different geological domains. Interpolating a distance function has been shown to be a useful method for estimating

the boundary location (Munroe & Deutsch (2008, a,b). One method for quantifying the uncertainty includes calibrating an additive parameter C, using available data in a way similar to the jackknife (Wilde & Deutsch 2011). Uncertain boundaries are problematic in many geo-engineering applications (Hosseini & Deutsch 2007). Geostatistical techniques have been developed to solve spatial modeling problems; however, they become inefficient when it comes to quantifying the uncertainty in the areal limits. The authors used the distance function (DF) because of simplicity, as well as a powerful methodology to characterize the space of uncertainty for areal limits. Their methodology was tested by using a large number of synthetic limits, and their conclusion was that the results were robust and the methodology can easily be incorporated in Monte Carlo Simulation to simulate any continuous attribute with uncertain areal limits.

Incorporation of the distribution uncertainty in input parameters is important; however, there is no established procedure for incorporating multivariate parameter uncertainty. Khan & Deutsch (2015) propose a multivariate spatial bootstrap resampling (MVSB) to sample the required global statistics. They incorporate multivariate parameter uncertainty in geostatistical resource modeling. The proposed workflow accounts for the prior uncertainty given the data locations and leads to the posterior uncertainty in the global distributions of all modeled properties. They concluded that the results are tractable and practically provide realistic assessments of the uncertainty. This accounts for large-scale parameter uncertainty, which is important in resource model.

The uncertainty quantification is valuable for many management decisions. However, resource uncertainty is underestimated or overestimated when the calculated parameter uncertainty is inaccurate (Rezvandehy et al., 2015). They developed a technique that improves the uncertainty in the univariate distribution for regionalized variables by using the spatial bootstrap and transferring through simulation. They compare their results to real uncertainty assessed through the scanning of a large image.

1.5 Research Contribution

Although the importance of uncertainty in resource model is well recognized, few studies provide a conceptual resource model with uncertainty. Uncertainty can have an impact on every aspect of modeling (Reckhow 1994; Klepper 1997; and Katz 2002). It is important to understand uncertainties coming from different input parameters during resource modeling and provide suitable best practices that can be used to minimize the uncertainty. A theoretical framework with best practices is developed. Case studies are presented to demonstrate the applicability of the concept. Outcomes will provide useful information to understand realistic uncertainty in input parameters. The main contribution of this thesis is to analyze existing techniques and select the best practices to assemble, capture, and transfer the uncertainty in input parameters in different geological settings.

1.6 Research Outline

This thesis is a study on resource modeling with data and parameter uncertainty with the goal of providing the best practices to measure the resource uncertainty. Each chapter targets one specific aspect of the study.

In Chapter 2, a conceptual geostatistical simulation workflow of resource modeling with uncertainty is presented. In this chapter, the basic concepts are introduced and discussed including conceptual geology, boundary, data, and model and model parameters and realizations, followed by implementation aspects. Additionally, some notations and details are reviewd. Unit operations are introduced and reviewed along with required geostatistical concepts and methodology to evaluate the uncertainty.

Chapter 3 shows Case Study 1 for a specific data set. This chapter provides an overview of the geology and available data. This will be followed by details of geostatistical modeling, result, and analysis.

In Chapter 4, Case Study 2 using another data set is presented. The outline of this case study is similar to Case Study 1.

In closing, Chapter 5 discusses conclusions, future work, and recommendations.

Chapter 2

A Conceptual Geostatistical Simulation Workflow for Resource Modeling with Uncertainty

At large scales, selection and implementation of the best and most applicable practices to meet the data and model requirements should be a top priority. A number of concepts can be applied to address this problem in a model. The goal of this chapter is to introduce and develop a conceptual workflow of resource modeling with uncertainty. A theoretical workflow with unit operations is developed. A conceptual basis will be first introduced for each unit operation followed by implementation aspects where realizations are simulated and full models of variables assembled. The plan for developing and implementing theoretical concepts for each input parameter/unit operation will follow the illustrative sketch shown in Figures 2.1 and 2.2. In the first figure, general hierarchical modeling workflow with unit operations is presented, whereas second figure illustrates a schematic illustration of assembling a resource model form all variables from simulated realizations.

The chapter starts with an introduction and purpose, Section 2.1 and Section 2.2. Conceptual geology is covered in Section 2.3, while unit operations including boundary uncertainty in Section 2.4, data uncertainty in Section 2.5, parameter uncertainty

and realizations in Section 2.6, post processing in Section 2.7, and recommendations in Section 2.8. With the purpose of full demonstration of the developd workflow, implementation aspects are presented at the end of each unit operation section. In addition, the implementation aspects will be directly linked to case studies as the workflow is fully implemented in case studies with different data. The scope of discussion is limited to those areas that are applicable to this thesis study.

2.1 Introduction

Uncertainty arises due to inadequate information, which can be of three sorts: inexactness, unreliability and ignorance (Funtowicz & Ravetz 1990). New information will decrease or increase uncertainty because the data may reveal the presence of previously unknown features. Any parameter in a resource model, or a geologic parameter can be a source of uncertainty. This source of uncertainty makes a modeling process difficult and challenging. A number of studies (Regal & Hook 1991 and Draper 1995) are presented on the impact of ignoring a model of uncertainty. Uncertainty should be captured and narrowed in a model.

Unit operations are selected based on best practices that are properly conditioned to the input parameters. The main purpose of the thesis study is to develop and select best practices/unit operations that will aid to reduce uncertainty and help in decision making. The developed workflow is robust and practical where uncertainty is assembled, quantified, and transferred, giving practitioners a range of alternative options to consider different uncertainty scenarios and evaluate them with confidence.

2.2 The Purpose

It is of primary importance to understand the phenomenon that we are modeling (Pyrcz & Deutsch 2014). A resource model is an important part of the mining system. Any uncertainty associated with the resource model may have an impact on a mining project as different types of uncertainty offer different challenges. Therefore, where possible, suitable data acquisition that reduce the uncertainty to an acceptable

level. The goals and purpose must be clearly established, and the workflow must be designed to meet these goals under the modeling constraints (Koltermann 1996). The purpose of the study is to develop, understand, and assemble a modeling workflow to fully integrate all available input parameters using best practices and expert knowledge. With the establishment of the workflow we can apply the modeling algorithms/methods to assess resource uncertainty.

2.3 Conceptual Geology

The conceptual geology provides the fundamental prerequisites required for resource modeling. These prerequisites allow to integrate all available information into a model with the goal of the best representation of uncertainty. Thus, there is a need to apply geological concepts in resource modeling. They serve as a base for resource modeling and the specific required characteristics of the modeling.

2.3.1 Hierarchical Modeling

The purpose of hierarchical modeling is to develop and establish a general modeling workflow. Hierarchical modeling is divided into five main unit operations. Considerations include a data inventory, formulating the conceptual basis, and making decisions on best workflows for a complete modeling process. The introduced hierarchical modeling is applicable for a variety of resource modeling approaches; however, different steps during a modeling process may also be considered depending on the goals of a project and different geological and parameter settings. Consider Figure 2.1 showing the general hierarchical modeling workflow adapted from Deutsch (2015).

Figure 2.1: General hierarchical modeling workflow, including formulation of a model setup, boundary, data, and parameter (distributions) uncertainty and realizations along with post processing in the uncertainty space adapted from Deutsch (2015)

The unit operations are developed and assembled based on latest thinking by considering best and applicable practices. In case of reservoir modeling, additional modeling steps may be required. This includes, but is not limited to, modeling of top surface structure and thickness, and/or facies modeling, and so on. These steps are still developed within the five unit operations framework.

In general, the first step starts off with setting up a model including formulation of the modeling workflow where exploratory data analysis (EDA) is performed. There is no strict set of requirements for performing EDA so it depends on a practitioner's preferences. The model set up also includes defining and setting up applicable software algorithms and input parameters used at each step of a workflow. The next step after model set up and performing the EDA, include boundary, data, and parameter uncertainty that will be performed within two steps including prior and posterior uncertainties, as well as post processing. The illustrated workflow with five steps in Figure 2.1 is to demonstrate general modeling concepts with uncertainty, whereas Figure 2.2 shows the modeling workflow with multiple realizations. The models are constructed hierarchically with correct dependencies between all input variables/parameters.

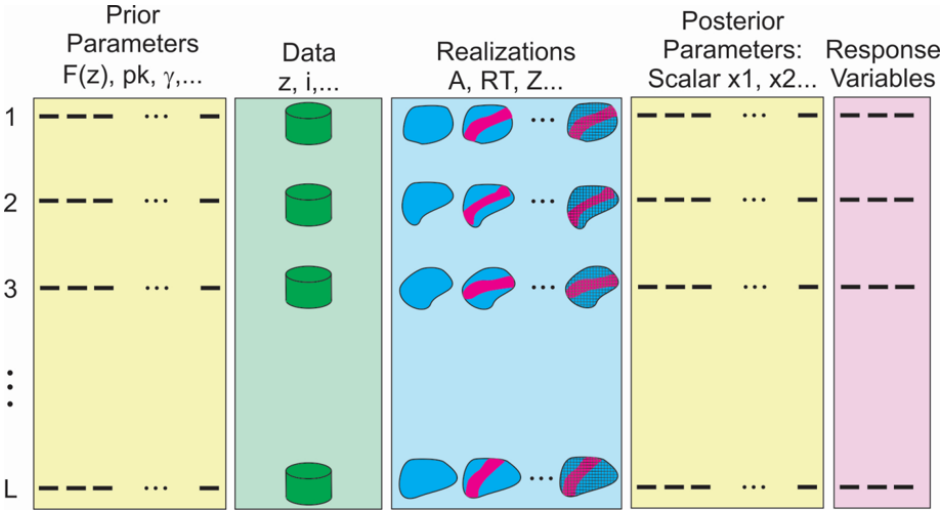

Figure 2.2: Illustration of the all realizations all time adapted from Deutsch (2015).

Understanding the large scale boundaries is a first step in the modeling workflow. Boundary uncertainty involves interpolating and mapping the uncertainty in

bounding surfaces (Hosseini & Deutsch 2007; Machuca-Mory, Munroe, & Deutsch 2009; and Wilde & Deutsch 2011). Data uncertainty is calculated based on analyzing the existing data and selecting the relative uncertainty format (Wilde & Deutsch 2010), such as understanding the data collection and processing. Parameter uncertainty includes simulation of all realizations from the modeling parameters. Post processing to evaluate the generated realizations comes at the end with sensitivity analysis in order to understand the importance and relationships between response and predictor variables by fitting a response surface.

Unit operations are an important part in establishing and developing a conceptual workflow that reasonably accounts for the uncertainty in input parameters and achieves the stated modeling goals. At some steps of the modeling workflow, different methodologies to assess the uncertainty could be used. There are, for example, many different facies modeling techniques includign indicator simulation, truncated (plori)Gaussian and multiple point statistics based techniques. Each unit operation targets one specific aspect of uncertainty including boundary surfaces, or data, or parameter uncertainty and realizations. The developed theoretical framework provides a realistic assessment of uncertainty and integrates all available input parameters into a resource model.

2.3.2 One-at-a-Time Approach

Depending on the complexity of a model, different methods varying from simple to relatively complex can be adapted. The MCS process can be summarized as: (1) problem formulation; (2) simulation of all variables; (3) post processing/transfer function; and (4) ssembling of all simulated response variables. A Monte-Carlo Simulation (MCS) is applied as a convenient modeling methodology where configurations of model inputs are drawn randomly from their distribution. And then resulting set of models outputs can be seen as a random sample of the distribution of the output of interest.

There is significant body of literature on modeling methodology addressing the workflow (Saltelli et al., 2000 and Kennedy & O'Hagan 2001). In this study, a MCS

workflow is adapted where values are drawn in a random manner from the distributions of each uncertain input parameter. Various approaches ranging from simple one-factor-at-a-time methods to comprehensive approaches are available based on MCS methods (Saltelli et al., 2005 and Cariboni et al., 2007). One-at-a-time approach is applied to understand the impact of each input parameters. This methodology allows the impact of each input parameter to be isolated and understood.

2.3.3 Overall Model Setup Approach

As more information or data for modeling becomes available to practitioners, there is a need to deal with them to constrain models of uncertainty. It is clear that some of tools for modeling uncertainty through traditional models are too rigid to handle all these complexities (Caers 2011). The reliability of a final model results and a relative contribution or importance of each uncertainty model is important. A schematic illustration of assembling a resource model from all variables from simulated realizations is adapted from Deutsch (2015) and shown in Figure 2.2. The overall model setup approach that will be used for the modeling workflow follows as:

1. Identifying and setting up all required parameters for modeling, where data is analyzed and a hierarchical workflow specified for how the realizations of all variables will be performed and assembled.

2. Prior parameter uncertainty defining base case parameters and uncertainty in each of those parameters. The input parameters include, but are not limited to thickness, grade values, and facies proportions, as well as variograms, and other input parameters depending on the data and modeling goals.

3. Data uncertainty of all input variables is then assessed. In this case, data imputation or sampling data error may be required in order quantify the uncertainty in the data (Barnett 2015).

4. Posterior uncertainty is understood after realizations of all variables are assembled. This includes all the steps identified in the model set up and unit

operations for every data and parameter realization. These are constructed hierarchically and checked to the greatest extent possible with correct dependencies between all input variables.

5. Post processing/process in transfer function includes calculation of resources/reserves with all realizations to understand uncertainty and in order to perform a sensitivity analysis.

The sensitivity comes at the end and is based on calculated scalar posterior parameters. A response surface can be created for each response variable using posterior uncertainty parameters with the purpose of analyzing and better understanding the importance/impact of each input parameter. The plan for the rest of this chapter is to introduce each unit operation [boundary, data, distributions, etc.] and demonstrate their implementations. This will help us to better understand and fully integrate the developed resource modeling workflow with uncertainty.

2.4 Boundary Modeling Uncertainty

Boundary modeling focuses on interpolating and mapping the uncertainty in boundaries. There are a variety of modeling approaches available to build boundary surfaces. In this thesis, the focus will be given to the distance function (DF) method to interpolate and map boundary uncertainty. Hosseini & Deutsch (2007) used the distance function to characterize the space of uncertainty in areal limits using a large number of synthetic limits. Their aim was uncertain areal limits. Munroe & Deutsch (2008, a, b) proposed another method to assess the uncertainty by calibration of two paramaters, C and β where C controls the width of the uncertainty and β controls the bias. These parameters are optimized to give appropriate uncertainty; however, optimizing these parameters requires multiple reference models and two objective functions. A simpler method for calibrating the distance function is proposed by Wilde & Deutsch (2011). Uncertainty quantification includes calibrating an additive parameter C, using the available data in a way to similar to the jackknife. This is less expensive compared to other methods.

2.4.1 Distance Function (DF)

The distance function (DF) used for boundary modeling is based on the Euclidean distance between a sample and the nearest sample with a different indicator type. This coding starts with a binary categorical indicator of the form (Deutsch & Journel 1998):

$$i(\mathbf{u}_\alpha) = \begin{cases} 1, & \text{if domain present at} \quad \mathbf{u}_\alpha \\ 0, & \text{otherwise} \end{cases}$$

Where $\mathbf{u}_\alpha$ is the sample location. The distance function is defined as positive outside the domain and negative within the domain of interest. The distance is calculated as follows in presence of anisotropy.

$$distance = \sqrt{\left(\frac{dx}{ax}\right)^2 + \left(\frac{dy}{ay}\right)^2 + \left(\frac{dz}{az}\right)^2}$$

Where d is the separation between the two points in each of the x, y, and z directions, and a is the geometric anisotropy defined for each of the x, y, and z directions. Illustration of the distance is measured to the nearest data location with positive or negative values depending on the location of the data inside or outside the domain is shown in Figure 2.3.

For each sample located at $\mathbf{u}_\alpha$, the nearest sample location ($\mathbf{u}_\alpha^{'}$) is determined such that $Min\left\{\mathbf{u}_\alpha - (\mathbf{u}_\alpha^{'})\right\}, i(\mathbf{u}_\alpha^{'}) \neq i(\mathbf{u}_\alpha^{'})$. The distance between the two locations is the distance function value at location $\mathbf{u}_\alpha$. If $\mathbf{u}_\alpha$ is within the domain, the distance is set to negative; otherwise the distance is positively signed:

$$DF(\mathbf{u}_\alpha) = +distance(\mathbf{u}_\alpha - \mathbf{u}_\alpha^{'}), \text{if } i(\mathbf{u}_\alpha) = 0$$

$$DF(\mathbf{u}_\alpha) = -distance(\mathbf{u}_\alpha - \mathbf{u}_\alpha^{'}), \text{if } i(\mathbf{u}_\alpha) = 1$$

Figure 2.4 illustrates the concept of the DF (Munroe & Deutsch 2010) where each illustration consists of two drillholes separated of ten units. The sample interval is

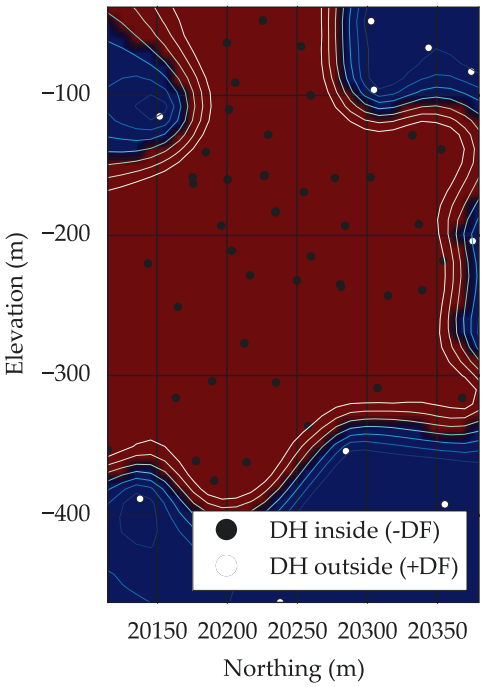

Figure 2.3: Illustration of drillholes locations inside and outside of the domain calculated from the DF values from the *Red* data using 46 drillholes coded inside of the domain. The units of the calculated DF values are in meters.

uniform at one unit. The white samples imply the presence of non-vein and are given a vein indicator code of 0, while grey areas signify vein and are given a vein indicator of 1.0. The numbers located on the each side of sample indicates the distance to the closest sample with vein indicators and are aided by the use of arrows.

2.4.2 Parameter Calibration

Interpolation of the distance function is useful for modeling boundaries with uncertainty; however, it requires an expensive calibration method to ensure that the uncertainty is unbiased and fair. A method to calibrate the distance function is proposed by Wilde & Deutsch (2011). This method uses the data to calibrate a single additive factor C, which modifies the DF values at the sample locations:

$$\widehat{DF}(\mathbf{u}_\alpha) = DF(\mathbf{u}_\alpha) + C, \text{ if } i(\mathbf{u}_\alpha) = 0$$

$$\widehat{DF}(\mathbf{u}_\alpha) = DF(\mathbf{u}_\alpha) - C, \text{ if } i(\mathbf{u}_\alpha) = 1$$

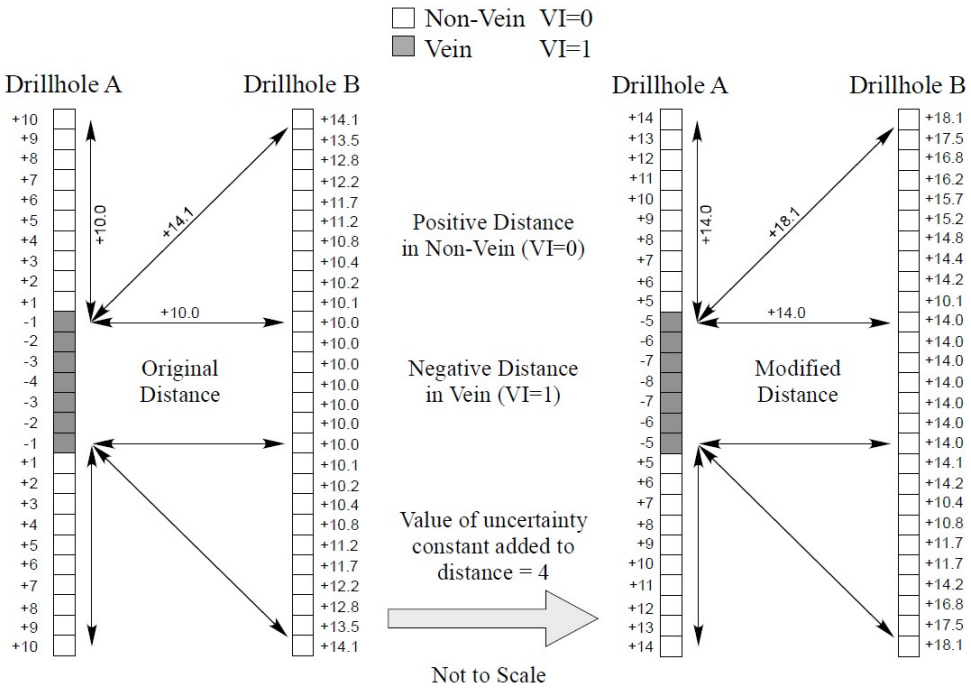

Figure 2.4: Distance function: sign dependent shortest distance between points with vein and non-vein indicators (Munroe & Deutsch 2010).

This modification is illustrated in Figure 2.5. The additive factor C increases positive and decreases negative distance function values. Once the C parameter is applied to the data, the modified distance function is interpolated. Calculated distance function values are modified at the sample locations. Modified DF estimates between (-C) and (+C) are within the range of boundary uncertainty.

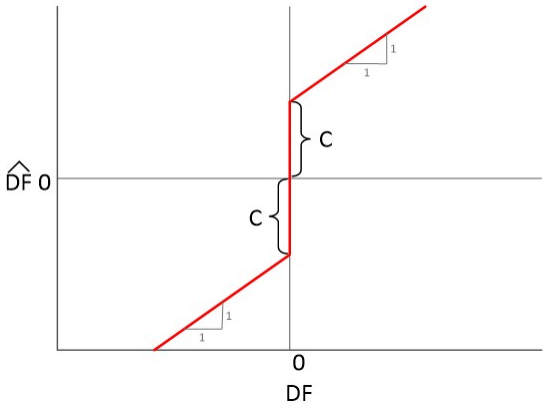

Figure 2.5: Conversion of distance function to modified distance function by the C parameter. The units of the C parameters are in meters.

2.4.3 Boundary Limits and Uncertainty

There is a need to define and know the limits of the uncertainty bandwidth. Determination of the limits by applying thresholds to the gridded model is an important step during the calibration process. With the defined limits, a distribution of areas can be determined. Consider Figure 2.6 that shows 1D schematic of distance function thresholds applied at boundary locations. As the distance function varies from positive (+C) to negative (-C) distance function values the boundaries erode to a smaller volume inside (Wilde & Deutsch 2011).

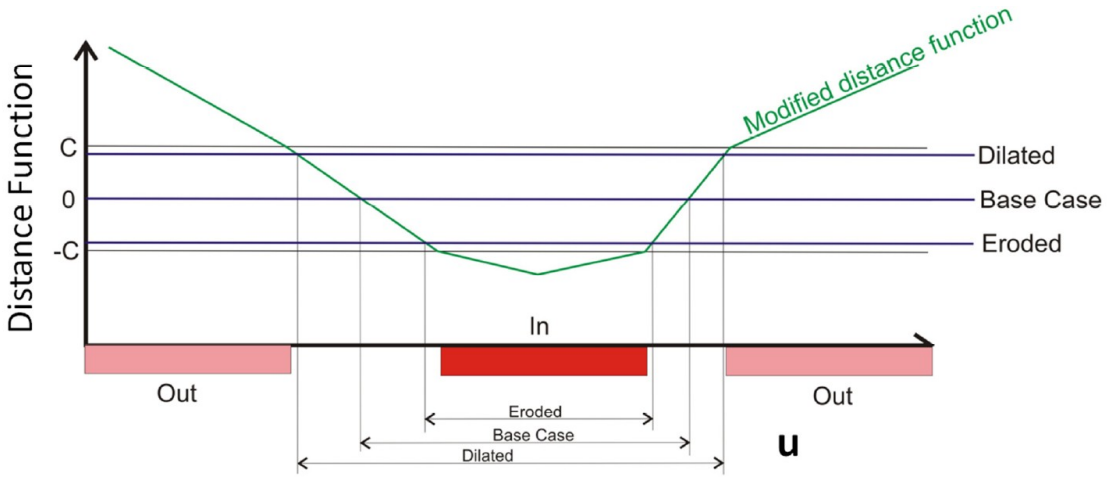

Figure 2.6: 1D schematic of distance function thresholds applied to arrive at different boundary locations (Wilde & Deutsch 2011).

A threshold of zero yields the base case; choosing a threshold near (+C) yields boundaries that are large everywhere (dilated boundary); and threshold near (–C) yields to be small everywhere (eroded boundary). Different boundaries can be extracted by applying a threshold between (-C) and (+C). The choice of a value for C parameter depends on the level of accuracy required versus the amount of time desired (Munroe & Deutsch 2008a). These values for C parameter can be subdivided into three categories: (1) empirical selection, (2) partial calibration, and (3) full calibration. Empirical selection is applied based on predetermined values and/or expert knowledge. In partial calibration the interpolated models are compared to a single solid model representation of an orebody. A value for the uncertainty constant C is

chosen based on the interpretation of representative sections and expert judgment. Lastly, full calibration uses multiple reference models for a complete, unbiased, and fair estimate of uncertainty. However, this calibration method requires considerable CPU time and increases with the size and number of reference models used as full calibration requires multiple iterations using different C values. In this study, the choice of the C uncertainty parameter bandwidth is based on expert judgment.

2.4.4 Implementation of the Boundary Modeling with Uncertainty

The calculation of the DF values could be done with a custom written program or the GSLIB-like program *DFcalc* demonstrated by Wilde & Deutsch (2011). An illustration of the calculated distance function values and location of drillholes inside/outside of the domain is shown in Figure 2.7 (a). A number of control points are then assigned at locations outside domain after calculation of the distance function values. Control points are chosen and assigned based on the drillholes that are coded (+DF) outside domain. The purpose of the control points is to constrain the ore and waste boundaries shown in Figure 2.7 (b). The full demonstration and more discussion on the uncertainty in boundary surfaces with defined/calculated distribution areas and corresponding probability distributions between the C=-30m and C=+30m thresholds will be presented in Case Study 1.

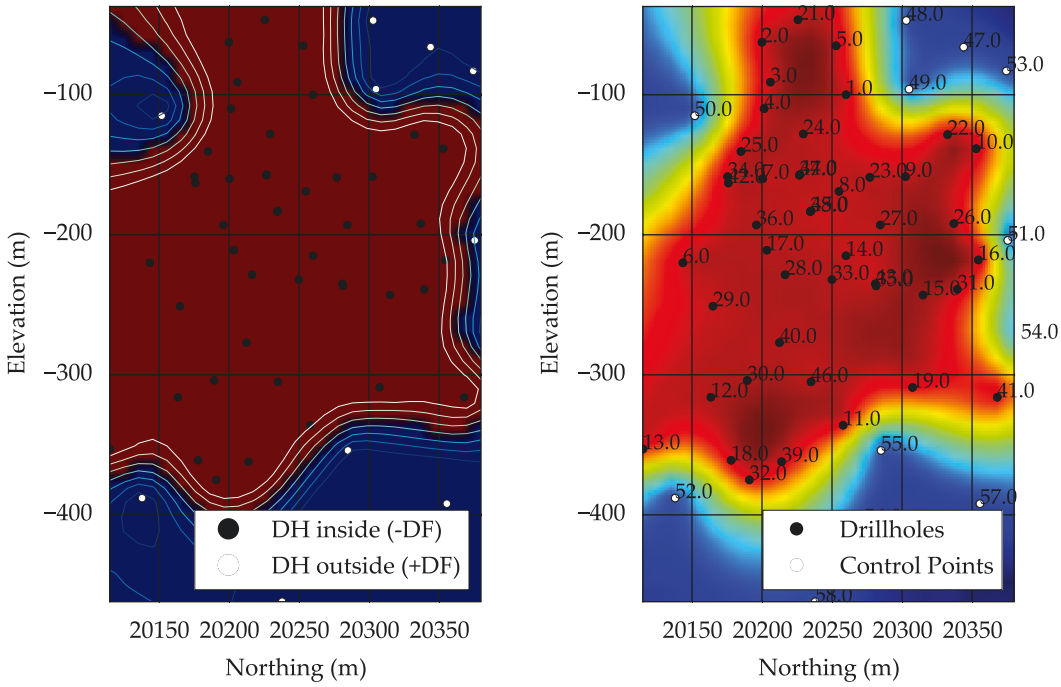

(a) (b)

Figure 2.7: Illustration of the drillholes located inside (-DF) and outisde (+DF) domain (a) and control points (b). Black=drillholes, White=control points. The units of the DF values are in meters.

2.5 Data Uncertainty

Error is an inevitable uncertainty that attends all measurements. An error does not carry the usual connotations of the terms of mistake or blunder (Taylor, 1997). Each sample has some sort of degree of uncertainty. Sample collections, preparation, and overall data handling are all sources of uncertainty (Rossi & Deutsch 2014). Data are often associated with uncertainty. It is useful to know how various measures of uncertainties respond to changes in data. A measurement inaccuracy or other errors arises due to limited sampling of the true distribution. A number of factors have an impact on the data uncertainty including the sampling protocol and intrinsic heterogeneity of the rock being measured.

2.5.1 Formats for Expressing the Data Uncertainty

Different formats are available to express uncertainty in data. Selection of these formats depend on prior experience, preference, and transparency. Available formats include a measure of the ± uncertainty, a probability to be within the ± measure of the uncertainty, and an absolute measure of the ± measure of the uncertainty. The relative uncertainty is expressed as a fraction or percentage to relative to the expected value. This gives an indication of how good a measurement is in a dimensionless format. A misclassification uncertainty could also be considered to present the uncertainty. This is a common procedure when there are two clear misclassification errors. This includes the probability of Type I errors (false positive) represented by α and the probability Type II errors (false negatives) represented by β. Figure 2.8 shows the illustration of normal probability distribution in units of standard deviation.

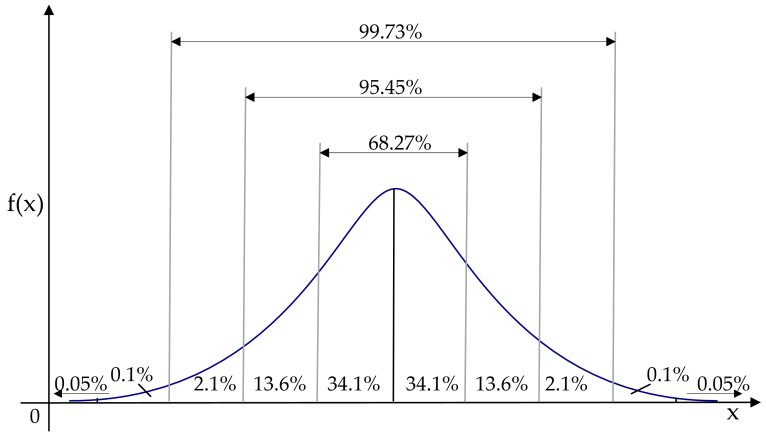

Figure 2.8: Illustration of normal probability distribution in units of standard deviations.

The figure above illustrates the well known result that there is a 68.27% chance that measurement falls within one standard deviation of the mean, and 95.45% chance that falls within two standard deviation of the mean, and three standard deviation within 99.73% of chance, respectively. The data value is considered as the mean and the true value is considered to fall within a probability distribution centered on this mean.

2.5.2 Implementation of Data Uncertainty

There is uncertainty in data that comes from the sampling protocol and data handling. It should be minimized, but may still be significant. In this study, the data are considered have a relative uncertainty. A relative format is recommended in most cases (Wilde & Deutsch 2010). A relative error can be expressed as:

$$\delta_{error} = \frac{X}{100} \times z$$

Where z is the true value related to the data and the X is a relative error value in percentage. The choice and selection of the acceptable relative error value is usually specified and selected by a practitioner. In this thesis study, a $\pm$ 10% relative error is selected to express the uncertainty in the data. This would have to be evaluated on a case-by-case basis. A small illustration of the data uncertainty using the relative error format will be demonstrated in Case Study 1.

2.6 Parameter Uncertainty

A variety of geostatistical techniques/methodologies to assess input parameters with different geological complexities exist. In order to obtain a better model of uncertainty, best practices and realistic parameter uncertainty should be considered. The process of transferring the prior parameter uncertainty to posterior paranmeter uncertainty model is achieved through geostatistical modeling with a number of modeling parameters. The random function (RF) concept is covered in many textbooks (Journel & Huijbregts 1978; Isaaks & Srivastava 1989; Goovaerts 1997; Grondona & Cressie 1991; and Chilès & Delfiner 2012). Some sources on different types of variogram-type measures of spatial variability include (Cressie & Hawkins 1980; Deutsch & Journel 1998 and Srivastava & Parker 1989). The spatial bootstrap (Journel & Bitanov 2004; and Feyen & Caers 2006) for a single variable is an extension of the bootstrap (Efron & Tibshinari 1986) resampling technique that accounts for

spatial correlation follows as:

1. Fit a normal score variogram model
2. Define the representative distribution $F(z)$
3. Simulate a realization of the data at the data locations
4. Calculate the statistic of interest from the resampled data, the experimental mean m_{sz} and variance from the realized vector z
5. Return to step 2 and repeat many times, say, $L = 1000$)
6. Assemble the distribution of uncertainty in the calculated statistic

2.6.1 Multivariate Spatial Bootstrap (MVSB)

In this thesis study, a multivariate workflow is applied for the parameter uncertainty. This new multivariate spatial bootstrap resampling (MVSB) method developed by Khan & Deutsch (2015) accounts for measuring the uncertainty in distributions in the context of a multivariate workflow. The general approach of the multivariate resampling workflow is:

- Sample correlation matrix $\mathbf{R}$ with elements ρ_{ij}, $i = 1...k$; $j = 1...k$
- Corresponding variogram models $\gamma_{zk}(\mathbf{h}) = C_{zk}(0) - C_{zk}(\mathbf{h})$ where $(\mathbf{h})$ is the lag vector
- Cumulative distributions functions $F_{zk}(z_k)$ and their summary means μ_{zk} and variances δ^2_{zk}

The applied multivariate workflow accounts for the prior parameter uncertainty coming from the multivariate spatial bootstrap resampling that is transferred to posterior distributions by conditioning data and clipping by domain boundaries. The applied approach provides realistic assessment of the uncertainty in parameters. The two programs *spatial bootstrap_ mv* and *parunce* may be used to implement the parameter uncertainty, see Khan & Deutsch (2015) and Rezvandehy et al., (2015). The

first program accounts for prior and second program uses for posterior uncertainty, respectively.

2.6.2 Principal Component Analysis (PCA)

Uncertainty in the correlation matrix is important because correlation coefficients quantify the relationships between variables. If the data deemed to be non-Gaussian then additional steps should be taken to understand the relationships (Deutsch & Deutsch 2011). Simulation methods for individual variables are frequently efficient (Lopes, Rosas, Fernandes, & Vanzela 2011); however, in many applications reproduction of the spatial dependence and joint simulation for multiple variables is critical. A variety of joint simulation methods for multivariable deposits can be applied. Over the years, practical and efficient co-simulation methods have been proposed and improved by many authors. The joint simulation based on the decorrelation of variables using principal component analysis (PCA) was introduced back in the 1980s. PCA is used abundantly in all forms of analysis because of its simplicity and utility in extracting relevant information from complex sets of data. Many variables can be reduced to a lower dimension.

2.6.3 Sphere-R Transformation

Barnett & Deutsch (2015) summarize the sphering and rotating of the factors from principal component analysis (PCA-R) that makes the results easier to understand compared to other co-simulation techniques including classical PCA. The PCA-R is used for effective geostatistical modeling. The theory behind the PCA-R is that matrices $\mathbf{A}$ are represented in terms of eigenvalues λ and eigenvectors υ. Then taking matrix $\mathbf{A}$ and rewriting in terms of sum of eigenvectors and eigenvalues, we have the following:

$$\mathbf{A}_{n\times n} = \sum_{i}^{n} \lambda_i \left[\frac{\mathbf{U}_i \times \mathbf{V}_i^T}{\mathbf{V}_i^T \times \mathbf{U}_i} \right] = \mathbf{P}_i \tag{2.1}$$

Where $\mathbf{P}_i$ is the eigenvector projection matrix, and the $\mathbf{U}_i$ and $\mathbf{V}_i$ are eigenvectors. Then rewriting the Equation 3.1, the eigenvector projection matrix will have the following form:

$$\mathbf{P}_i = \frac{[\mathbf{U}_i \times \mathbf{V}_i^T]}{(\mathbf{V}_i^T \times \mathbf{U}_i)} \tag{2.2}$$

By combining the Equation 3.1 and Equation 3.2 results the sphere principal component analysis (PCA-R), such as:

$$\mathbf{A}_{n\times n} = \sum_{i}^{n} \lambda_i \mathbf{P}_i$$

The multivariate data are passed through the PCA-R with an assumption that we know spatial and statistical relationships between the data, then decorrelated variables back onto the basis of the original variables. This is achieved by multiplying the transpose of the eigenvectors $\mathbf{U}_i$ and $\mathbf{V}_i$ to rotate the sphere variables back to the original basis where (1) variables are uncorrelated and variances are standardized; (2) the loading properties is not appropriate for a dimension reduction scheme is not considered; and (3) spatial continuity of original variables are likely preserved (Barnett & Deutsch 2015). Due to the the additional steps illustrated earlier, the mixing of loadings is minimized between the variables. By doing this, original variables will be resulted with higher probabilities for their spatial structure reproduced by modeling. For multivariate analysis of data including decorrelation of the variables being modeled, any of the co-simulaiton techniques [PCAs, MAF, LMC, etc] could also be considered for multivariate analysis of data.

The *Decorrelate* and *LoadingPlot* programs are can be implemented for multivariate analysis of data and demonstrate the sphere-R transformation (Barnett & Deutsch 2015). The authors also explain the program, which implements both conventional and sphere-R PCAs. Sources on a variety of co-simulation techniques include (Smith (2002); Barnett & Deutsch 2015; and Shlens 2005, 2014). The use of

the PCA-R technique will be demonstrated in case studies.

2.6.4 Implementation of the Parameter Uncertainty

Incorporation of parameter uncertainty in resource modeling is important. There are many existing approaches to quantify parameter uncertainty. This study uses the prior uncertainty and posterior uncertainty approach documented in (Khan & Deutsch 2015 and Rezvandehy et al., 2015). The prior parameter uncertainty is estimated from multivariate spatial resampling (MVSB) technique. The posterior uncertainty results from transferring and updating with the conditioning data and domain limits, see Rezvandehy et al., (2015). These techniques are used together to quantify the uncertainty in a multivariate context for large scale models.

A multivariate workflow defines prior parameter uncertainty; and then posterior distributions result from transferring the prior uncertainty updated by conditioning data. The parameter uncertainty framework starts off by checking the bivariate relationships and correlation matrix of the K variables (Deutsch & Deutsch 2011). The probability density function of each variable with a bivariate standard normal distribution is parameterized by correlation coefficient and presented for visual inspection. These contours are important in visualizing, inspecting, and detecting outliers of the individual scatterplots as it shows if the variables are bivariate Gaussian or not. Figure 2.9 shows illustration of bivariate plots and correlation coefficients between the five variables of the *Red* data. From the correlation plot, it can be seen that the variables are correlated. The highest correlation is between the copper (Cu) and gold (Au) grades. With few data points only extreme departures from bivariate normality can be detected with reasonable assurance (Johnson & Wichern 2002). The check becomes less powerful when there is a limited number of data being checked for Gaussianity. In this workflow, there is no need to reject any of the bivariate distribution as nonGaussian.

In practice, we require the prior distributions of the global statistics in the original units of the variables (Khan & Deutsch 2015). The prior distributions are first defined for the normal scores of each variable. The prior distributions of the global

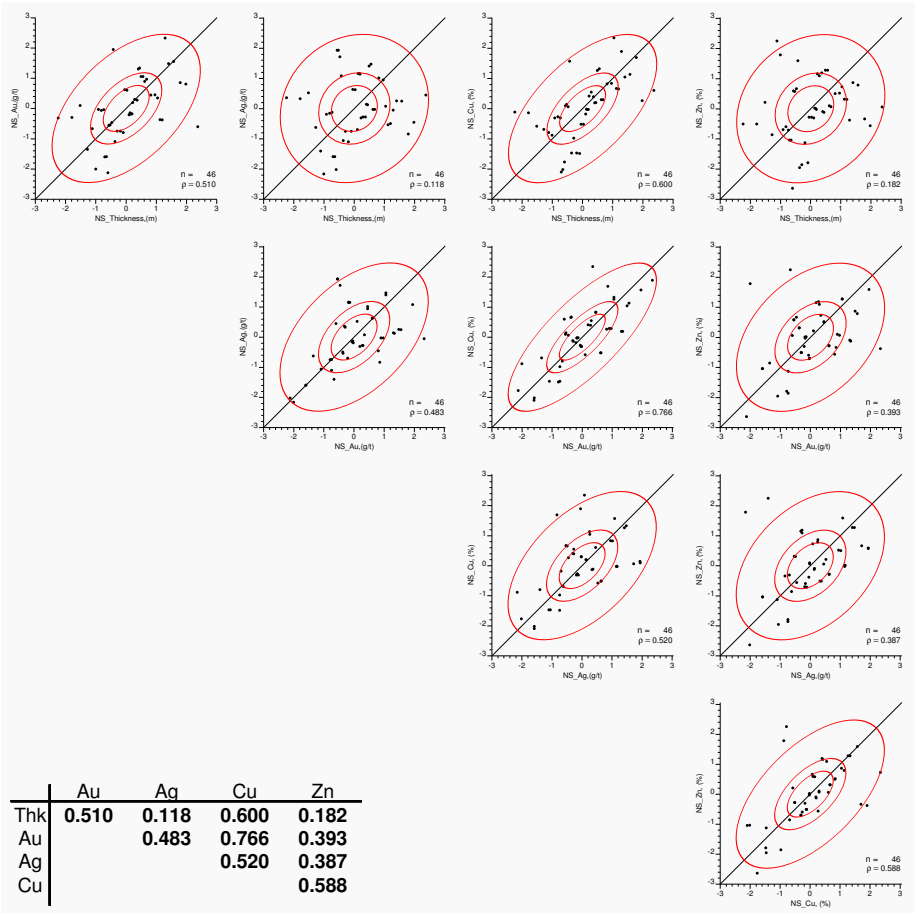

	Au	Ag	Cu	Zn
Thk	**0.510**	**0.118**	**0.600**	**0.182**
Au		**0.483**	**0.766**	**0.393**
Ag			**0.520**	**0.387**
Cu				**0.588**

Figure 2.9: Bivariare relationships and correlation matrix between the five variables of the *Red* data.

statistics of the mean and variance for each variable in original units are obtained. This is shown in Figure 2.10. These results in original units are used to transfer the prior uncertainty and update to the posterior uncertainty. The full context of this data will be explained in the next chapter.

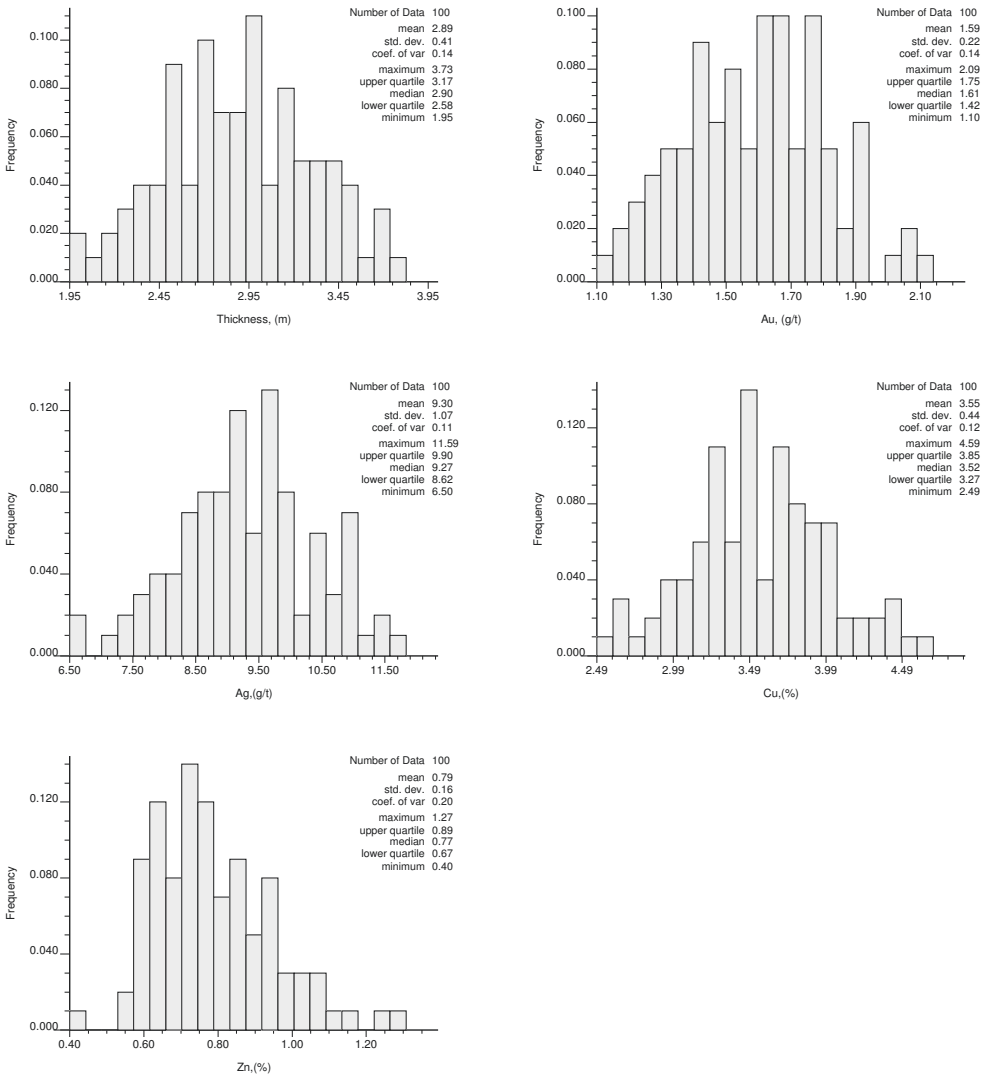

Figure 2.10: Prior distributions of the mean in original space of each variable from multivariate resampling technique from the *Red* data.

Each set of the prior distributions from the multivariate spatial resampling is correlated through a realization of the multivariate correlation matrix (Figure 2.9). That is, each set of prior distributions from the resampling honors the realizations of the correlation matrix. The distributions of the simulated correlated coefficients between the variables are shown in Figure 2.11. Some important considerations in the parameter uncertainty include (1) uncertainty in each input parameter is transferred through the prior sampling distributions of the mean, (2) the prior parameter

uncertainty is an important aspect because it uses to narrow the uncertainty in a model through data conditioning and clipping to an area of interest, and (3) the multivariate workflow is straightforward in terms of executing without any specialized algorithms other than a multivariate spatial bootstrap resampling.

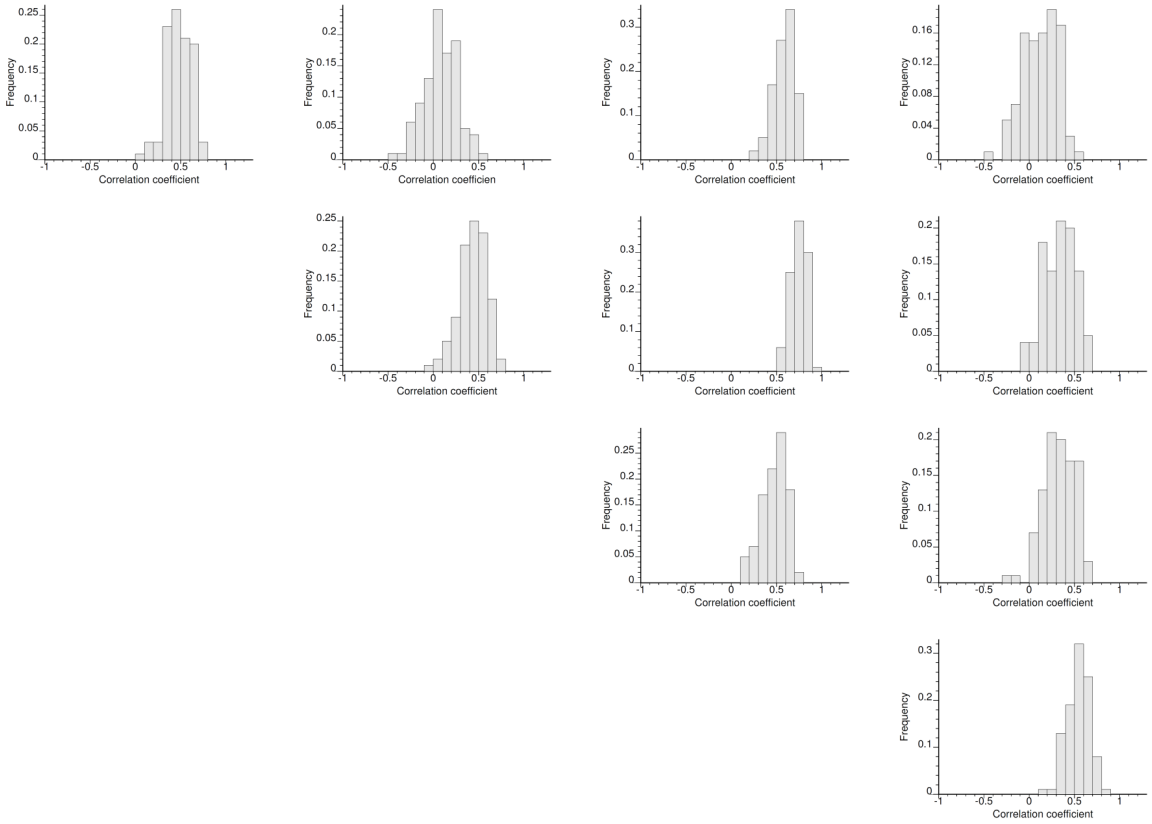

Figure 2.11: Realizations of sample correlation coefficients between variables obtained through multivariate spatial resampling of the *Red* data.

Figure 2.12 shows posterior distributions of the mean in the original space after clipping to the area of interest.

A simple way of quantifying the uncertainty in experimental variograms is demonstrated. Variogram uncertainty has been studied in a number of different contexts. For example, Webster & Oliver (1992) measured the uncertainty from different samplings and then determined whether these sampling were suitable for estimation or not. Other authors Bogaert & Russo (1999) proposed a technique on minimizing

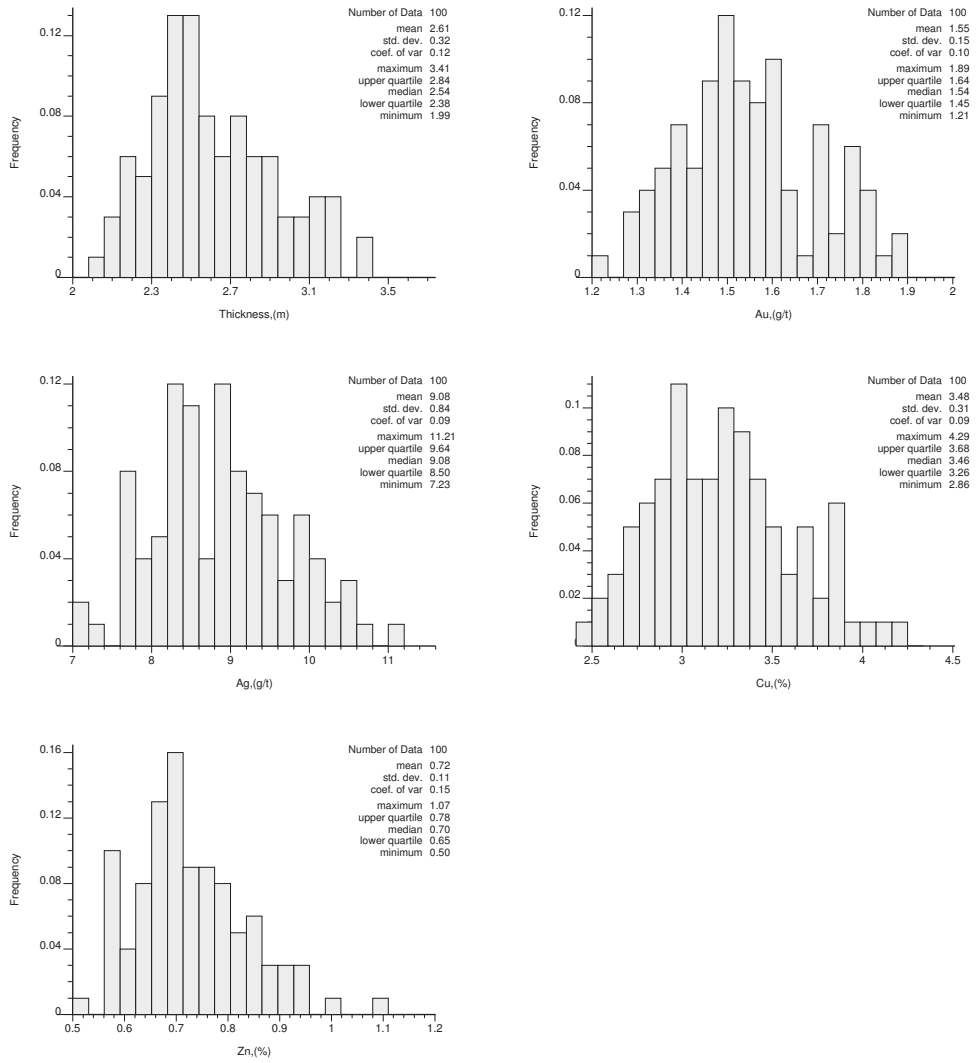

Figure 2.12: Posterior mean for each variable after clipping to the area of interest from the *Red* data.

the values of a theoretical expression of variogram uncertainty by positioning points and using sample schemes.

This study used the analytical method for assessing the uncertainty in the variogram proposed by Ortiz & Deutsch (2002). This method is based on estimating the uncertainty in the semivariogram directly from the data. The experimental variograms could be very noisy or redundant because of limited data, so choice of the final model will not be precise. In this case, it is possible to address this issue and

construct possible distributions of the variogram model ranges. The illustration of the uncertainty in experimental semivariogram using a fitted model with possible two scenarios for the variogram range is shown in Figure 2.13.

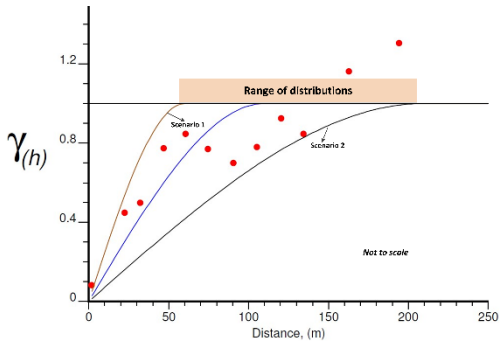

Figure 2.13: Illustration of the uncertainty in experimental semivariogram using the analytical method with possible scenarios for the variogram range.

To sample the uncertainty in the variogram range, random numbers $r \sim U(0,1)$ are drawn and then considered in the following equation:

$$a_i = a_{i,min} + r \times (a_{i,max} - a_{i,min}) \tag{2.3}$$

Where $a_{i,min}$-is the minimum base case variogram range distribution,i-is the number of variables ($i = 1...n$), r- is the random number $r \sim U(0,1)$, and $a_{i,max}$ - is the maximum base case variogram range distribution for a given variable. Figure 2.14 shows an illustrative example of different possible scenarios for the experimental variograms ranges derived from the analytical method where experimental semivariogram is shown in red dots with three possible semivariogram models.

By random sampling for each variable and using the equation above, new sets of variogram model ranges are defined.

The proposed method for the variogram uncertainty relies upon various statistical assumptions. Readers are referred to sources on the variogram uncertainty (Deutsch & Journel 1998; Ortiz & Deutsch 2002; and Koushavand & Deutsch 2008).

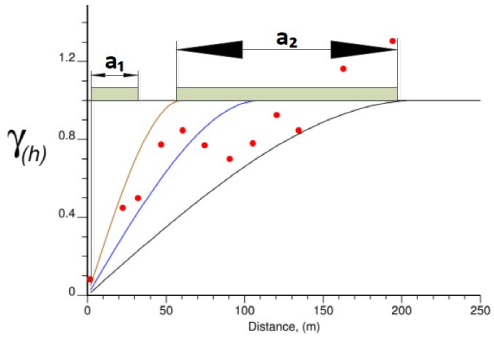

Figure 2.14: Uncertainty in the variogram. The experimental semivariogram (red dots) and three possible semivarigoram models.

2.7 Post Processing

Post processing involves evaluating realizations and computing response variables of interest. This includes uncertainty calculation and sensitivity analysis in order to understand the impact of each input parameter and help in further decision making.

2.7.1 Presenting and Understanding Uncertainty

Uncertainty can be communicated in a variety of ways. It is also necessary to define measures of uncertainty. The measures described herein have been found to be useful in a geostatistical context and include standard deviation, coefficient of variation, difference between specific percentiles, precision, and probability of misclassification. Some conventional ways of displaying and visualizing the uncertainty include summary statistics like the mean, or median, or standard deviation. Different probability p-intervals can also be applied to present the uncertainty. The probability that the unknown is valued within an interval (a,b) is calculated as the difference between the CDF values for thresholds band (Duggan & Dimitrakopoulos 2005):

$$\text{Prob}\left\{Z(\mathbf{u}) \in (a,b)\right\} = [F(\mathbf{u};b) - F(\mathbf{u};a)]$$

Other ways of presenting and understanding uncertainty may include in the form of a graphical presentation of obtained results such as grade-tonnage curves and

histograms. Grade tonnage curves are used for understanding the effect that different cutoff grades have on the number of tonnes in the deposit. If the deposit contains more than one metal of economic value, then calculation of the grade tonnage should be based on a metal equivalent relationship by comparing with different metal ratios.

2.7.2 Sensitivity Analysis

The goal of sensitivity analysis is to characterize how model outputs respond to changes in input with an emphasis on finding the input parameters to which outputs are the most sensitive (Saltelli et al., 2000 and Kennedy & O'Hagan 2001). A sensitivity analysis aims to assess the importance of different input parameters. Although uncertainty in each factor can be directly assessed, it is useful to quantify the importance and impact of each predictor variable in the response (Pinto & Deutsch 2014). The response variable is a resource or reserve measure and the predictor variables are factor that have some influence on the uncertainty. Linear or quadratic regression could be applied. The selection of the analysis methods depends on experiences, preferences, and the goals of the sensitivity analysis. In most cases, the results will be presented in a form of a tornado chart with the importance of the input parameters shown by the horizontal width. A non-parametric way of analyzing the sensitivity between the response and predictor variables includes alternating conditional expectation (ACE). Readers are referred to Zagayevskiy & Deutsch (2011) and Barnett & Deutsch (2013 a,b) for more information and discussion on these techniques.

2.7.3 Implementation of Post Processing

Post processing involves evaluating every realization for all calculations of interest. The correct approach to perform post processing is to use all realizations all the time and then distributions of the response variables of interest can be assembled by summarizing their outcomes. Resource uncertainty is calculated for all response variables in order to understand the uncertainty. The uncertainty in each response variable is calculated by considering all realizations. The expected response variables are obtained as an average of the responses.

The number of response variables depends on the data and the goals of resource modeling. However, as a common practice, some major response variables include the amount of ore, grade value, and quantity of metal. Equivalent grades are calculated based on the recovery and/or price for each variable and the minor metal(s) is/are converted and added to the grade of the major metal(s). Post processing is implemented with two different case studies in the following chapters where different data is used and a sensitivity analysis is performed. Some main graphical plots for summarizing the results from the sensitivity analysis include the tornado chart and others (Welch et al., (1992) and Deutsch et al., 2002).

2.8 Recommendations

In order to meet the goals under the modeling constraints, a clearly established conceptual theoretical workflow is recommended. Important uncertainties coming from different input parameters can be transferred through modeling by performing multiple scenarios for model of uncertainty. With the establishment of the conceptual basis the modeling algorithms can be applied to assess the uncertainty within the framework. In this case, all the best modeling options/practices must be evaluated in terms of ease of use, computational expense, and reliability of the final models.

2.8.1 A Common Format

There are many different models and realizations in a multivariate context. It is important to have a common format to ensure that the modeling processes are convenient and practical. Therefore, formats should be in a standardized form. In this thesis study, the open source GSLIB format is used throughout the modeling process as the standardized common format. When it is necessary this format is extended to other formats to read and write out the results, and demonstrate the implemented methods and outputs. These include, but is not limited to FORTRAN, Python, and MATLAB. These modules are helpful in implementing the modeling workflows and give some flexibility to a practitioner for transferring functions, methods, and

analyzing the results regardless of the selected method.

2.8.2 Complicating Factors

Dealing with the uncertainty in the model is an important factor. We can only assess the uncertainty in a model that we can imagine. Geological continuity is another complicating factor. It is difficult to sample, if the data are limited due to uneven continuity in the modeling area. Other complicating factors includes uncertainty in the data where this uncertainty must be considered in the model. In order to avoid some complexities at any stage of a modeling process, therefore, it is critical that uncertainty is considered explicitly early in the definition phase of a resource modeling.

2.9 Conclusions

Well-established theoretical concepts for resource modeling with uncertainty are important. This serves as a base framework to provide a practitioner with established workflows, methods, and uncertainty models to treat the uncertainty systematically throughout the modeling process. Selection of the workflows, however, should be based on each specific case. Complex geological processes and settings, prior experiences, and preferences are key factors in selecting suitable models of uncertainty. The selected models should give a flexibility in terms of ease of use, robustness, and practical computational expense. In order to account for different types of uncertainties coming from input parameters, more than one resource model may be considered throughout the modeling process with the goal of providing a range of possibilities to evaluate different scenarios for uncertainty with confidence and provide valuable decision support information.

In addition, unit operations to assess the uncertainty in input parameters vary. All available models should be based on prior experience, preference, and company policy. In this thesis study, developed theoretical workflow is used and implemented unit operations based on best practices by analyzing the existing techniques that are

properly conditioned to input parameters. Ideally, implemented methods/models should provide reasonable outputs of uncertainty assessment, and fully characterize the uncertainty in the modeling. This include adequate and reliable methods and contribution of each output of an uncertainty model.

A small change in any stage of a modeling process may have an impact on a final model of uncertainty. Uncertainty modeling at large scales can be problematic. Uncertainty in boundary surfaces is interpolated and mapped by applying efficient boundary modeling methods described above coming from by Munroe & Deutsch (2008, a,b) and Wilde & Deutsch (2011). Uncertainty in input parameters is quantified and captured (Khan & Deutsch (2015) and Rezvandehy et al., (2015)).

Chapter 3

Case Study: *Red* Data Set

This chapter shows a case study based on the *Red* Data set that was made available to the Mine Design project class at the University of Alberta. The objective of this case study is to assess and quantify the uncertainty in a resource model using the developed modeling practices. Section 3.1 provides information on the available data and an overview of the mineral deposit. Section 3.2 presents the exploratory data analysis (EDA) of the data; Section 3.3 demonstrates the geostatistical models used in assessing and quantifying the uncertainty; Section 3.4 includes post processing and resources uncertainty calculation; and finally, Section 3.5 provides conclusions.

3.1 Overview of the Geology and Available Data

The mineral deposit is a tabular, well-defined and steeply dipping zone of mineralization that strikes North-South. The main economic metal is gold, but there is also some silver, copper, and zinc. There are 67 drillhole intersections where the thickness of the deposit and the four grades have been measured. The case study considers all five variables over the plane of vein areas shown in Figure 3.1. The Northing coordinate shown on the horizontal axis is along strike. The Elevation coordinate shown on the vertical axis is down dip.

Figure 3.1 shows the location of the five variables colored between their minimum and maximum values. Table 3.1 shows an initial summary of the data.

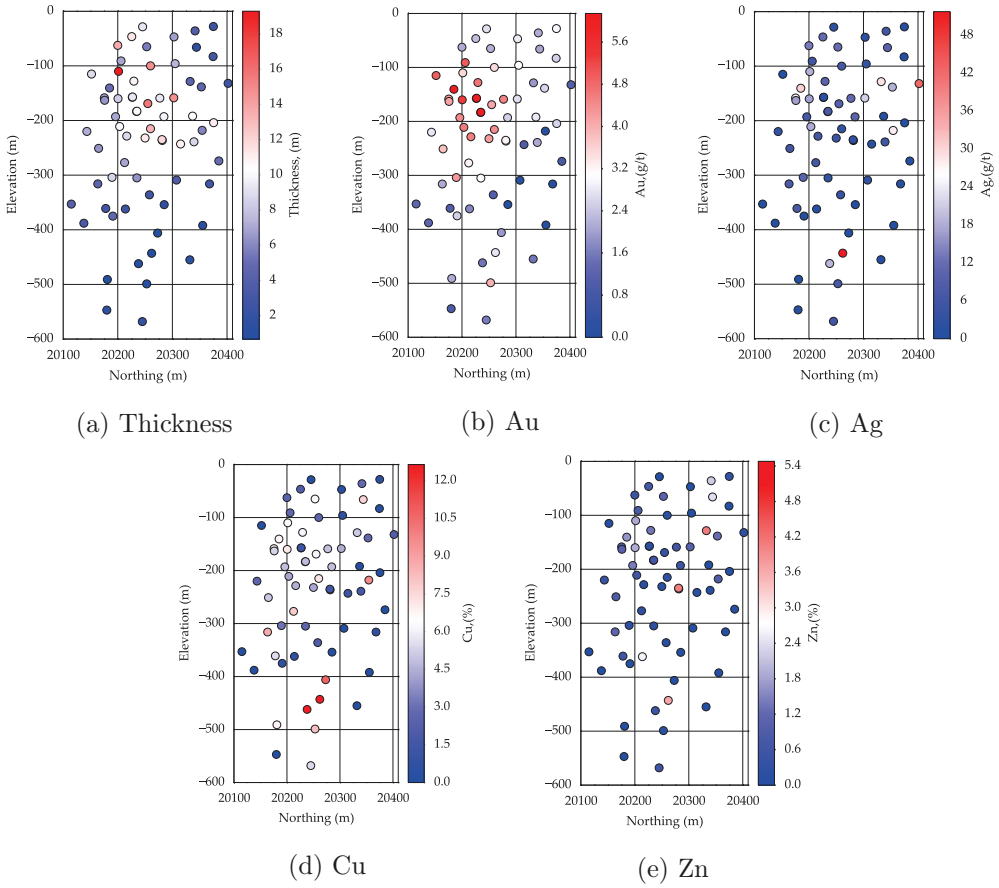

(a) Thickness (b) Au (c) Ag

(d) Cu (e) Zn

Figure 3.1: Locations maps of the five variables used in resource modeling.

There is no need to ignore a sample containing zero values because at same drillhole location other grade values might also be sampled with non-zero values, especially in deposits with steeply dipping zoning mineralization that may contain more than one economic metals. Therefore, all samples at all locations are used in this study. However, if given data contain non-zero null values then, there is a need to perform a data imputation because samples are taken at specific locations would have some other value. Including to analysis of data, some sort of criteria for below detection may also be useful and/or carefully reviewing the unprocessed data, if available.

Parameter	Units	Count	Minimum	Maximum
Thickness	m	67	0.67	19.3
Au	g/t	67	0	6.14
Ag	g/t	67	0	51.8
Cu	%	67	0	12.6
Zn	%	67	0	5.48

Table 3.1: Summary of the data set used for the resource estimation.

3.2 Exploratory Data Analysis

The exploratory data analysis (EDA) is an important aspect of geostatistical modeling. There are no strict requirements for performing EDA. Histograms for the given data are plotted on Figure 3.2 for all variables.

As data are rarely collected randomly and are spatially clustered in areas that are of greatest interest, there is a need to adjust the histograms and summary statistics to be representative of the entire volume of interest. Cell declustering is used for this purpose. Readers are referred Deutsch (2002) for more information on cell declustering. A cell declustering with cell size of 80 m is applied, since it approximately corresponds to an underlying regular grid of drilling. Table 3.2 illustrates summary comparison table between simple and declustered summary statistics.

Parameter	Units	Original mean	Declustered Mean	Difference (%)
Thickness	m	6.65	5.34	-19.7
Au	g/t	2.87	2.39	-16.7
Ag	g/t	8.61	7.44	-13.6
Cu	%	3.64	3.20	-12.1
Zn	%	0.78	0.60	-19.2

Table 3.2: Summary comparison table between simple and declustered histograms

The data were normal score transformed in preparation for the Gaussian simulation techniques. The bivariate relationships between the normal score transformed variables are examined by plotting correlation coefficients and the bivariate relationships between all pairs of variables, see Figure 3.3. The strongest correlation can be seen between silver (Ag) and copper (Cu), as well as silver (Ag) and zinc (Zn) grade values. The cross-plots appear reasonably Gaussian; there are too few data to

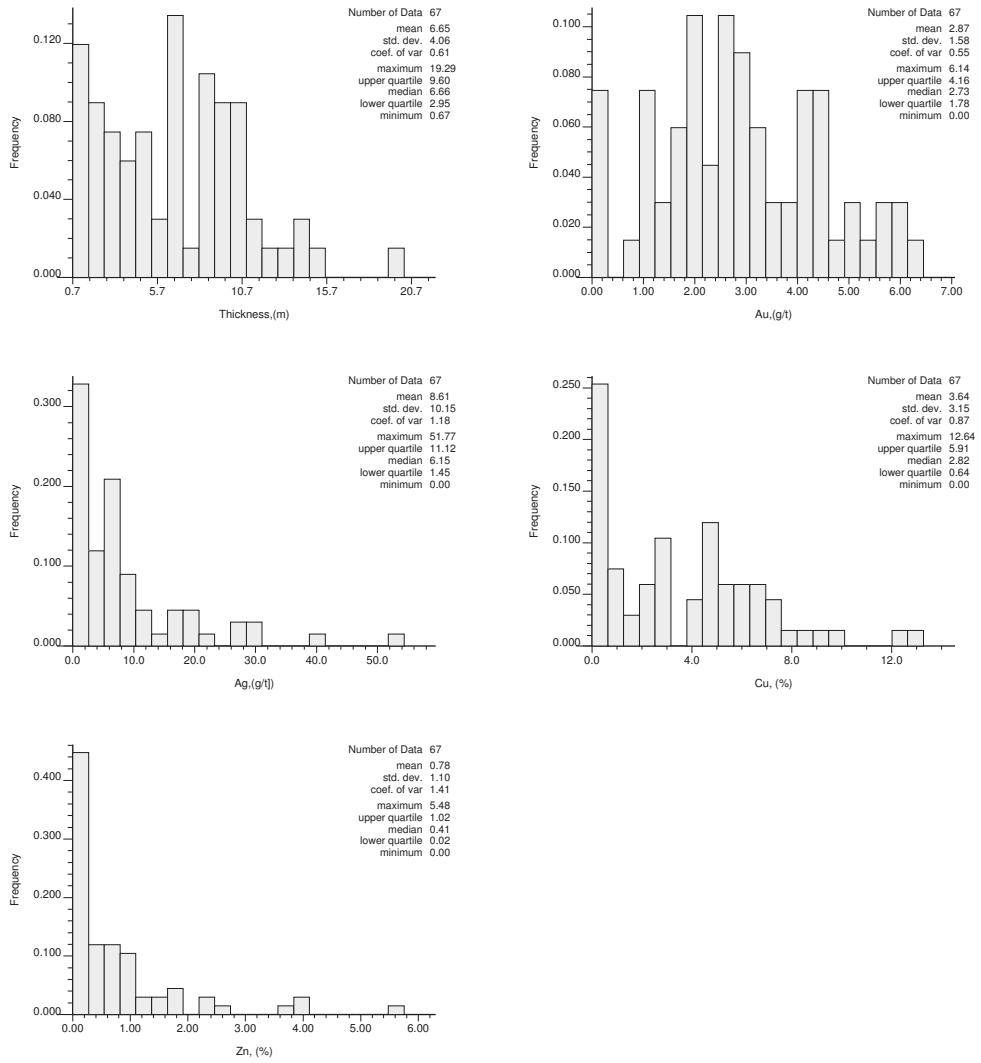

Figure 3.2: Histograms of the five variables used in resource modeling for the *Red* data.

reliably compute quantitative measures of Gaussianity.

As a result of limited data, there is uncertainty in the variograms that should be taken into account in resource estimation. The goal is to describe and represent the experimental variogram results as accurately as possible. Omnidirectional experimental variograms are calculated in original units and normal score (Gaussian) data and fitted with spherical type variogram models. Nugget effect of 20% is considered for copper (Cu) and zinc (Zn), and a nugget effect of 12% for silver—(Ag) grade, and no nugget effect for thickness and gold (Au). The illustrations of the original

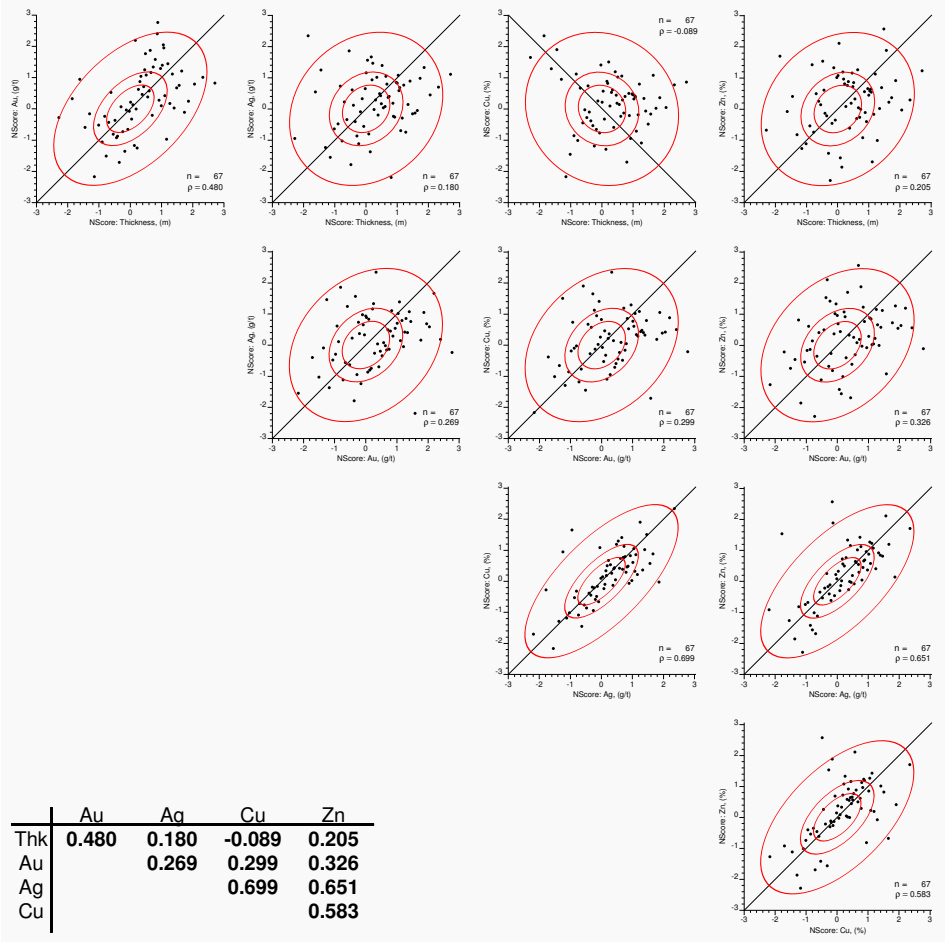

	Au	Ag	Cu	Zn
Thk	**0.480**	**0.180**	**-0.089**	**0.205**
Au		**0.269**	**0.299**	**0.326**
Ag			**0.699**	**0.651**
Cu				**0.583**

Figure 3.3: Bivariare relationships and correlation matrix between the five variables.

unit variograms for the five variables are shown in Figure 3.4. The normal score variograms are illustrated in Figure 3.5.

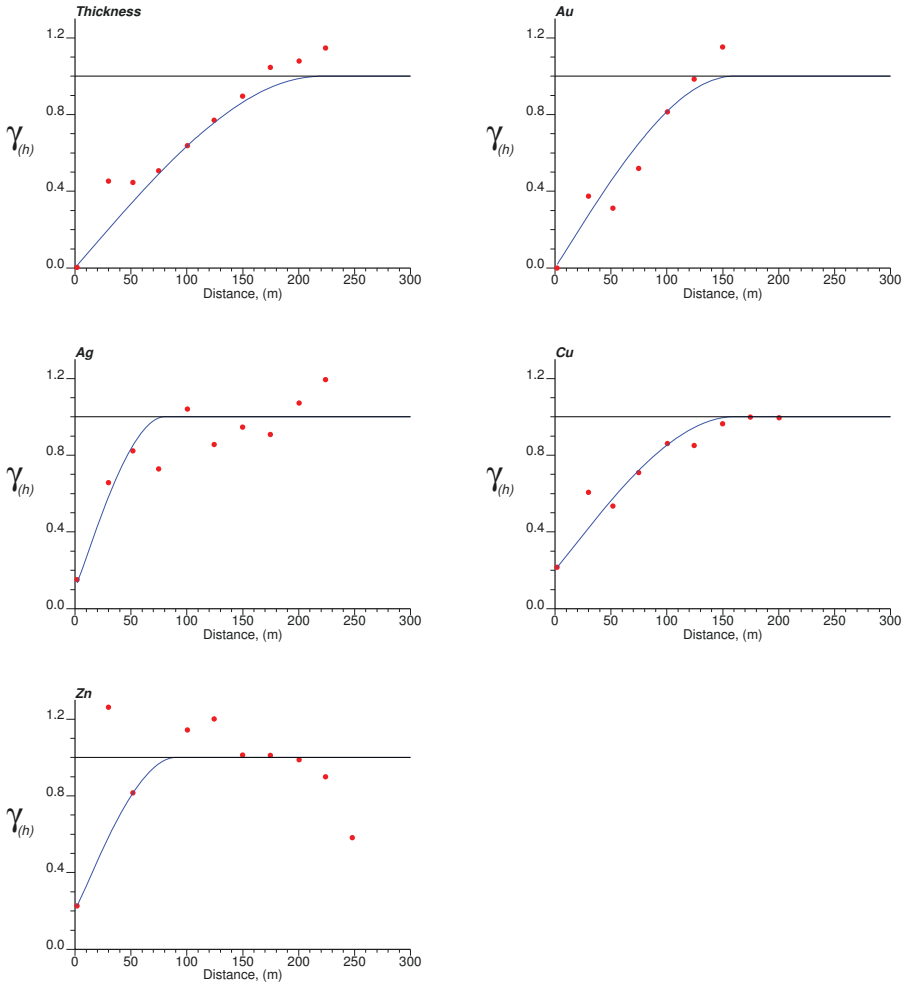

Figure 3.4: Illustration of original unit variograms for the five variables. The distance units are in meters and the variable units are in units of variance for the variable type.

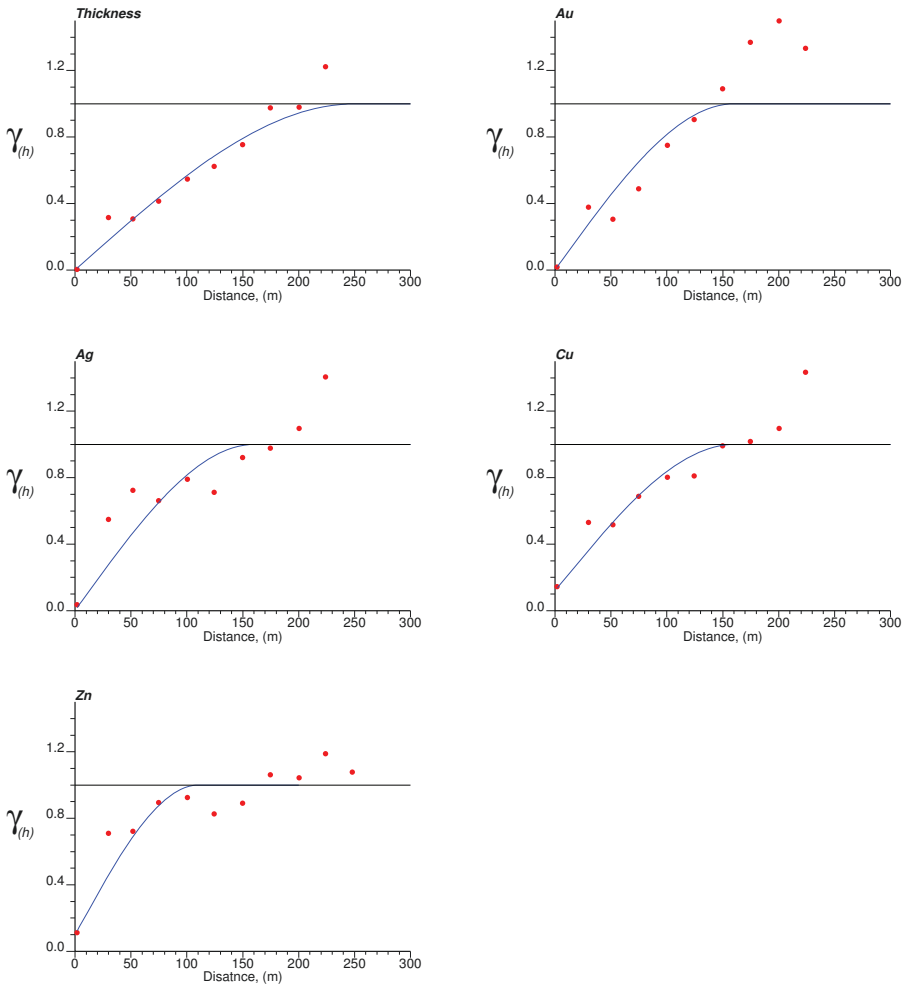

Figure 3.5: Illustration of normal score variograms for the five variables. The distance units are in meters and the variables units are standardized in normal score transform.

3.3 Geostatisitical Modeling

Geostatistical modeling is performed in the following order: (1) a distance function (DF) method is used for boundary modeling, Subsection 3.3.1; (2) distribution uncertainty is modeled with the multivariate spatial bootstrap (MVSB) technique, Subsection 3.3.2; (3) data uncertainty is demonstrated in Subsection 3.3.3; (4) and finally, consideration to be a processing and resources uncertainty calculation are documented in Subsection 3.3.4.

3.3.1 Boundary Modeling

Boundary modeling starts with distance function values calculation. The GSLIB-like program *DFcalc* calculates the distance function. The calculated distance function values depend on whether drillholes are located inside (-DF) or outside (+DF) the domain. The procedure of calculating and interpreting the distance function values is provided in Chapter 2. In general, boundary uncertainty modeling follows: (1) a distance function (DF) calculation and assigning control points, (2) mapping the distance function values, and (3) calibrating and applying the thresholds to the band of uncertainty.

An illustration of the DF calculation is demonstrated in Chapter 2. There are samples coded inside (red) and outside (blue) the domain. The distance to the nearest outside sample is calculated for each sample located inside/outside the domain. 47 of the 67 drillholes are considered to be inside the modeling domain. Figure 2.7 (a) shows the 46 drillholes that are considered inside. The samples that are coded outside considered as control points to define the boundary. Samples that are coded outside the domain are assigned a positive and samples that are coded inside the domain are assigned a negative distance function. The illustrative figure of the control points shows drillholes with black dots indicating an orebody and and blue area with white dots showing a waste see Figure 2.7 (b). There is a need for another exploratory data analysis (EDA) with the data considered to be inside the orebody. The procedure demonstrated in Section 3.2 is followed. Table 3.3 shows summary for 46 data considered to be inside the orebody.

Parameter	Unit	Count	Minimum	Maximum
Thickness	m	46	0.4	18.9
Au	g/t	46	0	4.5
Ag	g/t	46	0	30.4
Cu	%	46	0.02	9.1
Zn	%	46	0	5.5

Table 3.3: Summary of the 46 data used in the study.

Table 3.4 summarizes the original and declustered means of all variables. In the following steps of the workflow, the 46 drillholes considered inside the orebody are used, where the other 21 drillholes are not considered in the study.

Parameter	Unit	Original mean	Declustered Mean	Difference (%)
Thickness	m	4.3	3.5	-17.8
Au	g/t	1.7	1.3	-22.5
Ag	g/t	9.3	8.6	-7.6
Cu	%	3.4	3.1	-19
Zn	%	0.9	0.8	-13

Table 3.4: Summary comparison table between simple and declustered histograms with 46 data considered inside orebody

In the next step of boundary modeling, an additive factor C, modifies the distance function values, Wilde & Deutsch (2011). C is subtracted from distance function values that are inside and added to values that are outside. The C parameter at 0m and 30m is shown below, as well as selection of the C parameter is provided in Chapter 2.

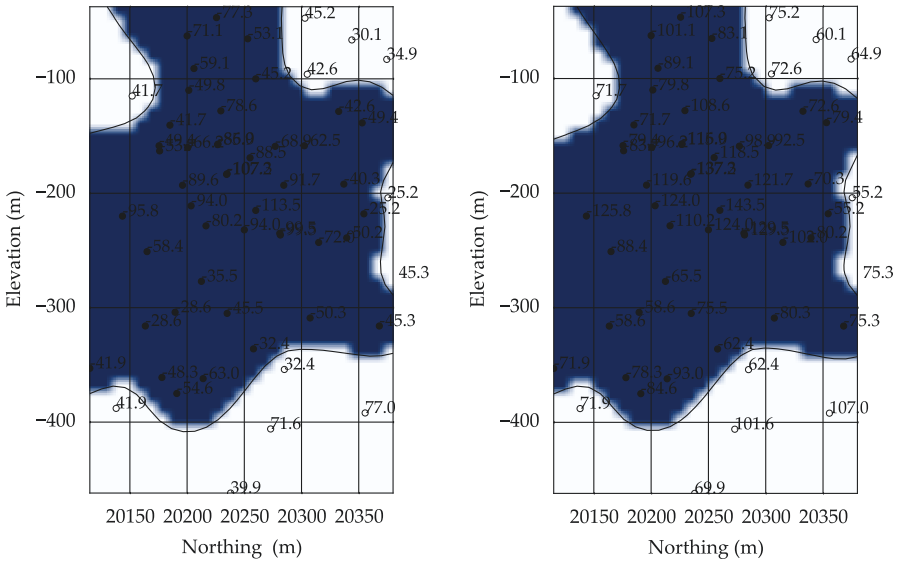

(a) C=0m (b) C=30m

Figure 3.6: DF calculated at each sample location and interpolated with C=0m and C=30m. Blue color indicates inside while white color shows outside domain. The units of the DF calculated values are in meters.

As C increases, the size of the boundary uncertainty region increases. There are a variety of ways to select the C parameter (Subsection 2.4.3, Chapter 2). In this case study, the C parameter is chosen to be 30m based on data spacing and expert judgment. A threshold of (C=0) gives a base case, near (-C) value the threshold is eroded (small everywhere) and choosing a threshold near (+C) is dilated (big everywhere). Once the limits are defined then we calculate a distribution of uncertainty in the area is calculated assuming that the threshold is uniform between -C and +C. Figure 3.7 illustrates the histogram of the calculated distribution areas. Figure 3.8 illustrates the uncertainty bandwidth for C=30m. Table 3.5 shows summary corresponding values. Figure 3.9 demonstrates illustration of different probability interval values *p10*, *p30*, *p50*, *p70* and *p90*. Figure 3.10 summarizes the calculated distribution areas between -30m to +30m.

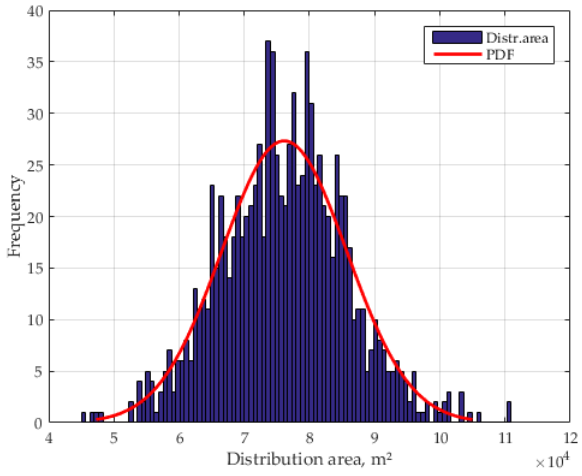

Figure 3.7: Distribution area uncertainty applied to the band between -30m to +30m. The units are in m^2

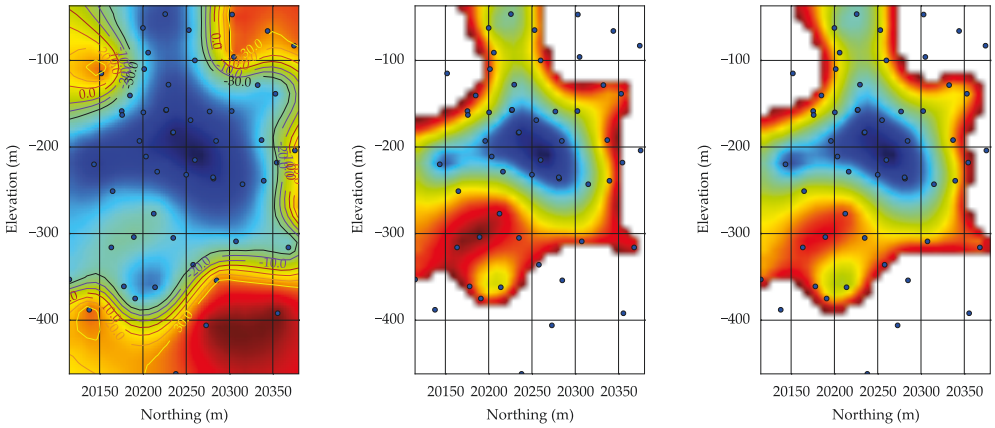

(a) SDF (b) C=-30m (c) C=-20m

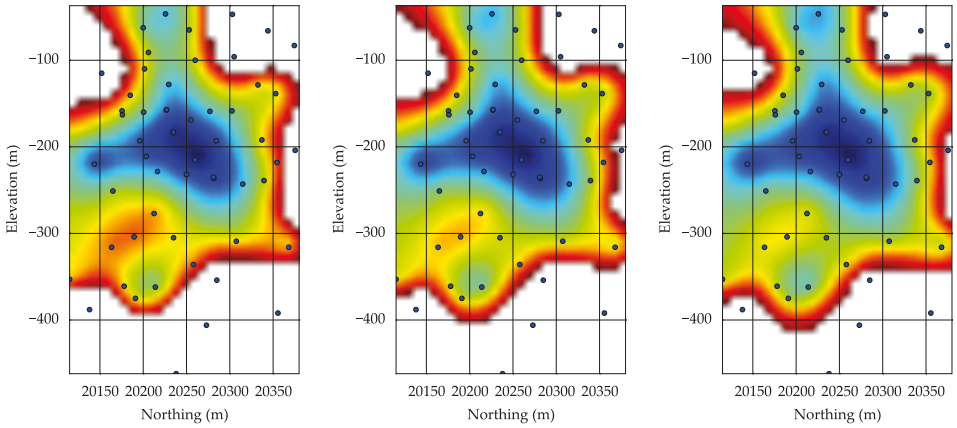

(d) C=-10m (e) C=0m (f) C=10m

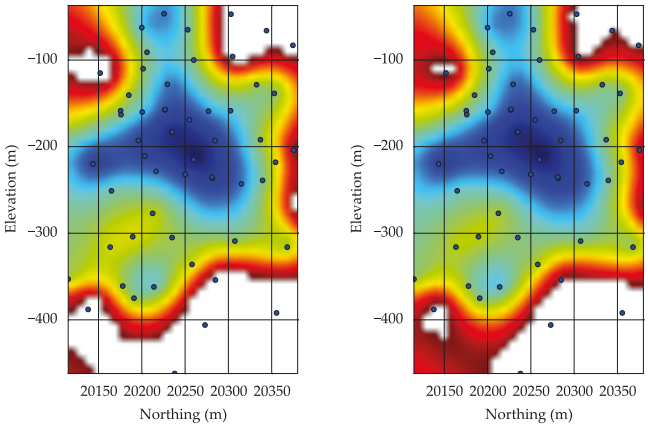

(g) C=20m (h) C=30m

Figure 3.8: Thresholds applied to different band between (-C) to (+C). The units are in meters.

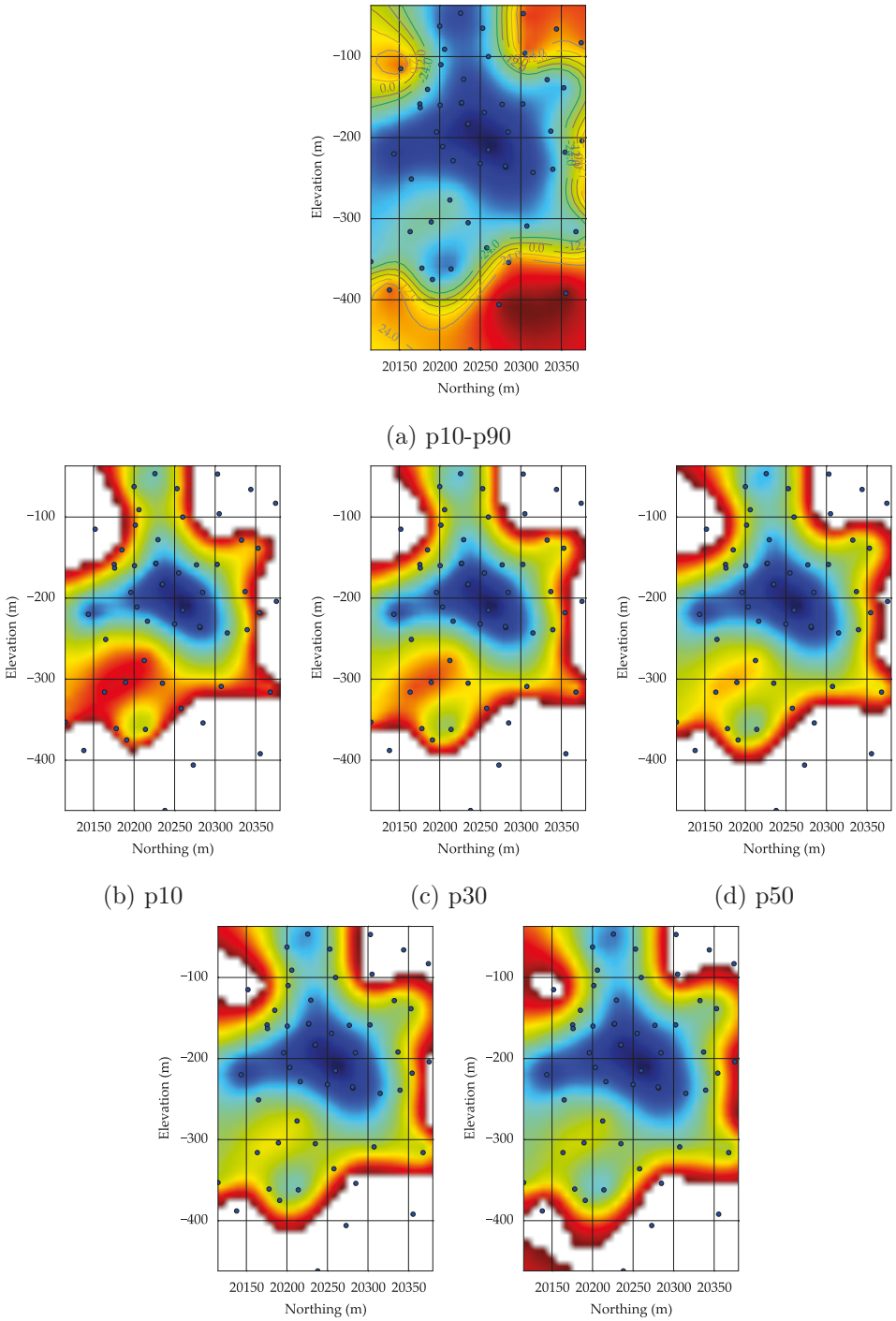

(a) p10-p90

(b) p10

(c) p30

(d) p50

(e) p70

(f) p90

Figure 3.9: Different probability intervals *p10*, *p30*, *p50*, *p70*, and *p90* applied between (-C) to (+C). The units are in meters.

Contour	Area, (m^2)	Contour	Area, (m^2)	Contour	Area, (m^2)
-30	59900	-9	71700	12	81800
-29	61100	-8	72400	13	82200
-28	62000	-7	72700	14	82900
-27	62700	-6	73300	15	83700
-26	63000	-5	73600	16	84200
-25	63500	-4	74000	17	84800
-24	63900	-3	74500	18	85200
-23	64400	-2	75000	19	86100
-22	64800	-1	75500	20	86800
-21	65200	0	76200	21	87300
-20	65800	1	76400	22	88000
-19	66600	2	77100	23	89000
-18	66900	3	77600	24	89400
-17	67700	4	78100	25	90400
-16	68100	5	78600	26	91200
-15	68700	6	79200	27	92900
-14	69300	7	79500	28	94100
-13	69500	8	80000	29	95000
-12	69800	9	80400	30	95500
-11	70400	10	80900		
-10	70900	11	81100		

Figure 3.10: Summary illustrative figure table of calculated distribution area for each band between chosen uncertainty bandwidth -30m to +30m. The units are in m^2

Corresponding p-values	Contour	Area, (m^2)
p10	-24	63900
p30	-12	69800
p50	0	76200
p70	12	81800
p90	24	89400

Table 3.5: Table of probability intervals *p10*, *p30*, *p50*, *p70*, and *p90* applied between (-C) to (+C).The units are in meters.

3.3.2 Parameter Uncertainty

A multivariate data analysis including principal component analysis, and the rotation transformation technique (Barnett & Deutsch 2015) is considered. The notion of the PCA-R is introduced in previous chapters. The PCA-R is applied to evaluate the given data in a multivariate context with one primary [thickness] and four [Au, Ag, Cu, and Zn] secondary variables with known spatial and statistical relationships. Scatterplots of the original data is shown in Figure 2.9. The primary variable is decorrelated using the sphere-R transformation technique. Due to reverse rotation, the correlation between the corresponding and output variables is maximized (Barnett & Deutsch 2015). This minimizes the required rotation to orthogonalize the variables, which leads to minimal mixing. Therefore, due to mixing effect observed in the loadings of the transformed variables, it is expected that the the sphere-R loads the decorrelated variables primarily onto their corresponding primary variable, see Figure 3.11.

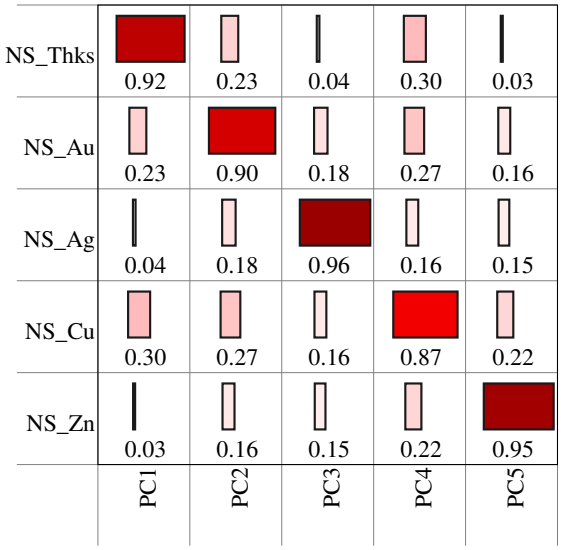

Figure 3.11: Loading plot with original vs. transformed variables.

The sphere-R variograms in Figure 3.12 overall close to original variograms due to rotation on associated axes which results in minimal mixing of the original variables. The mininal mixing is preferred in terms of geostatisitical modeling perspectives

since it can improve the probability where each variable will be reproduced. Figure 3.12 displays cross-variograms from the rotated variables.

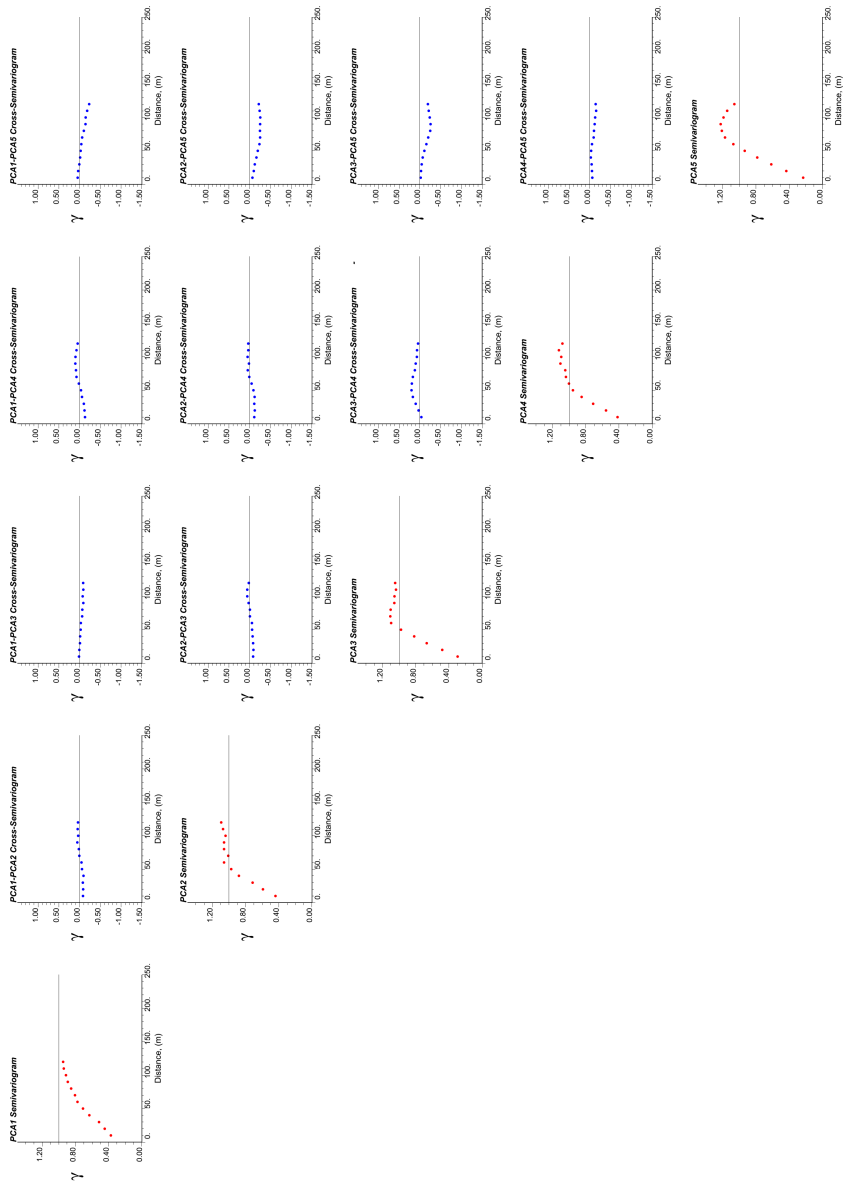

Figure 3.12: Direct and cross-variograms for the five transformed variables of the *Red* data.

The parameter uncertainty is calculated using the multivariate spatial bootstrap resampling (MVSB) workflow (Khan & Deutsch (2015) and Rezvandehy et al., (2015)). The notion of the multivariate spatial bootstrap resampling is introduced and discussed in Chapter 2. The uncertainty is estimated from the MVSB

sampling accounts for spatial correlation and the relationship between the variables. Consider Figure 2.9 showing the correlation matrix and bivariate relationships between the five variables. We are interested in the distribution of thickness as a response variable to the transfer of uncertainty in other four grade variables [Au, Ag, Cu, and Zn]. Each set of the prior distributions from the multivariate spatial resampling is correlated through a realization of the multivariate correlation matrix. That is, each set of prior distributions from the resampling honors the realizations of the correlation matrix. Realizations of sample correlation coefficients between the variables obtained through multivariate spatial resampling are shown in Figure 2.11.

The prior distributions of the mean simulated by MVSB technique in terms of normal scores transform first obtained of each variable of interest. These results are only shown with the purpose of tying back to the theoretical spatial resampling distributions. However, the main interest in this case study is the prior distributions of the global statistics in original units of the variables. The prior distributions of the global statistics of the mean and variance for each variable in original units are then obtained. These results in original units are used to transfer the prior uncertainty and update to the posterior uncertainty. These original space of the variables are used to transfer from prior parameter to the posterior parameter uncertainty. The prior distributions of the mean in original space of each variable from the MVSB technique is shown in Figure 2.10, Chapter 2.

In the next step, there is a need for transferring the prior parameter uncertainty to the posterior parameter uncertainty where the uncertainty is updated by conditioning and clipping by the boundary. This is documented by Rezvandehy et al., (2015). The posterior uncertainty accounts for: (1) conditioning data, (2) spatial correlation, and (3) area of interest. The idea of updating the prior uncertainty to the posterior uncertainty is to achieve realistic uncertainty distributions. The uncertainty for each variable is transferred through the prior sampling distributions of the global mean. Figure 3.13 shows the posterior mean for each variable after clipping to the area of interest.

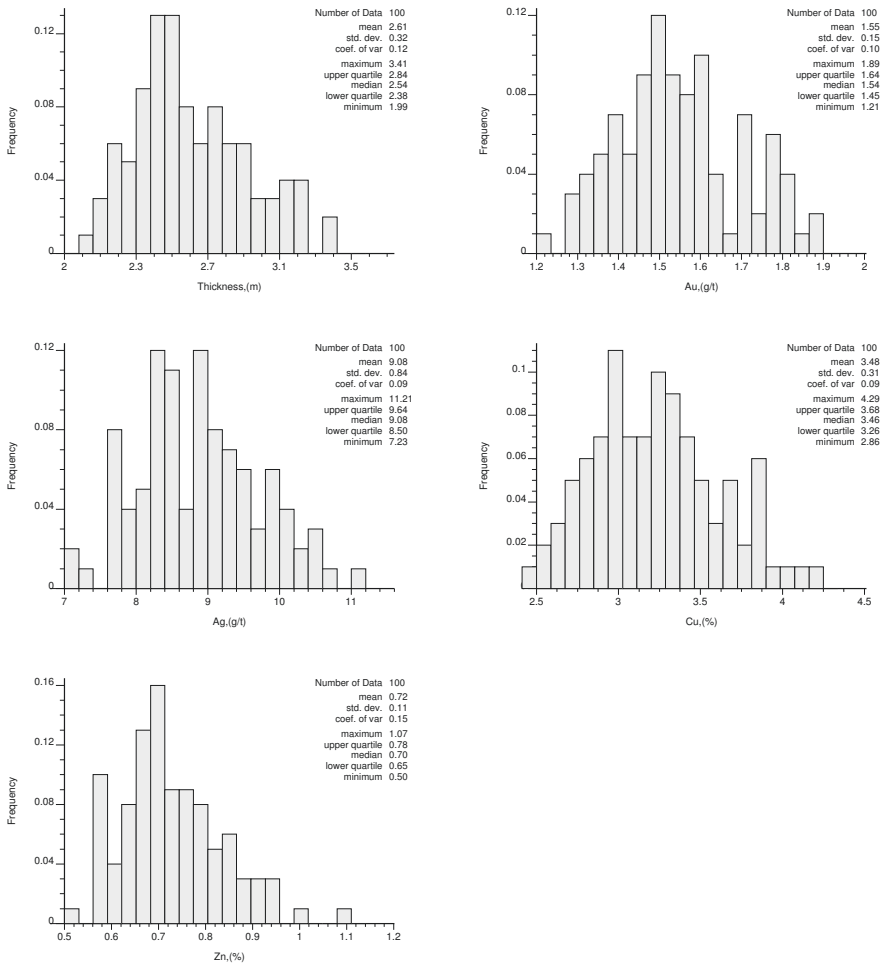

Figure 3.13: Posterior distributions of the mean in the original space of each variable after posterior realizations and clipping to the area of interest.

Realizations for each variable of the posterior uncertainty distributions of the mean in original space of each variable after realizations and clipping to the area of interest are shown in Figure 3.14 .

The results show that the uncertainty after transferring and updating to the posterior uncertainty is narrowed, as expected compared to the prior parameter uncertainty. The is resulted due to conditioning of local distributions by the data and clipping to the area of interest, see Figure 3.14. The clipping is based on: (1) calculated signed distance function (SDF) between (-C) and (+C), where C - is the uncertainty parameter involved in the SDF modeling process for boundary uncertainty

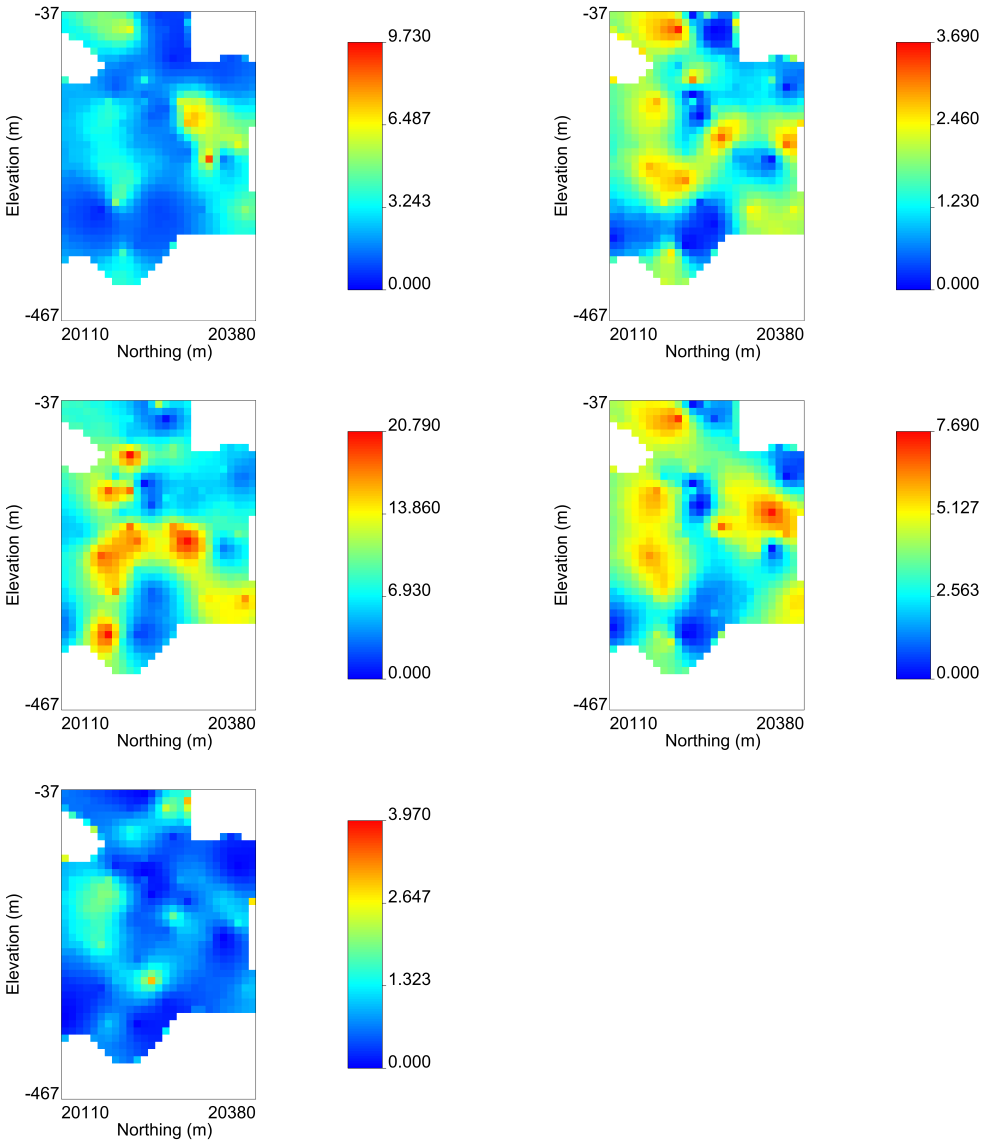

Figure 3.14: Posterior distributions of the mean for each variable after clipping to a domain of interest.

characterization; (2) posterior realizations of each variable of interest;(3)clipped areal limits with different indicators; and (4) trimmed locations to the area of interest. All variables are clipped to the domain of interest based on these steps where areal limits will be changed depending on the calculated areal limits/clipped regions, see Figure 3.14.

Response variable	Unit	Exp.value	Prior (variance)	Posterior (variance)
Thickness	m	2.89	0.41	0.32
Au	g/t	1.55	0.22	0.15
Ag	g/t	9.23	1.07	0.84
Cu	%	3.48	0.44	0.31
Zn	%	0.79	0.16	0.11

Table 3.6: Summary comparison table of the standard deviation of the global mean between prior and posterior uncertainty.

In order to roll up of the prior and posterior parameter uncertainty, we can compare these two parameter uncertainties. In addition, accounting for the mean of each variable enables a complete range of distribution shapes for each input variable. A summary comparison table of the standard deviation of the global mean between the prior and posterior uncertainty is shown in Table 3.6. The complete uncertainty in the input variables are sampled based on the MVSB and transferred through the posterior parameter uncertainty. The complete posterior uncertainty based on transferring through the simulation workflow is illustrated in Figure 3.15.

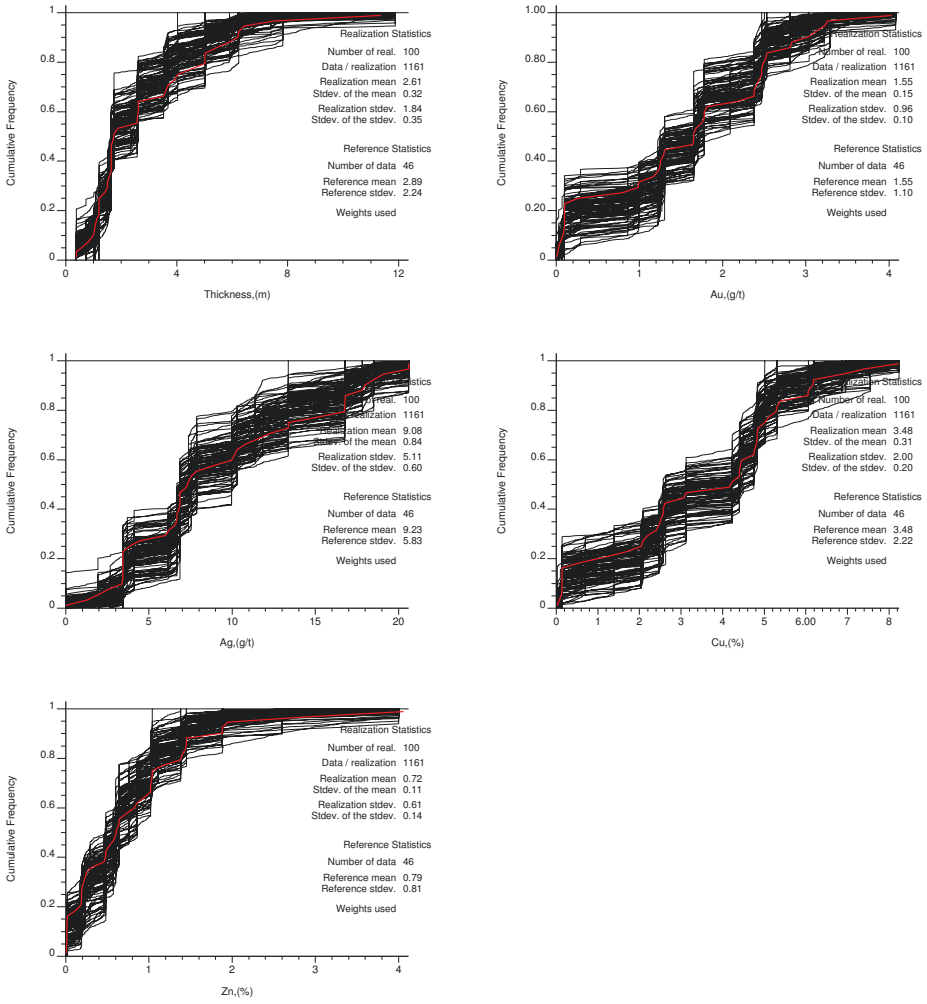

Figure 3.15: Posterior uncertainty in univariate distributions based on transferring a through the simulation workflow from the *Red* data.

The variogram uncertainty is not a main research topic here; however, the uncertainty in the variogram could be calculated by the analytical method (Ortiz & Deutsch 2002) and shown in Chapter 2. To demonstrate the uncertainty in the variograms, random numbers $r \sim U(0,1)$ were sampled to draw realizations of variograms for each variable and then mapped to different range values:

$$a_i = a_{i,min} + r \times (a_{i,max} - a_{i,min})$$

Where $a_{i,min}$ - is the minimum base case variogram range distribution,i - is the num-

ber of variables ($i = 1...n$), r - is the random number $r \sim U(0,1)$, and $a_{i,max}$ - is the maximum base case variogram range distribution for a given variable. Figure 3.16 shows an illustrative example of different possible scenarios for the experimental variograms ranges derived from the analytical method where experimental semivariogram is shown in red dots with three possible semivariogram models. Random

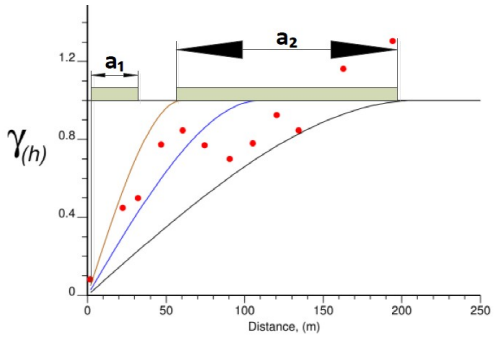

Figure 3.16: Uncertainty in the variogram. The experimental semivariogram (red dots) and three possible semivarigoram models.

sampling defines different variogram model ranges. Figure 3.17 shows one example of the variogram model for the Zn (zinc) grade value. In the variogram model, red dots show the experimental variogram with three variogram models (pink, blue, and black lines) that encompass variogram range uncertainty.

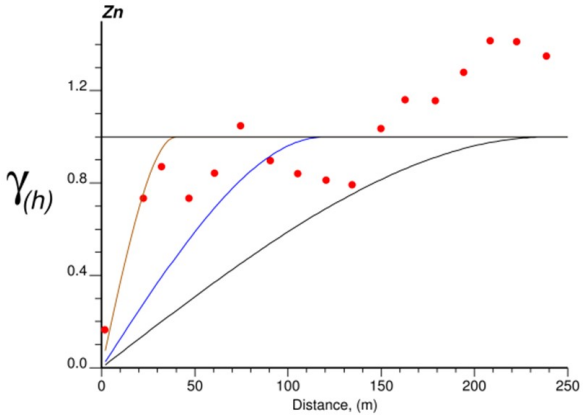

Figure 3.17: One illustration example of the variogram model for the Zn (zinc) grade value from the *Red* data. In the variogram model, red dot shows the experimental variogram with three variogram models (pink, blue, and black lines) that encompass distribution of the semivariogram range based on the analytical method.

3.3.3 Data Uncertainty

Available formats to express the uncertainty in the data include a relative/absolute measure of uncertainty, probability being within the measure, and so on. Consider Figure 2.8 illustration of normal probability distribution in units of standard deviation. In this case study, data uncertainty is considered to be a 10% relative error assuming that distribution of error values is Gaussian and relative to the measured data value. As an illustration, Figure 3.18 shows one example of calculation data uncertainty with 10% relative error for thickness at 0.38m with 95.45% chance that measure falls within two standard deviations of the mean.

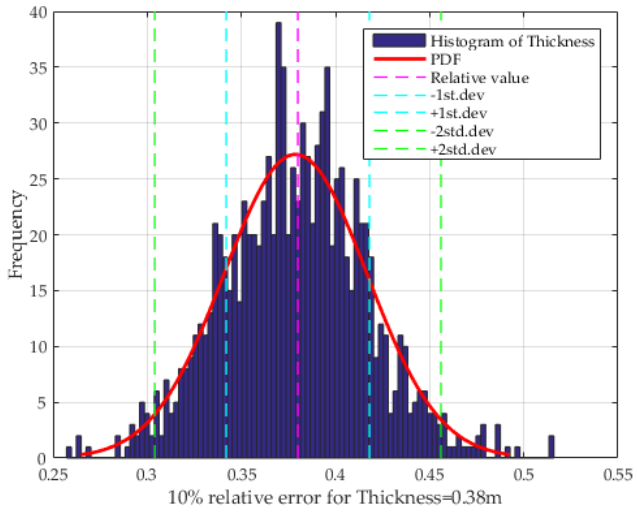

Figure 3.18: An example of illustration of the data uncertainty with 10% relative error applied for thickness at 0.38m. (Histogram bins are used only for an illustration purpose of the given data with a given value, not for the uncertainty).

3.3.4 Post Processing

Post processing includes evaluation of each realization for all calculations of interest. The post processing considers all realizations. The block averaging to a scale of interest is not performed assuming that the study area is related to underground deposit, and the scale of selectively is unknown, so the calculation of resources are performed on a point scale. The point scale realizations are used to calculate the

resources uncertainty, including tonnes of ore, grades, and metal content. Grade-tonnage curves from simulated realizations are calculated and the sensitivity analysis capturing the uncertainty impact from the input parameters is performed.

Grade tonnage curves are used for understanding the effect that different cutoff grades have on the tonnes in the deposit. As the deposit contains more than one metal of economic value, the calculation of the grade tonnage is based on a metal equivalent relationship. In this particular case, AuEq (gold equivalent) is used because it is the metal with greatest economic importance. This procedure is often applied for polymetallic deposits. The equivalent gold grade considers based on the recovery and price for each variable. The gold equivalent (AuEq) grade is calculated based on a recovery and price as follows:

$$AuEq_{AU} = Au(g/t) \tag{3.1}$$

$$AuEq_{AG} = Ag(g/t) \times \frac{Ag_{recovery(\%)} \times Ag_{price(\$/g)}}{Au_{recovery(\%)} \times Au_{price(\$/g)}} \tag{3.2}$$

$$AuEq_{CU} = \frac{\mathrm{Cu}_{(\mathrm{mass}\%)}}{100} \times 2200\frac{lb}{t} \times \frac{Cu_{recovery(\%)} \times Cu_{price(\$/lb)}}{Au_{recovery(\%)} \times Au_{price(\$/g)}} \tag{3.3}$$

$$AuEq_{ZN} = \frac{\mathrm{Zn}_{(\mathrm{mass}\%)}}{100} \times 2200\frac{lb}{t} \times \frac{Zn_{recovery(\%)} \times Zn_{price(\$/lb)}}{Au_{recovery(\%)} \times Au_{price(\$/g)}} \tag{3.4}$$

Combining equation (4.1), (4.2), (4.3), and (4.4) results in gold equivalent grade (AuEq) and it follows as:

$$AuEq = AuEq_{AU}(\frac{g}{t}) + AuEq_{AG}(\frac{g}{t}) + AuEq_{CU}(\frac{g}{t}) + AuEq_{ZN}(\frac{g}{t})$$

In the gold equivalent formula above, the minor metals are converted and added to the grade of the major metal. Figure 3.19 shows grade tonnage curve for the AuEq grade where tonnage will be decreased and grade will be increased as the cutoff

increases. Figure 3.20 illustrates the importance of each grade value used in the grades calculation.

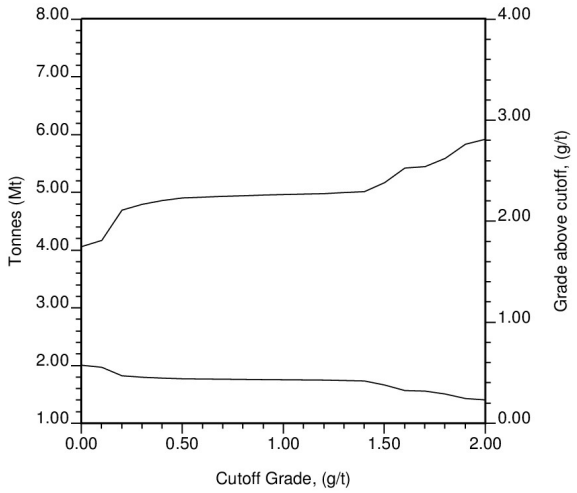

Figure 3.19: Grade-tonnage curve of gold equivalent (AuEq) grade.

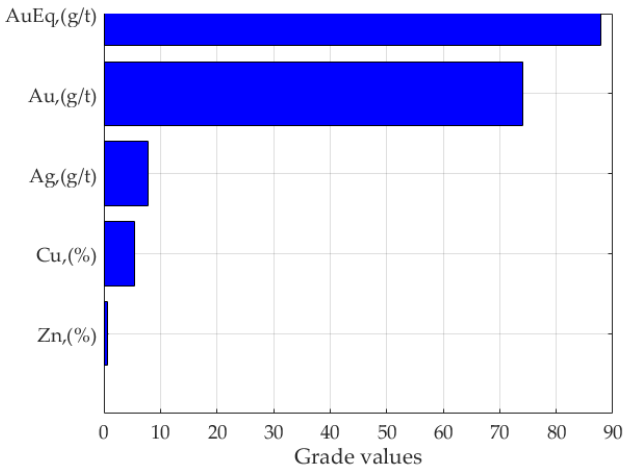

Figure 3.20: Importance of the grade values for the four grade values, including Au, Ag, Cu, Zn, and gold equivalent (AuEq) grade value.

After grade-tonnage calculation, tonnes of ore and quantity of metals can be calculated for resources uncertainty calculation. The resource uncertainty is then calculated for major summary statistics, including thickness, gold equivalent (AuEq) grade, tonnes of ore, quantity of metal (QM_AuEq) over the one hundred realizations. Figure 3.21 shows histograms over one hundred realizations for each variable

used to calculate the resource uncertainty. Analyzing the calculated resource uncertainty, we can see the average thickness is 2.52 g/t and and average gold equivalent (AuEq) grade is 1.80 g/t in the deposit.

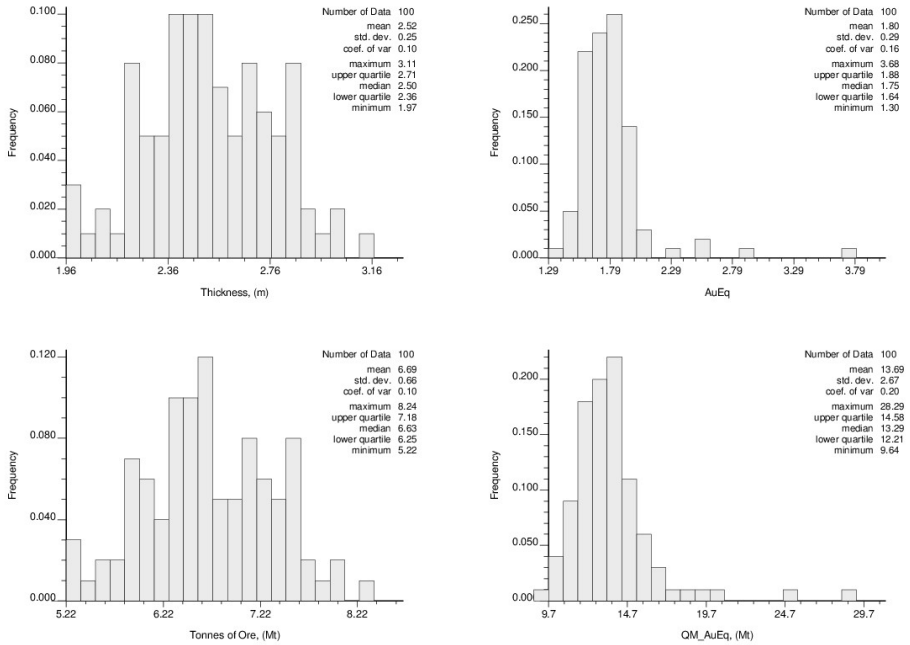

Figure 3.21: Resources uncertainty over the one hundred realizations in thickness (top left) gold equivalent (AuEq) grade (top right), tonnes of ore (bottom left), and quantity metal of gold equivalent (QM_AuEq) grade (bottom right).

Sensitivity is important as we want to know the level of the uncertainty and where is it coming from. Sensitivity analysis is performed to assess the impact of the uncertainty in each input parameter. The response variable is a summary measure such as ounces of gold, or tonnes of ore. The predictor variables are summaries of the input parameters, that is, factors that have some influence on the uncertainty.

In analyzing the sensitivity analysis, linear and/or quadratic regression can be applied. The sensitivity analysis study used the GSLIB-like program *SABOR*. The full description of the program can be found in Zagayevskiy & Deutsch (2011). In the tornado chart, the main middle part is divided into two bars. The bars on the right side of the tornado chart show either sensitivity coefficients and/or their standardized values. The bars on the left hand side show interaction terms between variables. The bars are plotted in the same order as bars on the right hand side of

the tornado chart. These values are plotted in descending order. Positive coefficients are shown in yellow color, whereas negative coefficients are drawn in green. All bars are scaled to the largest upper boundary of confidence level of any coefficient or interaction term. It can be seen from the plot that the regression coefficients have the largest value; however, interaction terms may also have larger values in some cases. We can also note that input variables with relatively short coefficients of bars and interaction terms could be discarded from a model.

Summary statistics including coefficient of determination, its adjusted value, standard error of model deviations, model utility test based on F statistic, and prediction power of the model (percentage ratio of standard deviations of predicted and actual values of model response) are presented in the upper left corner of the plot. The table with means, standard deviations, coefficients of correlation and variation, sensitivity coefficients and standardized sensitivity coefficients for model response and each input variable are tabulated in the table on the right of the chart. Coefficients, whose values are shown in blue in the table, are used for plotting bars. The specified confidence level is reported in the lower middle of the chart. Thus, the extended tornado chart visually summarizes results of sensitivity analysis and is useful for making decisions on the importance of input variables and the appropriateness of linear and quadratic models.

In both cases, the results will be shown as a tornado chart with the amount of explained uncertainty depending on the input parameter, and response variable. In order to better understand the importance and impact of each dependent versus independent variables, different scenarios are considered. To illustrate the sensitivity analysis study and expose the results, two main linear and quadratic regression models are used and compared to each other. The case study used three dependent, including tonnes of ore, quantity of metal, and gold equivalent (AuEq) grade with other seven independent variables. The independent variables include area, thickness, gold (Au) grade, variograms of thickness and gold (Au) grade, and relative error of data of the thickness and gold (Au) grade value. Among these independent variables, the two of them that are the most important are area and thickness.

Sensitivity analysis is then performed using these parameters.

Each time one response variable versus other independent variables are analyzed both for linear and regression analysis. The results show that both linear and/or qudratic regression model could be used for sensitivity study where each model indicates reasonable coefficient of determination value individually. During sensitivity analysis study, however, relative data error of thickness with thickness showed that these two could be the most important as well along with area and thickness, but relative error does not have much impact on the model, therefore this will not be used. After full analysis, a quadratic regression model is selected with QM_AuEq as a response variable. Predictor variables are plotted with a response variable — quantity of metal of gold equivalent grade (QM_AuEq). In this case, the both models resulted same results showing that thickenss and area are the most important dependent variables, but with slightly different coefficient of variation values of 22% and 56%, respectively.

In case of selecting the linear or quadratic model with quantity of metal as a response variable with other seven independent variables would suit better in this study. In both linear and quadratic models, thickness and area are resulted that these two parameters are the most important than other variables. The uncertainty could be explained by these variables. Figure 3.22 illustrates the tornado chart visualizing the effect of change in the value of an input parameter value for independent variables using the quadratic regression model with the quantity of metal for gold equivalent grade as a dependent and other seven independent variables, including area, thickness, variograms and relative data error of thickness and gold (Au) grade value.

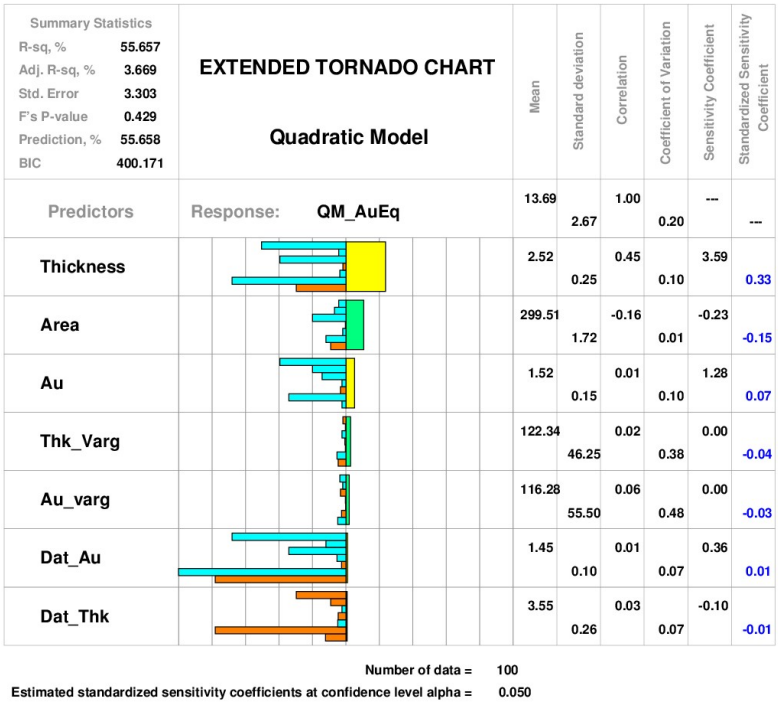

Figure 3.22: A tornado chart visualizing the effect of change in the value of an input parameter for predictor variables using quadratic regression models with the quantity of metal of gold equivalent grade as a response variable.

3.4 Conclusions

Accounting for uncertainty in different parameters is important for a realistic assessment of uncertainty. This case study demonstrates a workflow to assess the uncertainty in distributions with the purpose of understanding uncertainty. The uncertainty is assessed using unit operations developed specifically in this study. This case study is completed in the example of a vein-type deposit so consideration should be taken into account for different geological settings before proceeding to any geostatistical modeling. Different methodologies for assessing the uncertainty in distributions may be considered depending on a type of deposit, prior experience, and preferences.

Chapter 4

Case Study: *Oilsands* Data Set

This chapter demonstrates case study using the *Oilsands* data. The purpose of this chapter is to demonstrate the uncertainty assessment workflow with another deposit. Different methodologies are used for some steps due to different geological and parameter settings. Section 4.1 introduces the geology and data analysis, Section 4.2 provides the geostatistical modeling methodology and post processing used in the study; and conclusions are in Section 4.3.

4.1 Geology and Data Analysis

Oil sands are a mixture of sand, water, clay, and bitumen and can be found around the world, including Russia, Venezuela, and the United States, but the largest deposits of the oilsands are located in Canada (Alberta Energy 2015). The case study uses 3D data related to oilsands surface mining, which contain bitumen and fines grades, as well as a facies code. The data set over a $2km \times 2km$ area is sampled at 1853 sample locations. 3D displays of bitumen and fines grades in units of mass% are shown in Figure 4.1. Figure 4.2 shows histograms of the two grade values.

Parameter	Unit	Count	Minimum	Maximum
Bitumen	%	1853	0	18.428
Fines	%	1853	0.951	86.777

Table 4.1: Summary of the *Oilsands* data used in the case study.

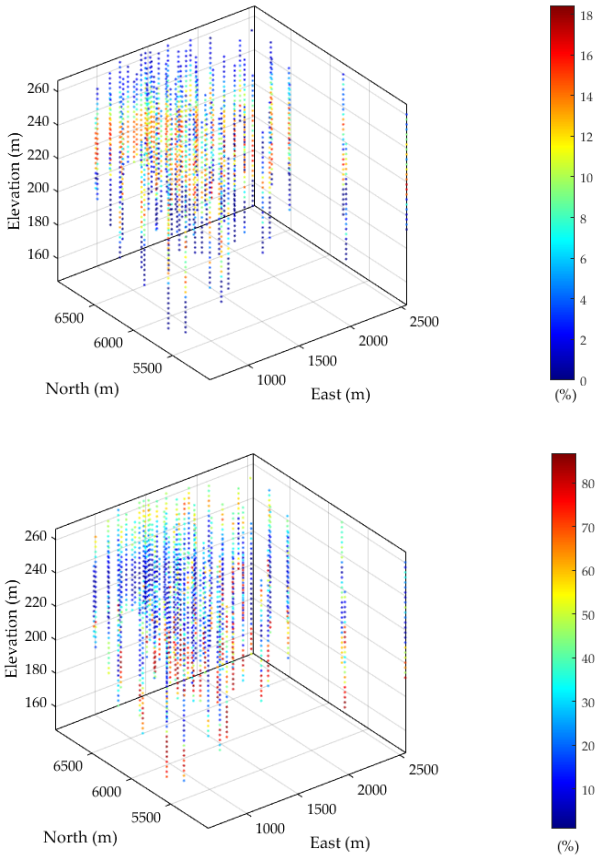

Figure 4.1: 3D visualization maps of the bitumen (top) and fines (bottom) grades. The units are in mass%.

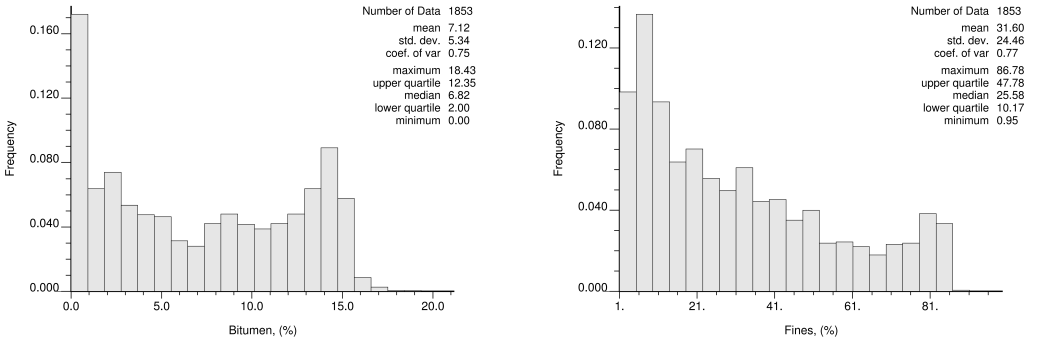

Figure 4.2: Histograms of bitumen and fines grade values.

Table 4.2 shows a summary table of simple and declustered statistics for the bitumen and fines grades.

Parameter	Unit	Original mean	Declustered Mean
Bitumen	%	7.120	6.020
Fines	%	31.600	34.830

Table 4.2: Summary comparison table between simple and declustered histograms

Original unit and normal score variograms for the two grades are plotted for major, minor, and vertical directions. In the horizontal variogram, the red dots and line is at at N40°E and the blue dots and line at N130°E. These are shown through Figure 4.3 to Figure 4.6.

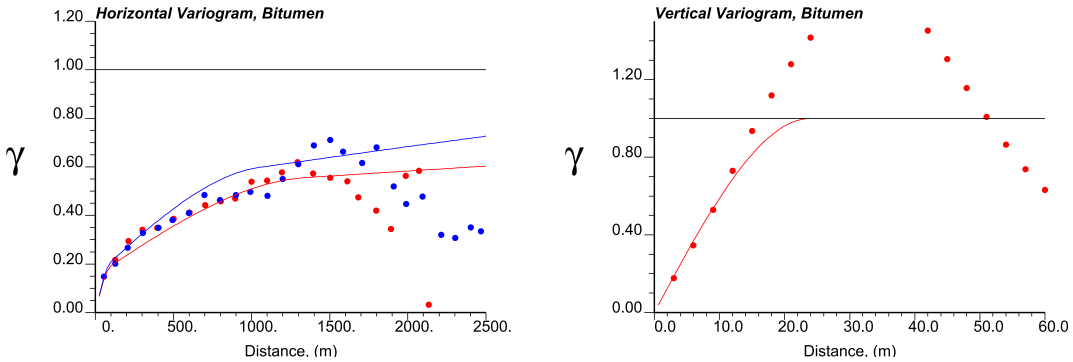

Figure 4.3: Original unit variograms of bitumen grade value for horizontal and vertical directions.

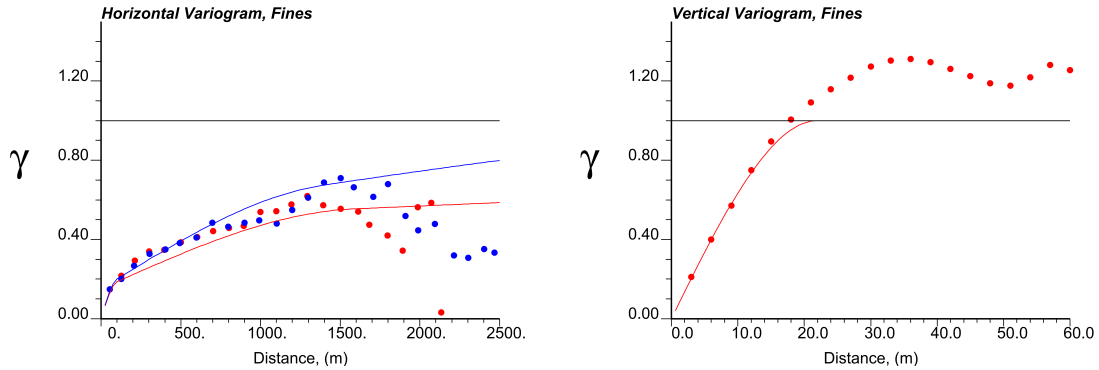

Figure 4.4: Original units variograms of fines grade value for horizontal and vertical directions.

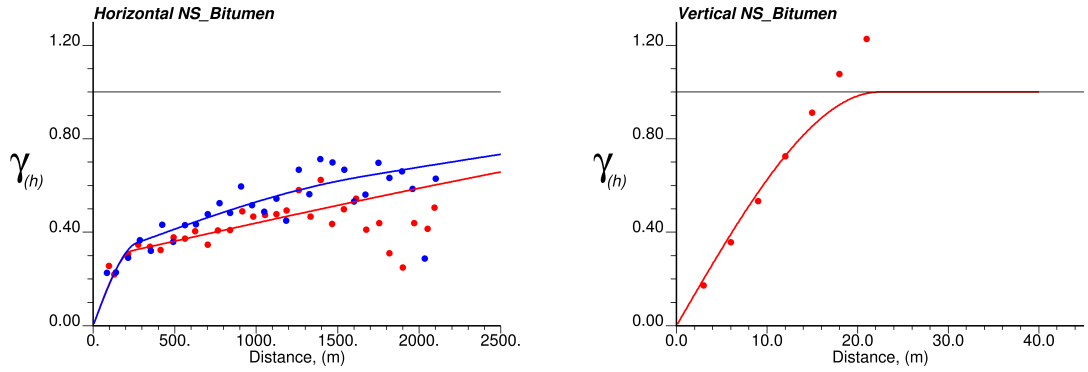

Figure 4.5: Normal score variograms of bitumen grade value for horizontal and vertical directions.

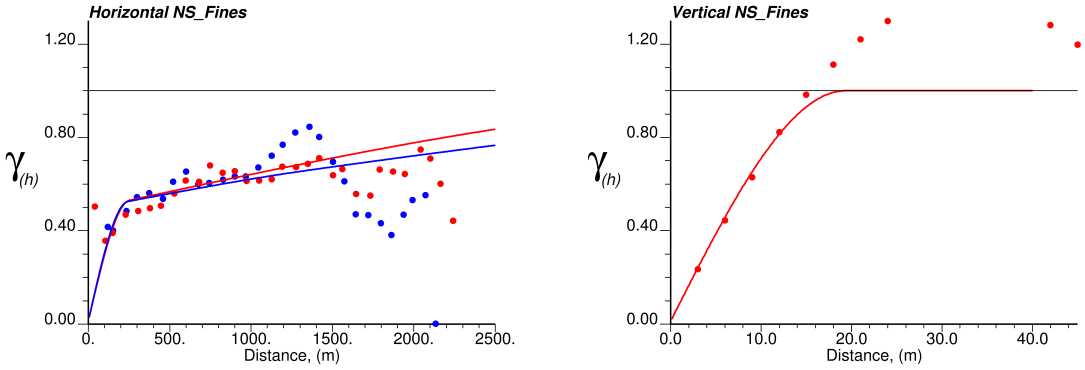

Figure 4.6: Normal score variograms of fines grade value for horizontal and vertical directions.

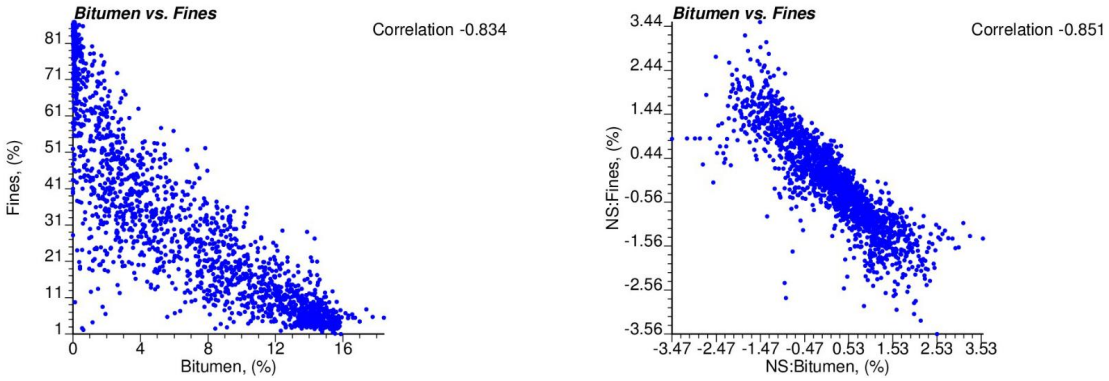

Figure 4.7: Cross-plots of bitumen versus fines grades in original units (left) and normal score space (right).

In the calculated original units and normal score calculated experimental variograms for the two major and minor directions, there is a zonal anisotropy where the variograms do not reach the expected sill/variance of 1.0 for large distances.

The notion and the use of the sphere transformation technique has already been introduced and discussed in the previous chapters of the study (Barnett & Deutsch 2015). The sphering technique (PCA-R) allows independent analysis of decorrelated variables. Figure 4.8 shows the PCA plot matrix loadings for the two variables in normals score units that are being modeled.

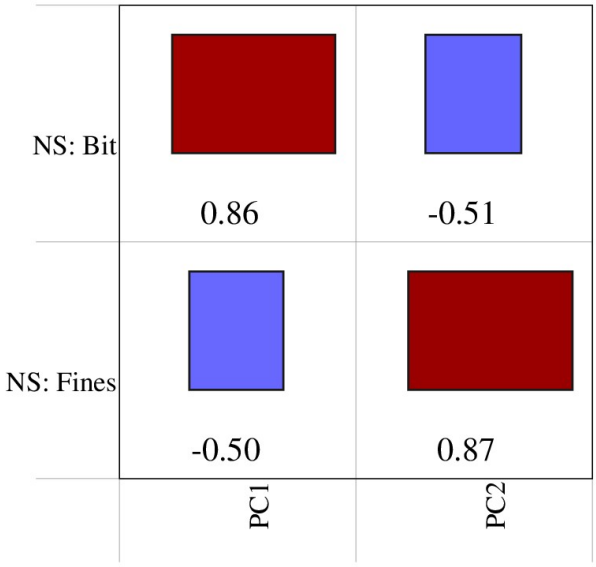

Figure 4.8: Loading plots of normal scores vs. transformed variables of the bitumen and fines grades.

In virtually all reservoir modeling cases, there is a need to model the joint distribution of multiple variables (Behrens et al., 1998). Multivariate analysis of the data can be difficult because of increasing dimensionalty in sizes for direct and cross-variograms. However, this issue could be solved by applying the PCA-R technique where decorrelated variables are could be modeled/analyzed independently. The variogram models are fit to each variable based on calculated experimental variograms, and the workflow for cross-variograms between the two variables for three directions is based on normal score variograms. The PCA-R is applied for cross-variograms between the two variables. This is a reverse PCA, which projects the orthogonal

variables back to original units. This minimizes the required rotation to orthogonalize the variables, which leads to minimal mixing. Direct and cross-variograms of the PCA-R values for three-major, minor, and vertical directions are shown through Figure 4.9 to Figure 4.11. Readers are referred to external sources for more information on the sphere-R principal component analysis.

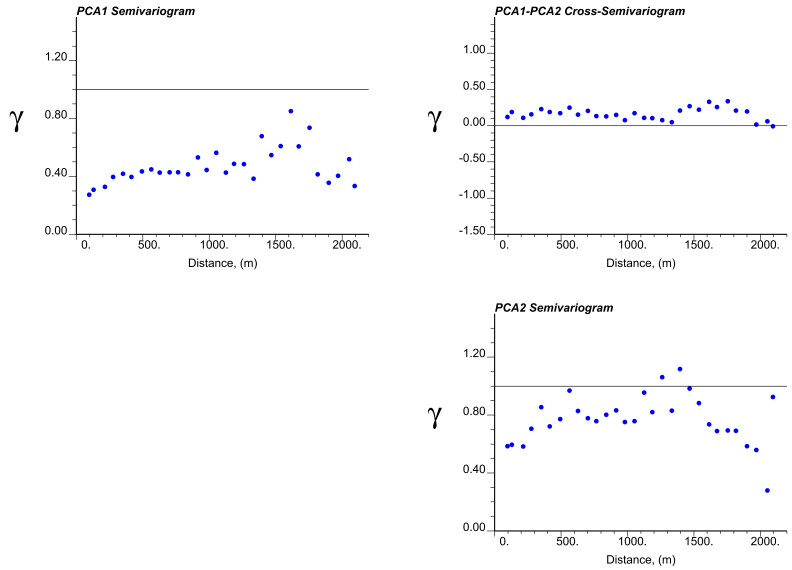

Figure 4.9: Direct and cross-variograms of PCA-R transformed values of bitumen, fines, and bitumen versus fines grades at N40°E major directions.

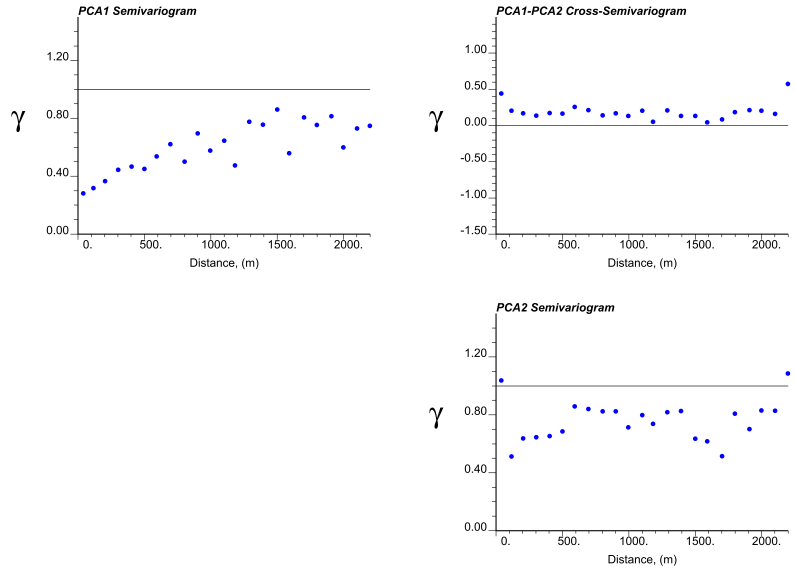

Figure 4.10: Direct and cross-variograms of PCA-R transformed values of bitumen, fines, and bitumen versus fines grades at N130°E minor directions.

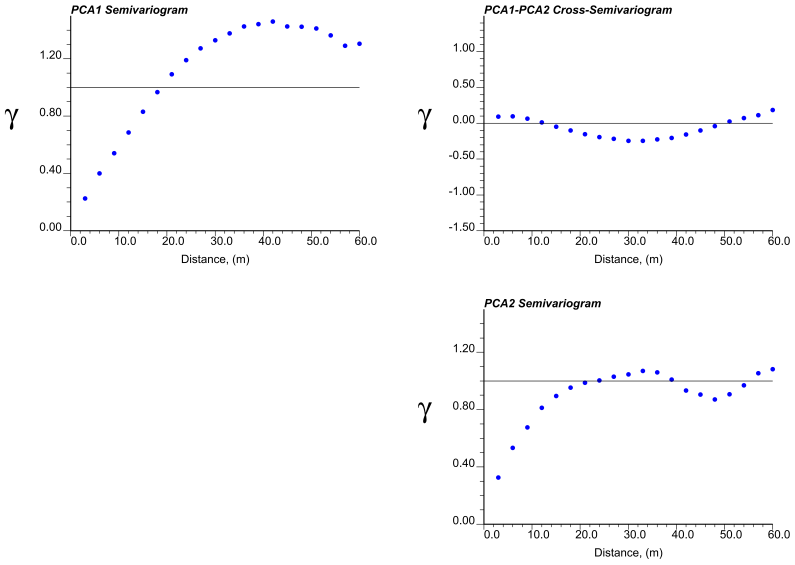

Figure 4.11: Direct and cross-variograms of PCA-R transformed values of bitumen, fines, and bitumen versus fines grades at vertcial directions.

4.2 Geostatistical Modeling Methodology

This case study uses slightly different geostatistical approaches compared to the first case study due to different geological and parameters settings of the *Oilsands* data.

The general approach follows as:

1. Analyzing and modeling boundary surfaces (Deutsch 2003)
2. Declustering data distribution where relevant statistics are representative in a deposit prior to modeling
3. Modeling of spatial continuity for all variables of interest
4. Facies modeling
5. Constructing uncertainty models for all variables of interest using geostatistical simulation
6. Performing post processing and sensitivity analysis in order to understand the impact of each input variable

These models can be applicable for both long and short term decision making. In the following steps, each of the modeling steps will be presented in more detail. The application is for more than one variables; however, the same workflow could also be applied to a single variable.

4.2.1 Structure Analysis and Modeling

As discussed above, it is essential to have a sound workflow for each modeling methodology. Some references on determination and analysis of stratigraphic coordinates and correlation include (Pyrcz & Deutsch 2014). Reservoirs are often made up of a number of layers where each layer corresponds to a specific period of time in the creation of the reservoir. The surfaces separating these specific layers reveal rapid or discontinuous geological changes. The most common correlation styles include proportional, truncation, onlap, and combination (Pyrcz & Deutsch 2014). A common approach for capturing stratigraphic continuity includes modeling continuity of facies and reservoir properties as proportional between top and base surfaces structures. Figure 4.12 shows a schematic illustration of stratigraphic coordinates corresponding to a proportional correlation style (Deutsch 2003). 2D maps of a top

surface structure and thickness from the seventy eight well locations are shown in Figure 4.13.

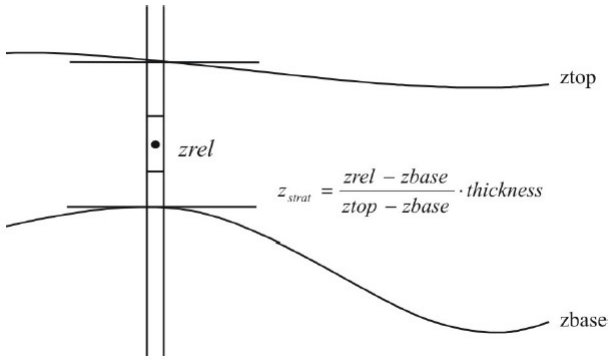

Figure 4.12: Schematic cross-section illustration of stratigrpahic transform for a proportional grid (Deutsch 2003).

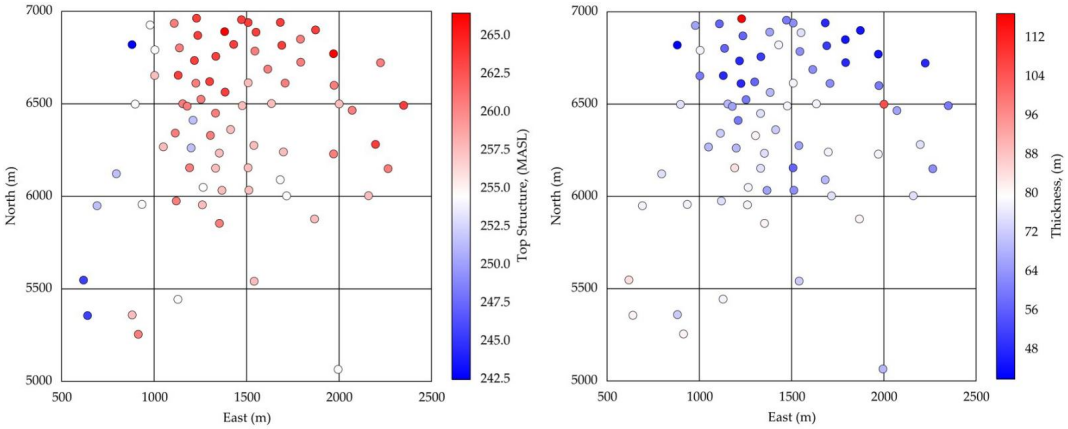

Figure 4.13: 2D location maps of a top surface structure (left) and thickness (right).

Histograms of the top surface structure and thickness are also illustrated in Figure 4.14. The minimum and maximum depth of the top structure are 242.5 MASL and 265.5 MASL, while the minimum and maximum thickness of the structure are 42.5m and 117m. Cell declustering of top surface structure and thickness is performed to determine appropriate weights. A cell declsutering with cell size of 450m is applied with same the weights both for top surface and thickness. The cell declustering diagnostic plot of these two structures is shown in Figure 4.15. The same cell size is used for thickness because of the same configuration of data. A normal scores

tranform is then performed.

Using the normal scores, variograms of the top surface structure and thickness are calculated and modeled. The variograms are calculated for the major direction at N40°E (red line) and minor direction at N130°E (blue lines) both for the top surface and thickness. The calculated and fitted experimental variograms are shown in Figure 4.16. The experimental variograms of thickness, see Figure 4.16 (right) show a slightly cyclic behavior.

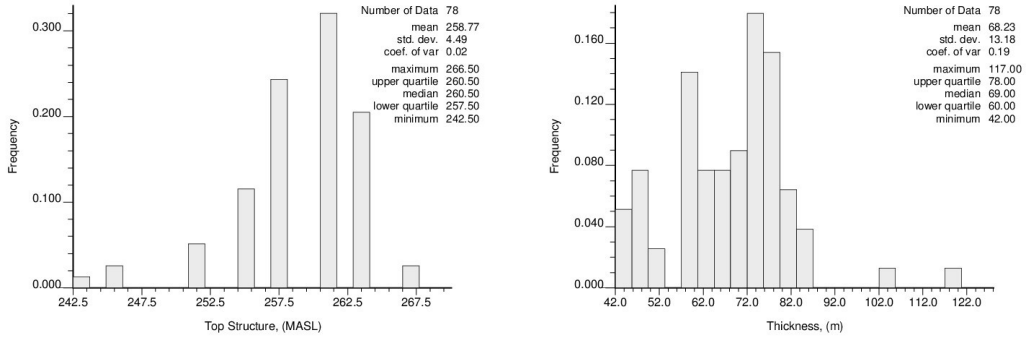

Figure 4.14: Histograms of a top surface structure (left) and thickness (right).

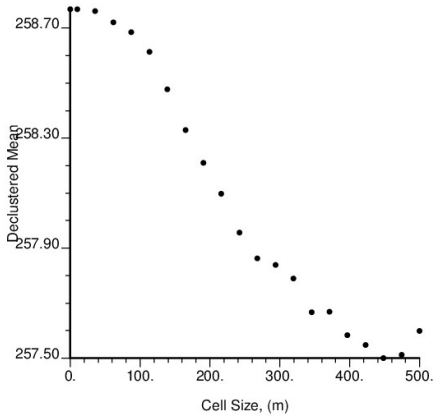

Figure 4.15: Declustered mean vs. cell size for top surface structure.

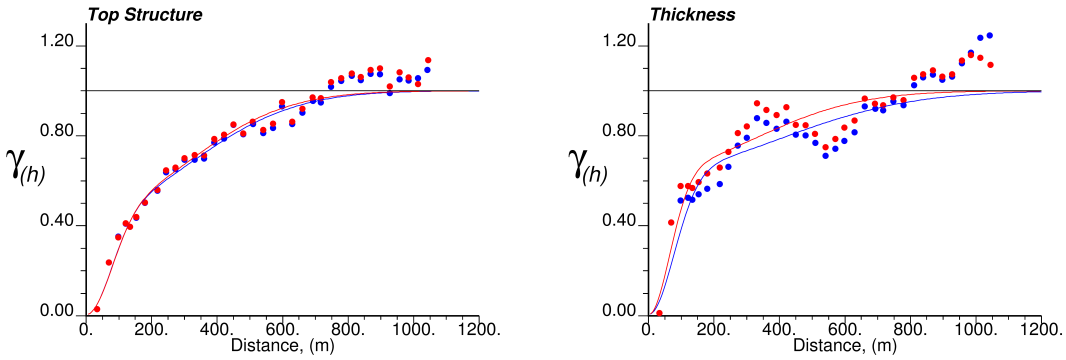

Figure 4.16: Experimental and fitted variograms models of a top surface structure (left) and thickness (right) for two diffrent directions.The major directions are chosen at N40°E (red line) and minor directions at N130°E (blue line).

Geostatistical modeling workflows rely on multiple realizations in order to fully characterize the uncertainty in distributions. Therefore, it is important to account for parameter uncertainty in the uncertainty calculations. The parameter uncertainty in the top surface structure and thickness is quantified using the spatial bootstrap (SBS). 100 realizations were drawn from the spatial bootstrap for the top structure and thickness. The uncertainty in the mean is of primary importance. In addition, uncertainty in thickness is also calculated. Figure 4.17 shows distributions of uncertainty for a top structure (a) and thickness (b) from over one hundred realizations. Figure 4.18 shows volumetric uncertainty obtained from the SBS over the one hundred realizations.

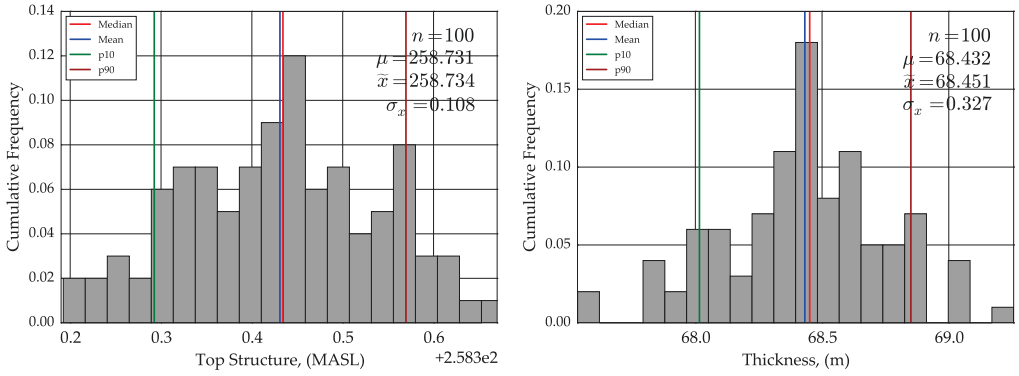

(a) (b)

Figure 4.17: Distributions of uncertainty in the mean top structure (a) and mean thickness (b) obtained from the spatial bootstrap (SBS).

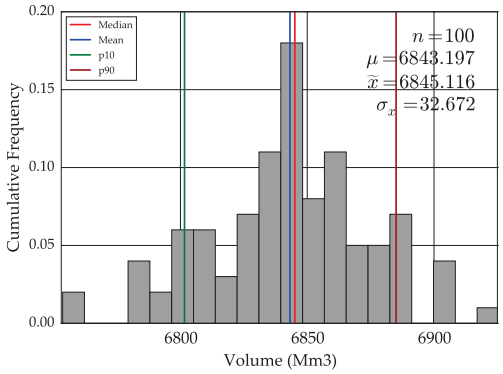

Figure 4.18: Volumetric uncertainty of thickness over the 100 realizations.

100 realizations of the top structure and thickness were generated using the conditional Gaussian simulation at the seventy eight well locations. The uncertainty in the distribution of top surface structure and thickness are transferred into realizations by different input distributions. Figure 4.19 shows a contour map of a top surface structure depth and thickness showing the distribution of seventy eight well locations from one realization. To analyze the top structure and thickness for different features, cross-sectional views are also plotted at different sections arbitrarily and these are shown in Figure 4.20 and Figure 4.21.

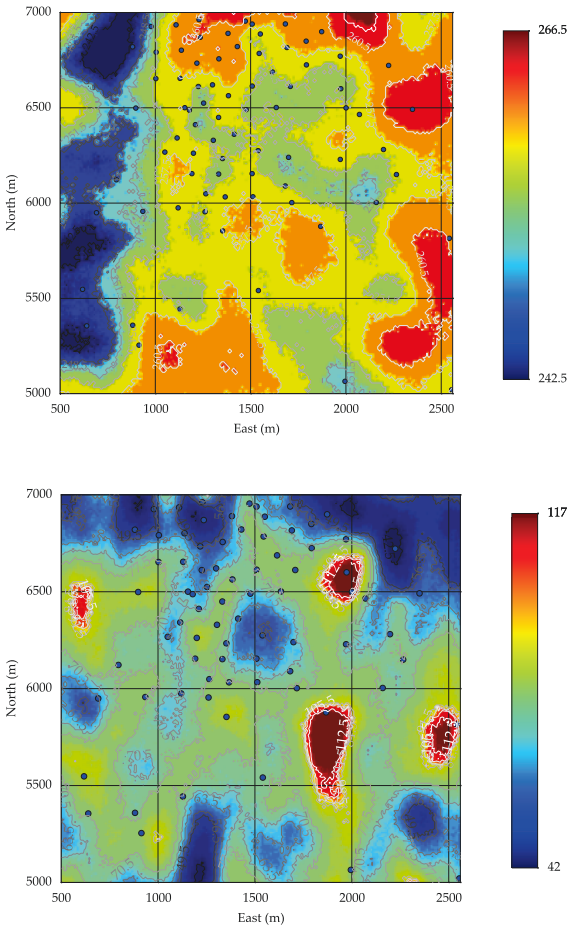

Figure 4.19: Contour map of a top structure depth(top) and thickness (bottom) showing the seventy eight well locarions from one realization. The units are in MASL and meters.

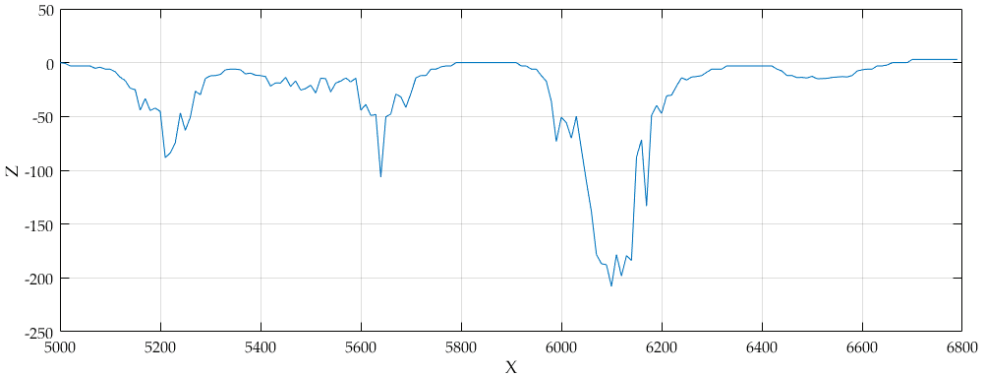

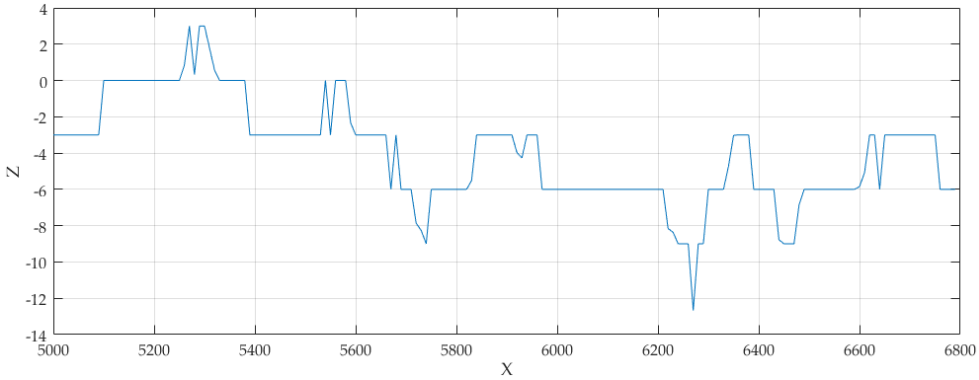

Figure 4.20: Cross-sectional views of top structure selected arbitrarily along X-axes at different reference values and slices. Reference value at 257.5 m and slice at 500m (top); Reference value at 260.5 m and slice at 1000m (bottom).

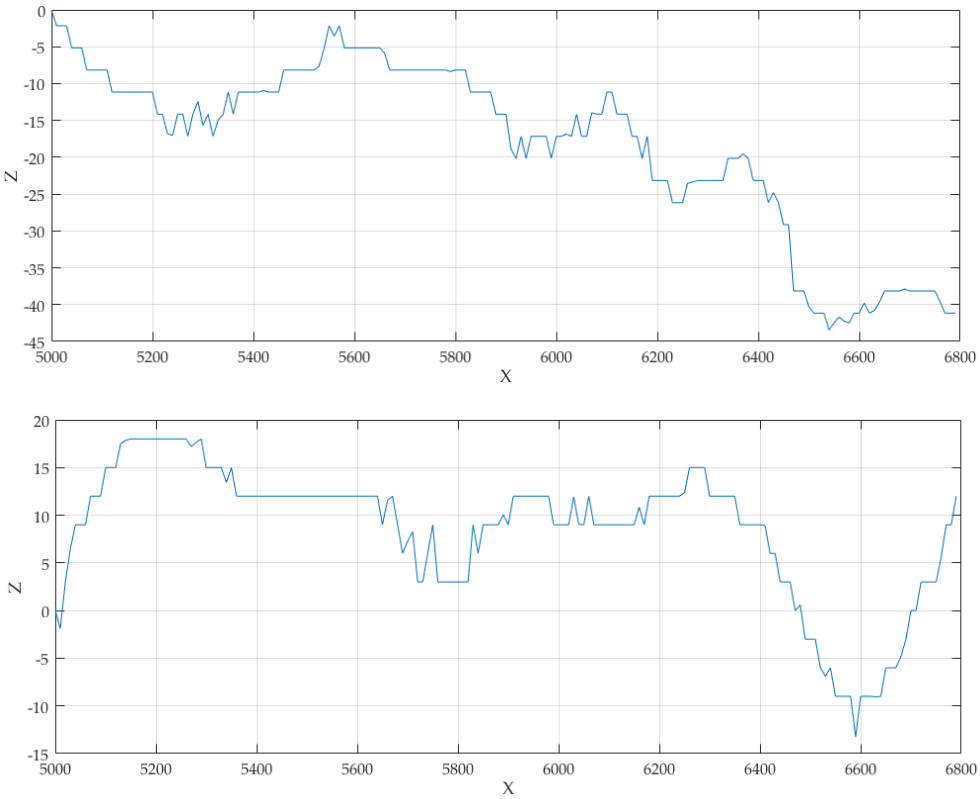

Figure 4.21: Cross-sectional views of thickness structure selected arbitrarily along X-axes at different reference values and slices. Reference value at 86.15 m and slice at 500m (top); Reference value at 66 m and slice at 1000m (bottom).

4.2.2 Facies Modeling

There is a need to group the facies together into high and low bitumen content sets because some of the original facies are very small in global proportion. High bitumen

content with corresponding low content for fines is considered as good (more ore), and low bitumen-content fines is considered bad (more waste). Some of the facies codes were combined due to limited data. The category that corresponds to the facies code [50] has average bitumen content of 8.1% and fines content of 27.5% responds to 1247 samples and assigned with facies indicator code of 1. The remaining facies codes [30, 31, 69, 70, 61, 40, and 60] are grouped together for total number of 606 samples are assigned with an indicator facies code of 0. A table of the averaged grades with their rankings and proportions is shown in Figure 4.22.

№	Facies codes	Average Bitument, (%)	Average Fines, (%)	Count	Rank	Global Proportions
1	50	8.092	27.516	1247	1	0.675
2	30	0.497	51.294	1	0	
3	31	0.899	36.982	3	0	
4	69	1.015	44.203	6	0	
5	70	2.208	41.409	5	0	
6	61	1.588	29.510	22	0	
7	40	2.475	39.968	59	0	
8	60	5.701	40.388	510	0	0.325

	Rank
High Bitumen content/Low Fines content	1
Low Bitumen content/High Fines content	0

Figure 4.22: Illustrative summary figure table with an extracted by $2km \times 2km$ area and with rankings and proportions.

Indicator variograms for major, minor, and vertical directions are calculated and fitted. Major directions are calculated at N40°E (red line) and minor directions at N130 °E (blue line). Figure 5.23 shows the calculated indicator variograms.

The uncertainty in distributions proportions quantified using the spatial bootstrap (SBS). 100 realizations of spatial bootstrap were run in order to quantify the uncertainty in distributions. Figure 4.24 shows one realization of distribution uncertainty in proportions obtained from the SBS for the proportion of combined facies one.

The vertical coordinate is defined as the relative distance between the surface top and base structure. This allows us to infer horizontal correlation and preserve geologic structure in the final numerical model. Proportional gridding is used to

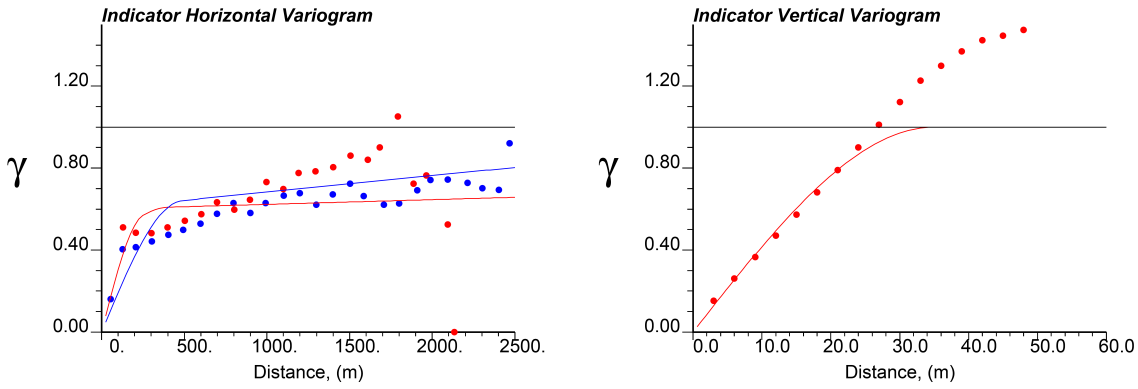

Figure 4.23: Experimental and fitted indicator variograms models of bitumen and facies grades for two diffrent directions.The major directions are chosen at N30°E (red line) and minor directions at N130°E (blue line) and vertical variograms (right).

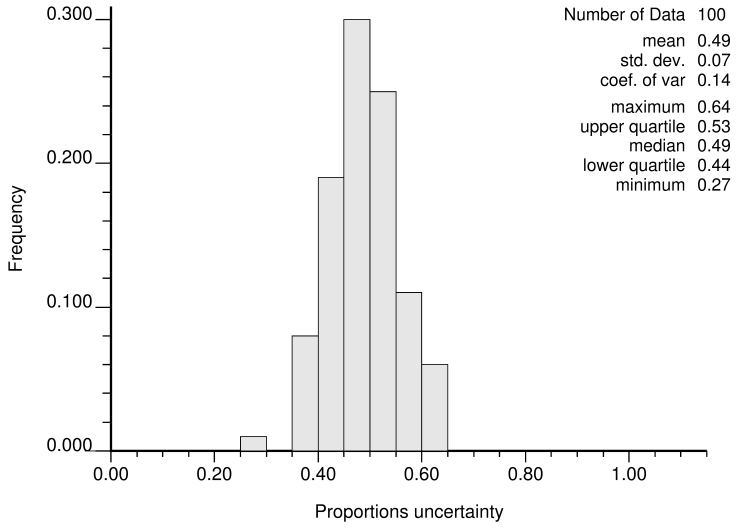

Figure 4.24: Distributions of uncertainty in proportions from one realizations using the spatial bootstrap (SBS) for combined facies one.

conform the existing top and base where proportional strata vary in thickness due to different geology such as compaction or sedimentation rate, or structurally deformed and faulted. The minimum thickness is fixed approximately at nine meters; and the correlation grids match with the existing grids. Readers are referred to (Pyrcz & Deutsch 2014) for more information on modeling prerequisites including stratigraphic correlation and coordinates.

Facies are important in reservoir modeling because properties of interest are highly correlated with facies type. Sequential indicator simulation (SIS) is applied

with the GSLIB-like program *BlockSIS* for facies modeling. Each time a different random number (RN) seed is used to generate multiple realizations One of the prerequisites for performing the facies modeling is to model indicator variograms and define global proportions. Indicators variograms are calculated and global proportions are defined from the available data. Figure 4.25 shows facies modeling results for different slices with realization 1.

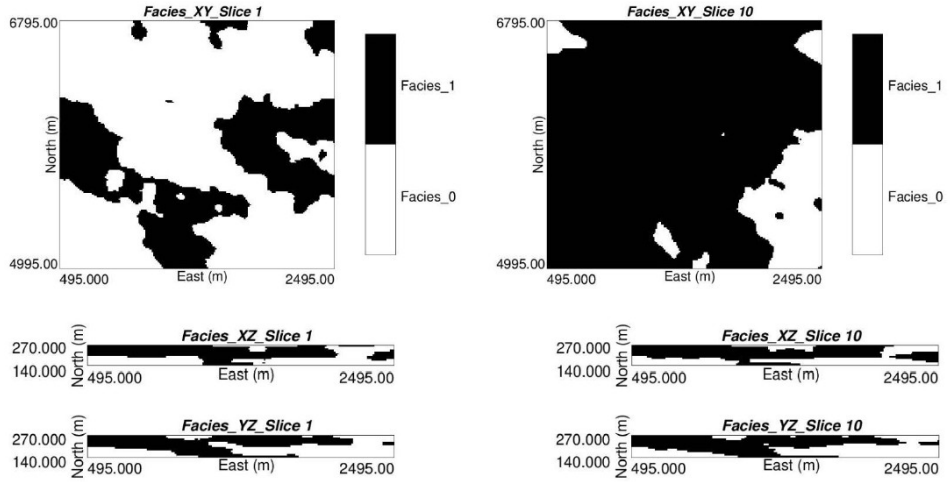

Figure 4.25: Facies modeling of Sequential Indicator Simulation (SIS) with two category types for XY, XZ, and YZ slice orientations at realization 1.

Post processing after facies modeling is then performed. The sequential Gaussian simulation (SGS) is performed over the 100 realizations for bitumen and fines grades. All maps from realizations show great variability; however, there are some similar features. The highest bitumen grade is located in the northwest. Realizations 25, 50, 75, and 100 are plotted to examine the highest and lowest regions in the deposit. The mapped realizations in Figure 5.26 show that realization 75 a low

region in the southeast, while realizations 25 and 50 illustrates almost similar area from low to high region in the northwest to southwest regions, respectively. The sim-

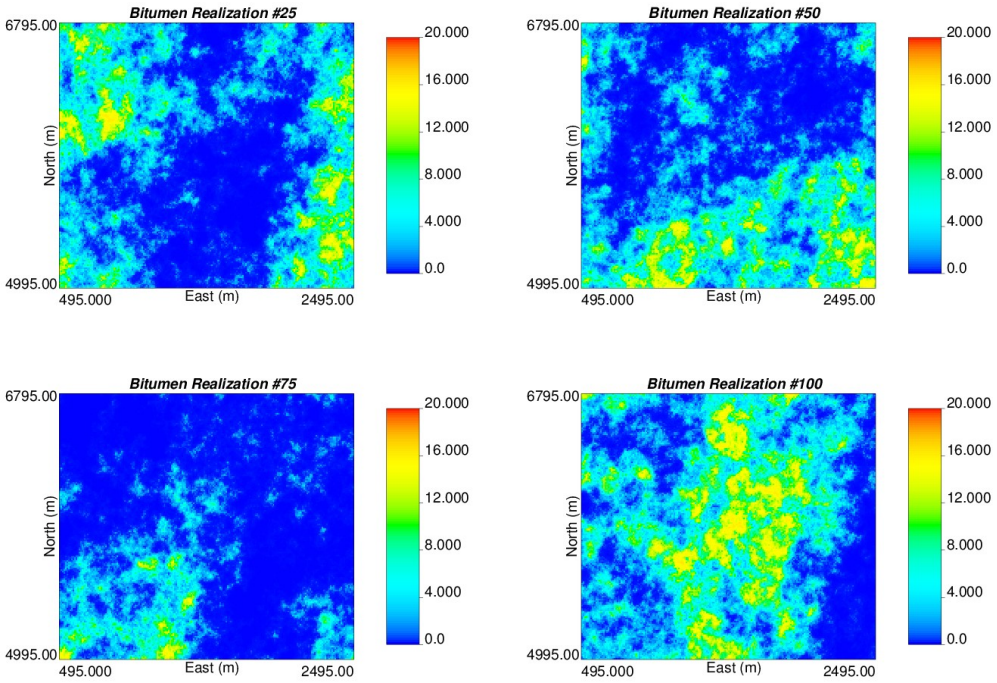

Figure 4.26: Four realizations of bitumen obtained from sequential Gaussian simulation.

ulated models are then checked for histogram reproduction. Figure 4.27 shows the histogram of realization from bitumen. In addition, histogram reproduction of the two variables are also checked over the 100 realizations, see Figure 4.28. The results show that realizations mean of bitumen and reference bitumen was 6.34 and 6.02 with a difference of 5%. The fines grade is also checked for histogram uncertainty and reproduction where the reference mean was equal to 34.83 and the mean from realizations equal to 33.02, which also a 5% difference approximately.

In the next step, we can pair each indicator simulation with different top structure and thickness, bitumen and fines realizations. In addition, bitumen and fines grades are merged based on their facies models. One facies realization is needed for each simulated realization. One realization of merged facies models with bitumen and fines is illustrated in Figure 4.29. In Figure 4.30 we can see the demonstration of pairing the top structure and thickness with different cross-sectional views.

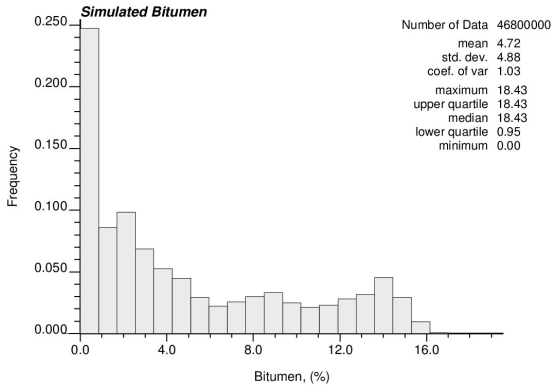

Figure 4.27: Histogram of simulated bitumen from one hundred realization. The units are in mass%.

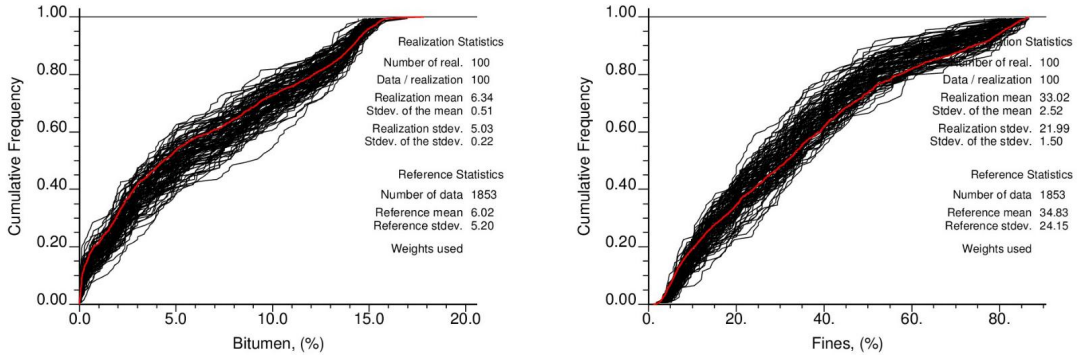

Figure 4.28: Histogram reproduction of bitumen and fines grade values.

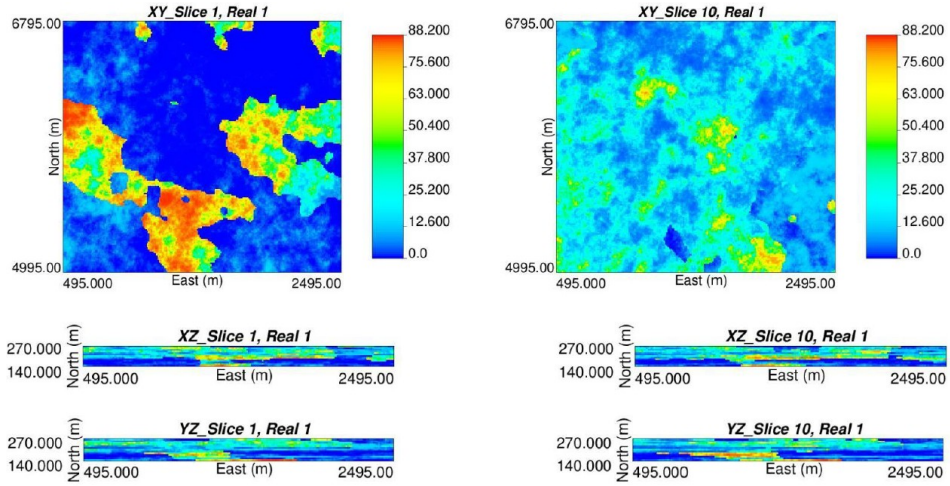

Figure 4.29: Merged facies realizations with simulated bitumen and fines grade realizations for XY, XZ, and YZ slice orientations at realization 1 arbitrarily.

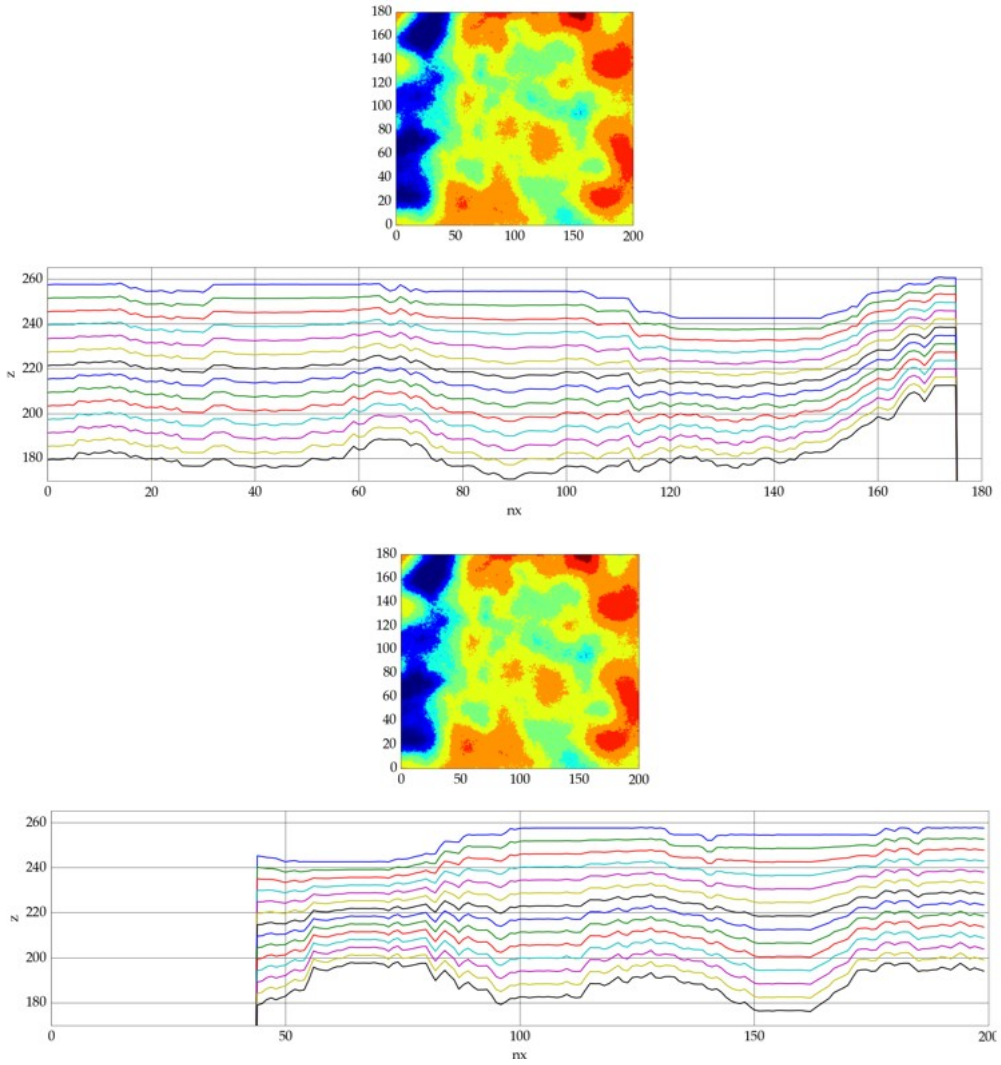

Figure 4.30: Illustration of pairing with top structure and thickness with different cross-sectional views. Cross-sectional views show slices at X=100 m and Y=90m (top) and X=90m and Y=100m (bottom)

4.2.3 Post Processing

In post processing, the resources uncertainty is calculated and sensitivity analysis is performed. Assume that the grade and fines can be considered with the AER recovery function by Equation 4.1 and the fines recovery function by Equation 4.2 (Sanford 1983). According to the AER operating criteria, a recovery function could be defined:

1. If the as mined bitumen grade (g) is $\geqslant$11, then the recovery is 90%

2. If the as-mined grade is <11%, then the recovery is defined by Equation 4.1

$$R(g) = -202.7 + 54.1g - 2.5g^2 \tag{4.1}$$

$$R(f) = 87.5 + 0.273f - 0.037f^2 \tag{4.2}$$

Where f is the fines. The bitumen cutoff grade given by AER is 7% and the recovery from the Equation 4.1 is 53.5%. Using a recovery function with multiple variables requires complex thresholds in order to define ore and waste. In practice, having a low fines content yields adequate recovery in terms of profitability. Using the mixture model the bitumen grades and fines are combined into a single variable termed as mass recoverable bitumen (MRB) based on the AER recovery function (Equation 4.1) and the fines recovery function (Equation 4.2) has the following:

$$R(g, f) = \frac{2 \cdot \mathrm{R(g)} \cdot \mathrm{R(f)}}{\mathrm{R(g)} + \mathrm{R(f)}} \tag{4.3}$$

The fines recovery function is calculated from the Equation 4.2. In this study, the mass recoverable mass bitumen cutoff grade is obtained based on the AER recovery function (Equation 4.1) and the fines recovery function from Sanford (1983), defined by Equation 4.2, which defined as mixture model defined by Equation 4.3. Every realization in each block has a unique recovery both for bitumen grades and fines. The bitumen for each block and realization gives function for bitumen whereas the fines for each block and realization gives the recovery function for fines. Then combining the bitumen grades and fines using the Equation 4.3, the mass recoverable bitumen (MRB) is defined, which is 3.078%. Tonnes of ore, waste, and other parameters are calculated using the MRB cutoff grade with raw bitumen density of $1012 kg/m^3$. Figure 4.31 shows histograms of MRB cutoff grade averaged over the 100 realizations.

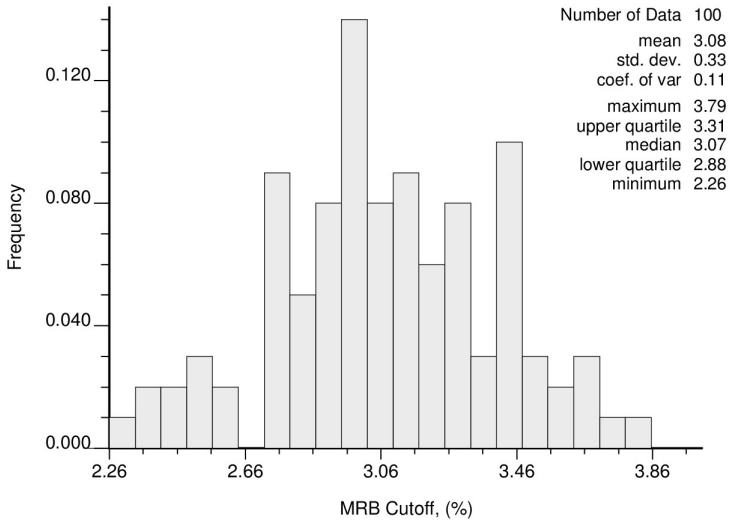

Figure 4.31: Mass recoverable bitumen (MRB) cutoff defined in terms of grade and fines.

Figure 4.32 (a) shows scatterplot between bitumen and fines grades in units of [mass%], and (b) shows cumulative distribution of bitumen grade with AER recovery and cutoff grade, and linear cutoff grade. Figure 4.32 (b) demonstrates a recovery function in terms of fines and grade's mixture model using the AER cutoff grade of 7% and fines cutoff grade derived from Sanford (1983). The blue and red lines show the AER cutoff grade and recovery function, which is 7% and 53.5%, respectively, whereas the blue line represents a nonlinear cutoff grade with a constant grade/recovery value of 6% approximately. Figure 4.33 shows ore/waste indicator (left) and bitumen grade obtained from the MRB cutoff grade calculation (right). Uncertainty for resources is calculated by evaluating every realization for all calculations of interest. This is done by computing the resource on every realization and assembling a distribution of the 100 values for each response variable of interest. Histograms of the calculated resources for bitumen grade, tonnes of ore, and quantity of bitumen is shown in Figure 4.34.

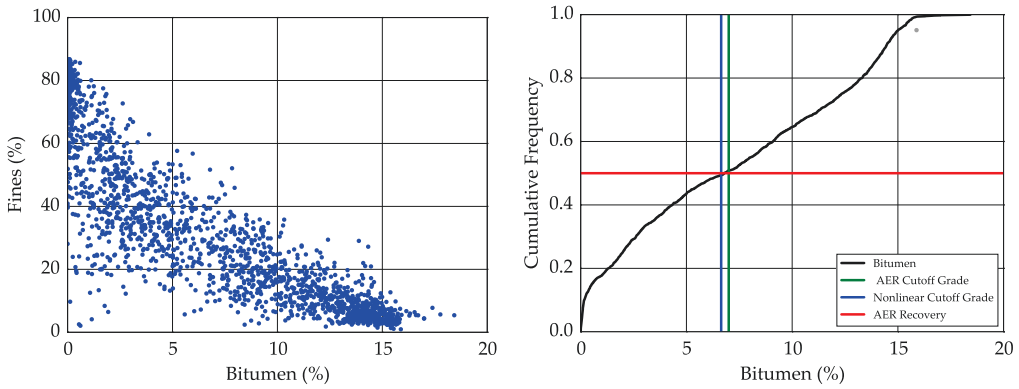

(a) (b)

Figure 4.32: Scatterplot between the bitumen and fines grades (a) and AER bitumen recovery, cutoff grade, and nonlinear cutoff grade (b).

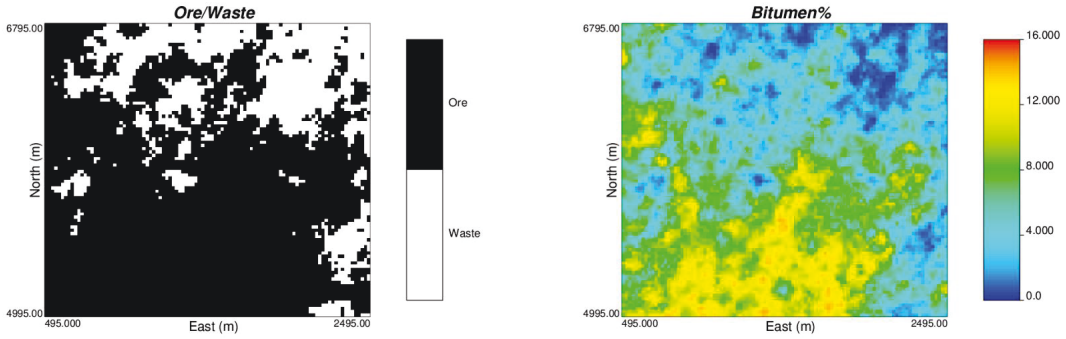

Figure 4.33: Illustration of ore/waste(left) and bitumen grade (right) based on MRB cutoff grade.

As the last step of the case study, sensitivity analysis is performed to assess the impact of each uncertainty. The sensitivity analysis is performed using the same methodology applied in the first case study. The sensitivity analysis used same GSLIB-like program called *SABOR* developed by Zagayevskiy & Deutsch (2011). In the tornado chart, the main middle part is divided into two bars. The bars on the right side of the tornado chart show either sensitivity coefficients and/or their standardized values. The bars on the left hand side show interaction terms between variables. The bars are plotted in the same order as bars on the right hand side of the tornado chart. These values are plotted in descending order. Positive coefficients are shown in yellow color, whereas negative coefficients are drawn in green. In the case of examining the linear regression model, other bars on the left side of the

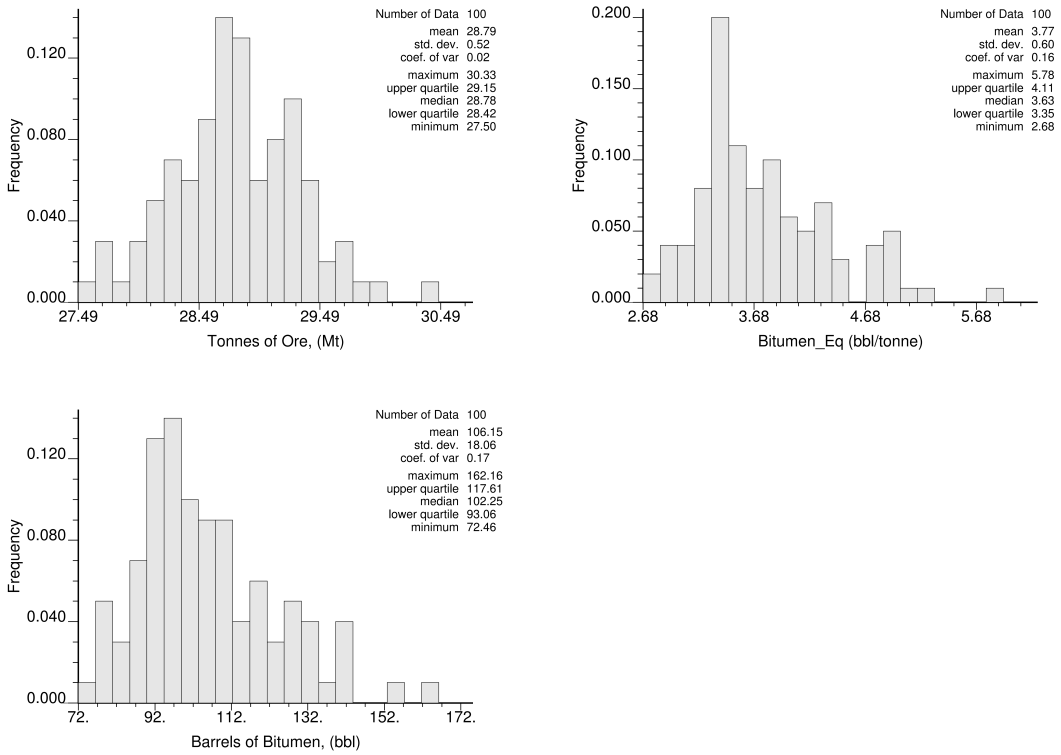

Figure 4.34: Histograms of calculated resources for tonnes of ore (top left), bitumen (top right), and bitumen quantity of metal (bottom left).

tornado represent either sensitivity coefficients or their standardized values without uncertainty. All bars are scaled to the largest upper boundary of confidence level of any coefficient or interaction term. It can be seen from the plot that the regression coefficients have the largest value; however, interaction terms may also have larger values in some cases. It also can be noted that input variables with relatively short coefficients of bars and interaction terms could be discarded from a model. In this particular case study, the linear model could be recommended for the given data set.

Summary statistics including coefficient of determination, its adjusted value, standard error of model deviations, model utility test based on F statistic, and prediction power of the model (percentage ratio of standard deviations of predicted and actual values of model response) are presented in the upper left corner of the plot. The table with means, standard deviations, coefficients of correlation and variation, sensitivity coefficients and standardized sensitivity coefficients for model response

and each input variable are tabulated in the table on the right of the chart. Coefficients, whose values are shown in blue in the table, are used for plotting bars. The specified confidence level is reported in the lower middle of the chart. Thus, the extended tornado chart visually summarizes results of sensitivity analysis and is useful for making decisions on the importance of input variables and the appropriateness of linear and quadratic models.

The dependent variables include tonnes of ore, bitumen equivalent grade, and barrels of bitumen. There are nine independent variables. The predictor variables include top surface structure, thickness, mean bitumen and fines grades, and facies proportions. In all cases, the sensitivity analysis shows that the uncertainty would be explained with three predictors. These three predictors include proportions, thickness, and bitumen grade. The coefficient of determination value in all cases was around R-sq=95%, where uncertainty is explained by the three most parameters mentioned above.

In this case study, a linear or quadratic regression models can be applied to understand the impact of each predictor variable as both of them could be applied after analyzing each response versus predictor variables. Figure 4.35 illustrates a tornado chart with a linear regression model. For illustration, the barrels of bitumen is selected as the response with the nine predictors in order shown in the figure. Three predictors have the most impact/importance: thickness, bitumen, and facies proportions.

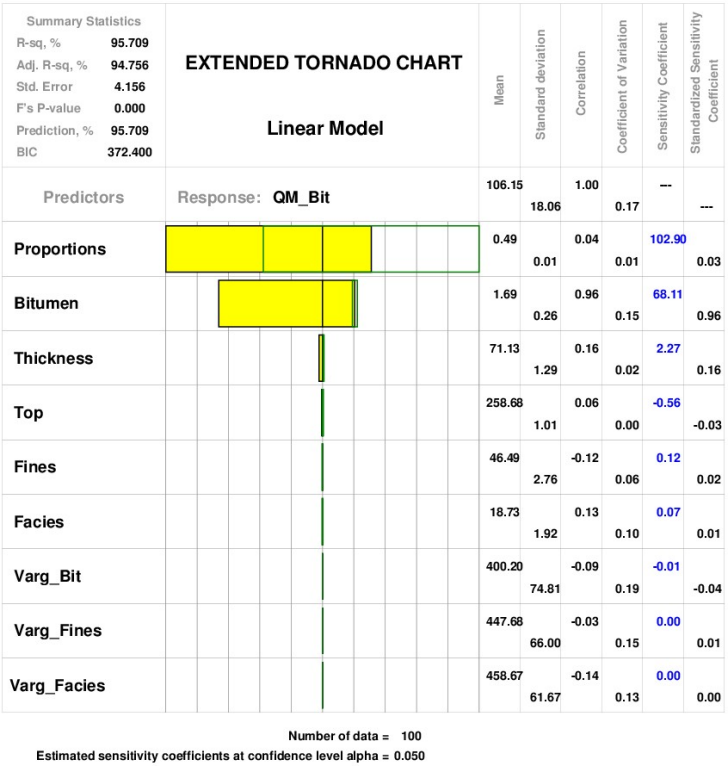

Figure 4.35: A tornado chart visualizing the effect of change in the value of an response versus predictor variables.

4.3 Conclusions

A reliable estimate of uncertainty is necessary in order to help decision makers in terms of reserve/resource classification, development decisions, and investment decisions. The case study for modeling some oilsands data show different geostatistical modeling methodologies in order to assess the resource uncertainty in a model. The used methodologies can be summarized as: (1) analyzing, determining, and modeling different structures, (2) facies modeling, including obtaining distribution of grades, modeling of spatial continuity, and (3) constructing uncertainty models followed by post processing and sensitivity analysis. The applied workflow accounts for the uncertainty in different input parameters.

Chapter 5

Conclusions

Assessing uncertainty in a resource model is an important task. One of the challenges during resource modeling is parameter and data uncertainty. In addition, uncertainty issues have not been fully addressed in modern work practices despite the importance of uncertainty in resource modeling. A development of this research is to capture, quantify, and assemble uncertainty into a practical modeling workflow. The goal is a realistic and fair measure of uncertainty in resource modeling. In this study, robust and practical concepts of resource modeling with uncertainty are developed.

5.1 Topics Covered and Contributions

Uncertainty depends on many factors, such as uncertainty in input parameters, data quality, and so on. These factors are discussed and a theoretical framework is developed and presented.

There are five main unit operations. These operations were incorporated and used to quantify and assemble uncertainty in different input parameters of interest. These include model setup, boundary, data, and parameter uncertainty, as well as post processing. General background and a review of relevant research is given in Chapter 1. A conceptual basis for resource modeling with uncertainty is introduced in Chapter 2. Each unit operation targets one aspect of the study; however, depending on the available data some of the unit operations vary from problem to

problem.

Chapter 2 also covers implementation aspects of resource modeling with uncertainty. Realizations of input parameters are generated and transferred to posterior realizations and assembled in order to perform post processing where evaluation is performed for every realization for all calculations of interest. The uncertainty is directly observed and the relationship between the input parameters are illustrated in a sensitivity study. Lastly, the developed conceptual workflow is presented with two case studies in Chapters 3 and 4. The presented case studies demonstrate the modeling process with two different deposits. Through each of these topics addressed the goals put forth in Chapter 1 are met. The outcomes of the conceptual workflow provides useful information to understand the uncertainty in complex geological settings.

The work provides three main contributions. The first is a conceptual workflow for assessing resource uncertainty. The developed theoretical workflow documents best practices to capture uncertainty. This considers different types of uncertainties and different implementation details depending on the deposit type.

The second contribution includes a clear documentation of the theoretical workflow. The documentation of the concepts for quantifying uncertainty is not fully defined in the literature with respect to each parameter for resource modeling. The presented workflow is applicable to resource modeling with uncertainty with deposits of varying complexity.

The third contribution is an understanding of uncertainties and their confounding factors. It is understood that uncertainty may have an impact on a project at any stage of mining. Considering uncertainty at early stages of a modeling process, therefore, is an important factor. Understanding uncertainty influences future decision making including additional drilling, long term planning and sequencing of mining operations.

5.2 Future Work

The concepts developed in this work show that the framework is practical for assessing uncertainty and is applicable for models from low to high complexity; however, future work remains. The following are some directions for future work:

- Determination of the acceptable level of uncertainty. The format for uncertainty statement could be customized depending on the deposit type and time in the mining lifecycle. There is no clear guideline for choosing the thresholds of acceptable uncertainty.

- Improved techniques to quantify parameter uncertainty. Different techniques could be applied to quantify the uncertainty in distributions. Selecting improved techniques would allow for the better integration of assessing uncertainty in input parameters that is practical.

- Data uncertainty with spatial correlation. Consideration of data uncertainty in the sampling is vital as the data may contain missing values or a sampling data error. Dealing with missing values and sampling errors in data with spatial correlation may be important.

- Understanding the number of realizations. In resource modeling, generating realizations/simulations is required, therefore, we run many realizations, but how many realizations is enough for assessing and modeling of uncertainty? It is necessary to understand and select realizations until the results are stable and enough to provide justification for a final model.

- Establishing a unified sensitivity analysis and addressing impactful parameters. Uncertainty is an important aspect of a resource modeling so we want to understand impacts of uncertainties coming from different input parameters and fully integrate sensitivity analysis.

- Uncertainty must also be transferred into mine planning and further decision making. The ability to transfer the assembled uncertainty through the mining

is essential. This will help decision makers in terms of long term economic feasibility, or mine planning, or risk assessment.

5.3 Recommendations

We wish for the lowest uncertainty possible. There are many parameters that influence resource uncertainty. In order to reduce uncertainty, it is important that the input parameters and their sources are known for more investigation. The presented concepts provides a framework for assessing uncertainty in a resource model. The presented conceptual workflow is robust and practical. Different methodologies may be considered to quantify uncertainty or improved resource modeling depending on the type of deposit.

Bibliography

Alshehri, N. and Deutsch, C. V. (2009). Reservoir uncertainty assessment. *Centre for Computational Geostatistics Annual Report*, 11.

Arvidson, H. (1998). KCGM-fimiston ore resource estimation practice, in *Proceedings Gold and Nickel Ore Reserve Estimation Practice Seminar*. pages 59–69. Australasian Institute of Mining and Metallurgy.

Babak, O. and Deutsch, C. V. (2006). A conditional finite domain (CDF) approach to parameter uncertainty. *Centre for Computational Geostatistics Annual Report*, 8.

Bailey, T. C. and Krzanowski, W. J. (2012). An overview of approaches to the analysis and modelling of multivariate geostatistical data. *Mathematical Geosciences*, 44(4):381–393.

Bárdossy, G. and Fodor, J. (2001). Traditional and new ways to handle uncertainty in geology. *Natural Resources Research*, 10(3):179–187.

Barnett, R. M. and Deutsch, C. V. (2011). Tools for multivariate geostatistical modeling. *Centre for Computational Geostatistics*, 13.

Barnett, R. M. and Deutsch, C. V. (2013a). Assessing the uncertainty and value of ACE transformation. *Centre for Computational Geostatistics*, 15.

Barnett, R. M. and Deutsch, C. V. (2013b). Tutorial and tools for ACE regression and transformation. *Centre for Computational Geostatistics*, 15.

Barnett, R. M. and Deutsch, C. V. (2015a). Imputation of geologic data. *Centre for Computational Geostatistics*, 17.

Barnett, R. M. and Deutsch, C. V. (2015b). Linear rotations: Options for decorrelation and analysis. *Centre for Computational Geostatistics Annual Report*, 17.

Barnett, R. M., Deutsch, J. L., and Deutsch, C. V. (2014). Practical workflows for geostatistical modeling with mean uncertainty. *Centre for Computational Geostatistics Annual Report*, 16.

Bear, J. and Cheng, A. H.-D. (2010). *Modeling groundwater flow and contaminant transport*, volume 23. Springer Science & Business Media.

Behrens, R. A., MacLeod, M. K., Tran, T. T., and Alimi, A. (1998). Incorporating seismic attribute maps in 3D reservoir models. *SPE Reservoir Evaluation & Engineering*, 1(02):122–126.

Berk, R. A., Bickel, P., Campbell, K., Fovell, R., Keller-McNulty, S., Kelly, E., Linn, R., Park, B., Perelson, A., Rouphail, N., et al. (2002). Workshop on statistical approaches for the evaluation of complex computer models. *Statistical Science*, pages 173–192.

Black, W. E. and Deutsch, C. V. (2015). Correlation reproduction of PCA and Sphere-R transformed multivariate data in the presence of secondary data. *Centre for Computational Geostatistics Annual Report*, 17.

Bogaert, P., Russo, D., et al. (1999). Optimal spatial sampling design for the estimation of the variogram based on a least squares approach. *Water Resources Research*, 35(4):1275–1289.

Bonneau, G.-P., Hege, H.-C., Johnson, C. R., Oliveira, M. M., Potter, K., Rheingans, P., and Schultz, T. (2014). Overview and state-of-the-art of uncertainty visualization. In *Scientific Visualization*, pages 3–27. Springer.

Caers, J. (2011). *Modeling uncertainty in the earth sciences*. John Wiley & Sons.

Cariboni, J., Gatelli, D., Liska, R., and Saltelli, A. (2007). The role of sensitivity analysis in ecological modelling. *Ecological modelling*, 203(1):167–182.

Carras, S. (1998). Let the orebody speak for itself. In *Proceedings Gold and Nickel Ore Reserve Estimation Practice Seminar*.

Chilès, J.-P. and Delfiner, P. (2012). Wiley series in probability and statistics. *Geostatistics: Modeling Spatial Uncertainty, Second Edition*, pages 705–714.

Cressie, N. (1993). Statistics for spatial data: Wiley series in probability and statistics. *Wiley-Interscience New York*, 15:16.

Cressie, N. and Hawkins, D. M. (1980). Robust estimation of the variogram: I. *Journal of the International Association for Mathematical Geology*, 12(2):115–125.

David, M. (2012). *Geostatistical ore reserve estimation*. Elsevier.

De Souza, L. E., Costa, J. F. C., and Koppe, J. C. (2004). Uncertainty estimate in resources assessment: a geostatistical contribution. *Natural Resources Research*, 13(1):1–15.

De Souza, L. E., Costa, J. F. C., and Koppe, J. C. (2005). Measures of uncertainty for resource classification. In *Geostatistics Banff 2004*, pages 529–536. Springer.

Deutsch, C. and Journel, A. (1998). *GSLIB: Geostatistical software library and user's guide*. Oxford University Press.

Deutsch, C. V. (2004). A statistical resampling program for correlated data: spatial_bootstrap. *Centre for Computational Geostatistics Annual Report*, 6.

Deutsch, C. V. (2015). All realizations all the time. *Centre for Computational Geostatistics Annual Report*, 17.

Deutsch, C. V., Monteiro, M., and Leuangthong, O. (2002). Procedures and guidlines for assessing and reporting uncertainty in Geostatistical reservoir modeling. *Centre for Computational Geostatistics Annual Report*, 4.

Deutsch, J. L. and Deutsch, C. V. (2011). Plotting and checking the bivariate distributions of multiple Gaussian data. *Computers & Geosciences*, 37(10):1677–1684.

Draper, D. (1995). Assessment and propagation of model uncertainty. *Journal of the Royal Statistical Society. Series B (Methodological)*, pages 45–97.

Duggan, S. and Dimitrakopoulos, R. (2005). Application of conditional simulation to quantify uncertainty and to classify a diamond deflation deposit. In *Geostatistics Banff 2004*, pages 419–428. Springer.

Edwards, A. (2001). Mineral resource and ore reserve estimation: the AusIMM guide to good practice. Australasian Institute of Mining and Metallurgy.

Efron, B. (1983). Estimating the error rate of a prediction rule: improvement on cross-validation. *Journal of the American Statistical Association*, 78(382):316–331.

Efron, B. and Tibshirani, R. (1986). Bootstrap methods for standard errors, confidence intervals, and other measures of statistical accuracy. *Statistical science*, pages 54–75.

Feyen, L. and Caers, J. (2006). Quantifying geological uncertainty for flow and transport modeling in multi-modal heterogeneous formations. *Advances in Water Resources*, 29(6):912–929.

Funtowicz, S. O. and Ravetz, J. R. (1990). *Uncertainty and quality in science for policy*, volume 15. Springer Science & Business Media.

Glacken, I. and Snowden, D. (2001). Mineral resource estimation. *Mineral Resource and Ore Reserve Estimation-The AusIMM Guide to Good Practice, The Australasian Institute of Mining and Metallurgy: Melbourne. P*, pages 189–198.

Gnanadesikan, R. (2011). *Methods for statistical data analysis of multivariate observations*, volume 321. John Wiley & Sons.

Goovaerts, P. (1997). *Geostatistics for natural resources evaluation*. Oxford University Press.

Grace, K. (1986). The critical role of geology in reserve determination, in Ranta, D. E.,(ed.). *Applied Mining Geology*, pages 1–7.

Gringarten, E. and Deutsch, C. V. (2001). Teacher's aide variogram interpretation and modeling. *Mathematical Geology*, 33(4):507–534.

Grondona, M. O. and Cressie, N. (1991). Using spatial considerations in the analysis of experiments. *Technometrics*, 33(4):381–392.

Hengl, T., Minasny, B., and Gould, M. (2009). A geostatistical analysis of geostatistics. *Scientometrics*, 80(2):491–514.

Hosseini, A. L. and Deutsch, C. V. (2007). A distance function based algorithm to quantify uncertainty in areal limits. *Centre for Computational Geostatistics Annual Report*, 9.

Isaaks, E. and Srivastava, R. (1989). *Applied geostatistics*. Oxford University Press New York.

Johnson, R. and Wichern, D. (2002). *Applied multivariate statistical analysis*. Pearson International Edition.

Journel, A. (1986). Geostatistics: models and tools for the earth sciences. *Mathematical Geology*, 18(1):139.

Journel, A. and Huijbregts, C. (1978a). *Mining Geostatistics*. London - New York - San Francisco Academic Press.

Journel, A. G. and Bitanov, A. (2004). Uncertainty in N/G ratio in early reservoir development. *Journal of Petroleum Science and Engineering*, 44(1):115–130.

Journel, A. G. and Huijbregts, C. J. (1978b). *Mining geostatistics*. Academic Press.

Katz, R. W. (2002). Techniques for estimating uncertainty in climate change scenarios and impact studies. *Climate Research*, 20(2):167–185.

Kennedy, M. C. and O'Hagan, A. (2001). Bayesian calibration of computer models. *Journal of the Royal Statistical Society: Series B (Statistical Methodology)*, 63(3):425–464.

Khan, K. D. and Deutsch, C. V. (2015). Practical incorporation of multivariate parameter uncertainty in geostatistical resource modeling. *Natural Resources Research*, pages 1–20.

King, H, F., McMahon, D, W., and Butjor, G. J. (1982). A guide to the understanding of ore reserve estimation. Supplement to the AusIIM Proceedings. Number 2. Australasian Institute of Mining and Metallurgy.

Klepper, O. (1997). Multivariate aspects of model uncertainty analysis: tools for sensitivity analysis and calibration. *Ecological modelling*, 101(1):1–13.

Knights, P., Dunn, D., et al. (2008). Geological uncertainty and risk: Implications for the viability of mining projects. *Journal of Coal Science and Engineering (China)*, 14(2):176–180.

Kogan, R. (1989). Interval estimation of mineral propsects. *Mathematical geology*, 21(6):607–618.

Koltermann, C. E. and Gorelick, S. M. (1996). Heterogeneity in sedimentary deposits: A review of structure-imitating, process-imitating, and descriptive approaches. *Water Resources Research*, 32(9):2617–2658.

Koushavand, B. and Deutsch, C. V. (2008). A methodology to quantify and transfer variogram uncertainty through kriging and simulation. *Centre for Computational Geostatistics Annual Report*, 10.

Kupfersberger, H., Deutsch, C. V., and Journel, A. G. (1998). Deriving constraints on small-scale variograms due to variograms of large-scale data. *Mathematical Geology*, 30(7):837–852.

Leuangthong, O., Khan, K. D., and Deutsch, C. V. (2011). *Solved problems in geostatistics*. John Wiley & Sons.

Leuangthong, O., Schnetzler, E., and Deutsch, C. V. (2004). Geostatistical modeling of McMurray oil sands deposits. *Centre for Computational Geostatistics Annual Report*, 6.

Li, S. and Knights, P. (2008). Quantifying geological/geotechnical risk associated with coal reserves estimation. *Australian Mining*, 191.

Lopes, J., Rosas, C., Fernandes, J., and Vanzela, G. (2011). Risk quantification in grade-tonnage curves and resource categorization in a lateritic nickel deposit using geologically constrained joint conditional simulation. *Journal of Mining Science*, 47(2):166–176.

Lutherborrow, C. (1999). Evaluation of resource and reserve estimation methods at Pasminco Broken Hill mine southern underground operations, in *Proceedings Resource and Reserve Estimation Practice in the Central West New South Wales Mining Industry*. pages 3–10. Australasian Institute of Mining and Metallurgy.

Mann, C. J. (1993). Uncertainty in geology. *Computers in Geology–25 Years of Progress, Oxford University Press, Oxford*, pages 241–254.

Marchant, B. and Lark, R. (2004). Estimating variogram uncertainty. *Mathematical Geology*, 36(8):867–898.

Matheron, G. (1962). *Traite de Geostatistique Appliquee*. Technip, Paris, France.

Mory-Machuca, D. F., Munroe, M. J., and Deutsch, C. V. (2009). Tonnage uncertainty assessment of vein-type deposits using distance functions and lcoation-dependent correlograms. *Centre for Computational Geostatistics Annual Report*, 11.

Munroe, M. J. and Deutsch, C. V. (2008a). A methodology for modeling vein-type deposit tonnage ucnertainty. *Centre for Computational Geostatistics Annual Report*, 10.

Munroe, M. J. and Deutsch, C. V. (2008b). Full calibration of C and Beta in the

framework of vein-type deposit tonnage uncertainty. *Centre for Computational Geostatistics Annual Report*, 10.

Murphy, R., Landmark, J., Warner, J., Riddington, D., and Ekers, B. (2008). Towards a better resource estimate–The GSML Experience, in *Proceedings Gold and Nickel Ore Reserve Estimation Practice S*eminar. pages 101–120. Australasian Institute of Mining and Metallurgy.

Ortiz, J. and Deutsch, C. V. (2002). Calculation of uncertainty in the variogram. *Mathematical Geology*, 34(2):169–183.

Philip, G. and Watson, D. (1986). Matheronian geostatistics—Quo vadis? *Mathematical geology*, 18(1):93–117.

Pinto, F. A. C. and Deutsch, C. V. (2014). Factors influencing data spacing and uncertainty. *Centre for Computational Geostatistics Annual Report*, 16.

Pyrcz, M. J. and Deutsch, C. V. (2014). *Geostatistical reservoir modeling*. Oxford University Press, Second edition.

Reckhow, K. H. (1994). Importance of scientific uncertainty in decision making. *Environmental Management*, 18(2):161–166.

Refsgaard, J. C., Van der Sluijs, J. P., Brown, J., and Van der Keur, P. (2006). A framework for dealing with uncertainty due to model structure error. *Advances in Water Resources*, 29(11):1586–1597.

Refsgaard, J. C., van der Sluijs, J. P., Højberg, A. L., and Vanrolleghem, P. A. (2007). Uncertainty in the environmental modelling process–a framework and guidance. *Environmental modelling & software*, 22(11):1543–1556.

Regal, R. R. and Hook, E. B. (1991). The effects of model selection on confidence intervals for the size of a closed population. *Statistics in Medicine*, 10(5):717–721.

Rezvandehy, M. K., Khan, D., and Deutsch, C. V. (2015). ParUnce: Code for parameter ucnertainty. *Centre for Computational Geostatistics Annual Report*, 17.

Rossi, M. E. and Deutsch, C. V. (2013). *Mineral resource estimation*. Springer Science & Business Media.

Saltelli, A., Chan, K., Scott, E. M., et al. (2000). *Sensitivity analysis*, volume 1. Wiley New York.

Sanford, E. (1983). Processibility of athabasca oil sand: Interrelationship between oil sand fine solids, process aids, mechanical energy and oil sand age after mining. *The Canadian Journal of Chemical Engineering*, 61(4):554–567.

Schuenemeyer, J. H. and Power, H. C. (2000). Uncertainty estimation for resource assessment—an application to coal. *Mathematical Geology*, 32(5):521–541.

Shlens, J. (2005). A tutorial on principal component analysis, systems neurobiology laboratory, university of california at san diego. *URL http://www. snl. salk. edu/˜ shlens/pca. pdf*.

Shlens, J. (2014). A tutorial on principal component analysis. *arXiv preprint arXiv:1404.1100*.

Sinclair, A. and Blackwell, G. (2002). *Applied Mineral Inventory Estimation*. Cambridge University Press.

Smith, L. I. (2002). A tutorial on principal components analysis. *Cornell University, USA*, 51(52):65.

Srivastava, R. M. and Parker, H. M. (1989). Robust measures of spatial continuity. In *Geostatistics*, pages 295–308. Springer.

Taylor, J. R. (1997). *Error analysis: the study of uncertainties in physical measurements*. University Science Books; 2nd ed.

Tukey, J. W. (1977). Exploratory data analysis.

Uusitalo, L., Lehikoinen, A., Helle, I., and Myrberg, K. (2015). An overview of methods to evaluate uncertainty of deterministic models in decision support. *Environmental Modelling & Software*, 63:24–31.

Villalba, M. E. and Deutsch, C. V. (2009). Review of techniques to calculate uncertainty in the mean. *Centre for Computational Geostatistics Annual Report*, 11.

Wackernagel, H. (2013). *Multivariate geostatistics: an introduction with applications*. Springer Science & Business Media.

Walker, W. E., Harremoës, P., Rotmans, J., van der Sluijs, J. P., van Asselt, M. B., Janssen, P., and Krayer von Krauss, M. P. (2003). Defining uncertainty: a conceptual basis for uncertainty management in model-based decision support. *Integrated assessment*, 4(1):5–17.

Webster, R. and Oliver, M. A. (1992). Sample adequately to estimate variograms of soil properties. *Journal of soil science*, 43(1):177–192.

Welch, W. J., Buck, R. J., Sacks, J., Wynn, H. P., Mitchell, T. J., and Morris, M. D. (1992). Screening, predicting, and computer experiments. *Technometrics*, 34(1):15–25.

Wilde, B. J. and Deutsch, C. V. (2009). Automatic determination of uncertainty versus data density. *Centre for Computational Geostatistics Annual Report*, 11.

Wilde, B. J. and Deutsch, C. V. (2010). Formats for expressing acceptable uncertainty. *Centre for Computational Geostatistics Annual Report*, 12.

Wilde, B. J. and Deutsch, C. V. (2011a). A new way to calibrate distance function uncertainty. *Centre for Computational Geostatistics Annual Report*, 11.

Wilde, B. J. and Deutsch, C. V. (2011b). Simulating voundary realizations. *Centre for Computational Geostatistics Annual Report*, 11.

Wu, J. and Li, H. (2006). Uncertainty analysis in ecological studies: an overview. In *Scaling and Uncertainty Analysis in Ecology*, pages 45–66. Springer.

Youden, W. J. (1951). *Statistical methods for chemists*. Wiley New York.

Zagayevskiy, Y. V. and Deutsch, C. V. (2011). Updated code for sensitivity analysis based on regression. *Centre for Computational Geostatistics Annual Report*, 13.